Laboratory Studies of Stratospheric Dust – Relevance to the Theory of Cometary Panspermia

By

Norimune Miyake
BSc

Thesis submitted in candidature for the degree of Doctor of Philosophy at Cardiff University

ProQuest LLC
789 East Eisenhower Parkway
P.O. Box 1346
Ann Arbor, MI 48106-1346

CARDIFF UNIVERSITY
PRIFYSGOL CAERDYDD

DECLARATION

This work has not previously been accepted in substance for any degree and is not concurrently submitted in candidature for any degree.

Signed .....(candidate) Date ...31/09/08...

STATEMENT 1

This thesis is being submitted in partial fulfillment of the requirements for the degree of .....PhD.....(insert MCh, MD, MPhil, PhD etc, as appropriate)

Signed .....(candidate) Date ...31/09/08...

STATEMENT 2

This thesis is the result of my own independent work/investigation, except where otherwise stated. Other sources are acknowledged by explicit references.

Signed .....(candidate) Date ...31/09/08...

STATEMENT 3

I hereby give consent for my thesis, if accepted, to be available for photocopying and for inter-library loan, and for the title and summary to be made available to outside organisations.

Signed .....(candidate) Date ...31/09/08.

STATEMENT 4: PREVIOUSLY APPROVED BAR ON ACCESS

I hereby give consent for my thesis, if accepted, to be available for photocopying and for inter-library loans **after expiry of a bar on access previously approved by the Graduate Development Committee.**

Signed .....(candidate) Date ...31/09/08...

Contents

Acknowledgements

First of all, I like to record my sincere thanks to my supervisor Professor Chandra Wickramasinghe for suggesting the topic of my thesis, and for many discussions throughout the period of my study. His amazing ideas have always inspired me, I am very grateful to him for giving me an opportunity to work in this exciting field. He has encouraged me when I needed it the most, and I cannot thank him enough for that.

I also like to thank Professor David Lloyd (School of Biosciences, Cardiff University) and Dr. Gordon Webster (School of Earth & Ocean Sciences, Cardiff University) for letting me use their facilities, as well as technicians Pete Fisher, Anthony Oldroyd and Lindsey Axe for their support on the use of equipment.

My special thanks go to Dr. Max Wallis, Dr. Anthony Hann and Dr. Shirwan Al-Mufti for their tremendous support, mentally and technically to complete this thesis.

Finally, I like to dedicate this thesis to my family: my sister Kae, her husband Scott, my nephew, Eileen, Gerald, and my parents who endlessly encouraged me throughout my academic career.

Norimune Miyake
Cardiff Centre for Astrobiology, Cardiff Iniversity
26 September 2008

Summary

This thesis presents results of laboratory investigations of stratospheric dust that have a direct bearing on the theory of cometary panspermia.

Chapter 1 deals with the historical backdrop to panspermia theories, with a summary of recent relevant work on comets, meteorites and IDP's (Interplanetary Dust Particles).

In Chapter 2 I describe the techniques that have been used over several decades to collect stratospheric dust with a view to identifying a cometary and possible biological components. The Cryosampler technique deployed by ISRO in 2001 provides the best hope for preserving small fragile particles of cometary origin, even those of possible biological provenance. The source material for my laboratory investigations was collected using the Cryosampler technique in a balloon flight on 21 January 2001.

The description of techniques for stratospheric air collection, extraction of aerosols, analysis by SEM, EDX and the results of my investigations using these techniques form the main bulk of Chapter 3. Over 30 individual IDP's were imaged, analysed, catalogued and classified. Many biologically relevant particles including putative bacterial spores and nanobacteria were discovered.

In Chapter 4 DNA extracts from the stratospheric samples were analysed using PCR amplification of 16S rRNA gene sequences. Evidence of actinobacteria (96% homology) and chloroplast sequences (99% homology) point to an extraterrestrial origin of these genes. Arguments for contamination are discussed, and ruled out.

In Chapter 5 present a preliminary analysis of the 2001 Kerala Red Rain samples. SEM, TEM images were obtained, and staining tests for DNA carried out. The origin of the red rain cells remains inconclusive.

CHAPTER 1

Introduction

1.1 General Introduction

Evidence of biology in space and in the Earth's upper atmosphere has been sought for many decades. From astronomical spectroscopy and space probes over the past 3 decades, we now know that the primitive biological materials do exist in space. No decisive evidence of any viable organisms in space has been discovered to date, however.

According to the Hoyle-Wickramasinghe theory of cometary panspermia (1978), viable organisms exist within the comet's nucleus, and seed habitable planets with life. The discovery of various extremophiles supports the possibility of microorganisms surviving in the hostile environments of space and in the interior of comets. Recently, possibly controversial evidence of fossilised microorganisms was found inside carbonaceous meteorites (Hoover *et al.*, 2004), which were thought to originate from comets (Ehrenfreund *et al.*, 2001). This shows that even now extraterrestrial life is possibly entering the Earth's atmosphere within the meteorites and cometary debris.

Microorganisms originating in comets and meteorites can be collected in the upper atmosphere. In 2001, the Indian Space Research Organization carried out a balloon-borne investigation using prototype of a cryogenic sampler to obtain extraterrestrial aerosols from the upper stratosphere. In the same year, the Red Rain Phenomenon in India was observed and samples were collected. In both cases, the samples were investigated at the Cardiff Centre for Astrobiology, Cardiff University. In this thesis, I present the investigation of these samples in relation to the theory of panspermia.

1.2 Abiogenesis

The origin of life has been discussed in many different forms in religion, philosophy and science as if it is the ultimate question for humans. Abiogenesis is a topic that has been discussed for many centuries. It is the study of life-formation from inanimate organic and inorganic molecules. The standard modern theory of abiogenesis began when Oparin (1924) and Haldane (1929), working independently, proposed that the

life may have begun in a 'primordial soup' of organic molecules and developed on a primitive Earth. Their hypothesis was that a mixture of inorganic molecules such as water, methane, ammonia, and hydrogen cyanide were broken down by the action of the sun's ultraviolet rays and strong electric discharges in lightning in the atmosphere of the early Earth. Fragments of broken down inorganic molecules may have recombined into prebiotic organic molecules and rained down into the primitive ponds. Here further reactions of prebiotic molecules for millions of years may have started life.

This theory was supported by the classic experiments of Miller and Urey (1959). They showed that when a gas mixture of inorganic molecules (e.g. H_2O, CH_4, and NH_3) such as were thought to exist in the early atmosphere by Oparin and Haldane, was heated and subjected to electrical discharges, organic molecules that may serve as life's building blocks, such as simple sugar and amino acid, were formed. Although the current theories of the Earth's early atmosphere are different from that of Oparin and Haldane prediction, many new experiments have achieved similar results using various corrected atmospheric compositions and conditions (Rode, 1999; Hanic *et al.*, 2000).

The Miller-Urey experiment, however, does not explain later stages in the processes that led to the origin of life, such as the evolution of a simple genetic code or processes leading to cellular membrane formation. The question of how simple organic molecules lead to the formation of a protocell is unanswered but there are many hypotheses. The currently popular RNA-world hypothesis is based on the evidence that short stretches of RNA molecules, which could have spontaneously formed from simple organic chemicals, can act as the enzymes thus catalysing their continuing replication (Woese, 1968; Gilber, 1986). Proteinoids, which are protein-like molecules produced when amino acids are heated, can then form a pre-cellular membrane called 'a microsphere' protecting these short strands of RNA.

In 1980's, Wächtershäuser (1988) proposed the iron-sulfur world hypothesis, where the organic molecules are formed through catalytic processes in deep sea vents. In contrast to the Oparin-Haldane theory, which invokes the energy from the lightning and UV rays to form the organic molecules, his hypothesis uses the energy from the redox reaction of iron sulfides (such as pyrite) and other minerals in hot vents to synthesize prebiotic organic molecules. He also argued that the energy released from this reaction is enough to form lipid polymers, which form the 'microsphere' containing organic molecules inside. He further argued that a complex metabolism like DNA formation evolved after the microsphere moved to an ideal environment. However, it is still not clear whether this proposed mechanism could actually work.

Cairns-Smith (1985) proposed another hypothesis based on clay. He argued that the surface of silicate crystals can act as catalysts to organic molecules in solution enabling complex protogenes to form. Clay crystals grown at the stream bed can convey the molecules to more favourable environments thus function also as vehicle.

The cosmic view of life-formation on the Earth has a long history. Du Noüy (1947) calculated that a single simple protein molecule would take 10^{243} Ga to form by the workings of chance and error. And this single protein molecule was still very far from the life itself. Hoyle and Wickramasinghe (1982) calculated that the probability of forming the crucial enzymes for life from the necessary amino acids in a primordial soup is 1 in $10^{40,000}$. These numbers point dramatically to the non-feasibility of life formation within the allowed time scale on the primitive Earth.

The recent discovery of detrital zircon crystals in metamorphosed sediments proved that water existed in liquid form at about 4.4 Ga (Wilde *et al.*, 2001), which opened only a small window of time scale possible life-formation on the Earth. The oldest fossilised stromatolites are dated at 3.5 Ga, so that abiogenesis if it happened on earth had to take place within a timescale less than 1 Ga. However, starting of abiogenesis within a small liquid volume in the hostile environment of 4.4 Ga ago is very doubtful. Together with the fact that no satisfactory theory for the origin of nucleic acid and

protein is found on Earth yet, many biologists and astronomers started to look for answers in space, where timescales for abiogenesis pose no concern.

The improbability of abiogenesis on the Earth has led Napier *et al.* (2008) to suggest that the totality of all the comets around all the stars in the galaxy could provide a more promising prospect for an origin of life. Once life originated on some comet somewhere, its spread to other comets and other planets appears to be relatively easy (Wickramasinghe, 2007).

1.3 Theory of Panspermia

Panspermia is another theory that has been argued alongside abiogenesis from many centuries ago. It is a theory that the life is ubiquitous all over the universe in the form of "seeds", and they may deliver life or have delivered life to the habitable bodies such as the Earth. The idea of panspermia was first mentioned in the writings dating back to 5th century B.C. in Greece. After a long latent period, the theory was revisited by many scientists in 19th century. Berzelius (1834) discovered complex carbon compounds in addition to clay minerals in the Alais meteorite and speculated that this might provide the proof to the life originating in space. In 1864, Pasteur disproved the widely discussed theory of the spontaneous generation of life by means of a simple experiment (Dubos, 1950). Using a sterilised flask with bent neck he demonstrated that the microorganisms cannot begin to grow in any culture medium if there are no organisms previously.

These concepts prompted Kelvin and Helmholtz to propose the basics of lithopanspermia in 1871. Their hypothesis was that microscopic life can be conveyed in a rock such as a meteorite or comet. In the presidential address to the British Association for the Advancement of Science, Kelvin stated:

"Should the time come when this earth comes into collision with another body, comparable in dimensions to itself... many great and small fragments carrying seeds of living plants and animals would undoubtedly be scattered through space. Hence, and because we all

confidently believe that there are at present, and have been from time immemorial, many worlds of life besides our own, we must regard it as probable in the highest degree that there are countless seed-bearing meteoric stones moving about through space. If at the present instance no life existed upon this earth, one such stone falling upon it might, by what we blindly call natural causes, lead to its becoming covered with vegetation."

1.4 Problem with Solar Radiation

In the beginning of 20th century, Arrhenius (1903) proposed a different hypothesis of panspermia, which lifted undeveloped ideas to the level of serious scientific theory. His argument was that the direct propagation of microscopic spores between planets can be done by the radiation pressure of starlight. He suggested that, subject to the low temperatures in space, spores would be able to remain viable for very long periods. However, as regards the effect of solar radiation, he had many critics. Becquerel (1924) and others used laboratory experiments to argue that the microorganisms like bacteria cannot survive long-time exposure to the hostile environment of space, especially the solar radiation.

Ultraviolet radiation can produce a covalent linkage between two adjacent pyrimidine bases in DNA to form dimers (e.g. thymine dimers called TDHT), which then leads to the deletion of one or more base pairs during the DNA replication causing disastrous damage to the cell. Damage like formation of TDHT is not easily amenable to cellular repair processes. Hoyle and Wickramasinghe (1981) argued that if bacteria exist in colonies, a very thin surface layer of graphite for each colony (~0.02 μm thick) would be sufficient to give protection to the bacteria inside, because the UV radiation penetrates only a small distance into organic material. Interstellar clouds can also give the protection since roughly a third of all interstellar carbon is found to be in the form of graphite. The graphite can absorb UV light over the wavelength range of importance for biology.

For an unshielded cell, ionising radiation from the cosmic rays is considerably more lethal than UV radiation. It can knock out some electrons in DNA which produces

reactive free radicals and also cause the breakage of DNA strands. Although it is difficult to estimate the dose of cosmic rays received by a naked bacterium in a typical location in interstellar space, within the solar system it is estimated to be in a range of 0.1-0.45 MGy (1 Gy = one joule of energy absorbed per kg of matter) per million years depends on the distance from the sun and the phase of solar activity. The discovery of viable bacterial spores in a 250 Myr salt crystal (Vreeland *et al.*, 2000) is relevant, because the integrated dose from radiopotassium is calculated to be of similar magnitude and to induce sufficient DNA double strand breakage to kill most of the spores (Nicastro *et al.*, 2002). Ultra-low fluxes delivered over timescales as long as 250 Myr appear to be much less effective, however.

In the dormant state of spore-forming bacteria, which is normally triggered by the depletion of nutrients or sudden changes to the surrounding environments, spores have no detectable metabolism and exhibit a high degree of resistance to inactivation by various physical insults, such as extreme heat and cold, desiccation by vacuum or oxidising agents. However, UV radiation and cosmic rays (total of 4.8 Gy) exposure to the naked-spore (*B. subtilis*) for 6 years in space gave only a small survival rate (Horneck, 1993; Horneck *et al.*, 1995).

Mileikowsky *et al.* (2000) assumed that a few μm of meteorite material would give enough protection against UV, a few mm would be required to shield against X-rays, and about 10 cm against ionising radiation. Horneck *et al.* (2001) has shown that the solar radiation exposure to *B. subtilis*, which is embedded in clay or rock materials with similar ratio as occurring in terrestrial soil, for 2 weeks in space, gave 100 % survival rate. She also showed that the spores survived in a simulated Martian meteorite (Zagami) at the same condition.

1.5 Cosmic Dust

Cosmic dust in the form of submicron to micron sized particles are found ubiquitously in space. It is a vital component in many astrophysical processes. In the early stage of

a star's life cycle, it exist in the form of an interstellar cloud fragment (nebula), and this diffuse dust cloud collapses under its own gravity and forms stars and planets. Cosmic dust also accumulates in interstellar molecular clouds, from material ejected from a star nearing the end of its life called a red giant or by a stellar explosion of a bigger star called a supernova. The solar system condensed from such a cloud of gas and dust.

Most of the dust is formed by processes within the cloud itself, but a fraction predates the collapse of the cloud and such particles are called the presolar grains. There is evidence that the solar system's condensation was started by the pressure wave from a supernova because the interplanetary dusts contain a fraction of those presolar grains from a supernova. This is further discussed in a later section.

Wickramasinghe (1974) discovered evidence for polymers similar to formaldehyde in the interstellar dust by using astronomical observations of infrared spectroscopy. It was the first discovery of complex organic polymers in interstellar space. Subsequently he showed the infrared absorption of interstellar dust at 2.9-3.5 μm regions which had a close correspondence to that of spore-forming bacteria in laboratory (Allen and Wickramasinghe, 1981). He argued that the prestellar molecular clouds favour formation of grains coated with carbonaceous materials.

Wickramasinghe also identified aromatic molecules including polysaccharides using ultraviolet absorption spectra of the interstellar dust clouds (Hoyle and Wickramasinghe, 1977; Wickramasinghe *et al.*, 1989). Lacy *et al.* (1991) discovered interstellar methane also by infrared spectroscopy. These discoveries are now the basis of the recent researches on Panspermia. The modern techniques used to study the cosmic dust particles *in situ* are discussed in Chapter 2.

1.6 Comets

A comet is a 'small' solar system body that orbits the sun. It is typically a few kilometres across, containing ice, organics, dust and rocky particles. The comets are thought to have formed from condensation of the leftover materials in the cooler outer region of the solar system after formation from the interstellar molecular cloud. They reside in regions called the Oort cloud and to a lesser extent in the Kuiper Belt.

In 1978, Hoyle and Wickramasinghe proposed the theory of cometary panspermia where a small fraction of microorganisms in the interstellar cloud was incorporated within newly formed comets. This small population would be amplified in the warm liquid interiors of primordial comets that subsequently became hard frozen when the original radioactive heat sources died out. Collisions between the cometary bodies ejected a fraction of life-containing comets into both outer and inner solar system. Comets that were deflected to inner solar system delivered microorganisms onto the Earth and other planets. Wallis (1980) argued that the radiogenic heating due to aluminium-26 can maintain warm liquid water condition at the centre of comets, providing an ideal niche for the viable microorganisms (Hoyle and Wickramasinghe, 1985).

The nature of comets has been studied *in situ* by the space probes. The first observation of comet Halley near perihelion in 1986 showed the presence of organic materials. From the Giotto mission's dust impact mass spectra, Wickramasinghe *et al.* (1986a, b) argued that complex organic grains that have a composition consistent with the biological hypothesis are found, while Allen (1987) discovered methane and ammonia in the coma and Huebner (1987) found the formaldehyde polymer polyoxymethylene, all of which favour to the ideas of cometary panspermia.

In 2005, NASA's space probe 'Deep Impact' collided with the nucleus of comet Tempel 1. The spectral analysis of the ejecta increased an amount of organics such as formaldehyde and methanol (A'Hearn *et al.*, 2005). It also discovered evidence of

phyllosilicate (probably clay minerals), which had to be formed in presence of liquid water (Lisse *et al.*, 2006; Wickramasinghe *et al.*, 2008). This shows that the interior of Tempel 1 must have had liquid water some time in its formation history where microorganisms could be amplified. The space missions to the comet Halley and Tempel 1 are further discussed in chapter 2.

1.7 Meteorites and Dust particles in Atmosphere

Dust and meteorites in the solar system are mostly associated with planets, asteroids or comets. Some of this material was generated by impact ejection from planets, collisions of comets and asteroids that fragment planetary bodies. Dust and meteorites are important too in studying the history of our solar system, since they are found to contain presolar grains. These grains have unique isotopic signatures, which prove they formed via condensation from the cooling outflows of supernova or a red giant.

In the 1960s, xenon and neon components with unusual isotopic ratios were discovered in the primitive meteorites, and it was later found that diamond and silicon carbide grains were the carriers of these noble gases (Grady and Wright, 1990). Since then many different types of refractory minerals containing presolar grains, such as C, TiC, TiO_2, Si_3N_4, Al_2O_3, spinel and silicate minerals, have been found in the dust particles collected in the stratosphere and in meteorites (e.g. Nagashima *et al.*, 2004; Hoppe *et al.*, 2004; Krot *et al.*, 2005; Sunshine *et al.*, 2008). The discovery of a pure refractory Ti-crystal embedded in a stratospheric dust particle is discussed in Chapter 3.

Meteorites

One of the best studied meteorites, the Orgueil meteorite, fell in France in 1864. It was the first time that a meteorite was proposed to contain fossilized bacteria (Tan and VanLandingham, 1967). Continuing investigations of this fossil have shown its extensive similarity to a magnetotactic bacterium (e.g. *Rhodopseudomonas rutilis*) (e.g. Hoover *et al.*, 1998). More recently, Hoover *et al.* (2004) discovered more evidence of fossilised bacteria in the Orgueil meteorite. His Field Emission Scanning

Electron Microscope (FESEM) images and EDX spectral analysis showed indigenous microfossils and microbial assemblages, which closely resemble mats of known terrestrial fossilised cyanobacteria (e.g. *Phormidium tenuissimum*).

Discovery of microbial fossils in the Martian meteorite ALH84001, which was preserved in Antarctica for about 13,000 years, was first claimed by McKay *et al.* (1996). The exceptionally small size of the microstructural fossils (20 ~ 500 nm) was initially criticised on the grounds that microorganisms are generally much larger. However, it was noted that such sizes of nanobacteria are common within the terrestrial environment (e.g. Allen *et al.*, 1997; Kazmierczak and Kempe, 2003). The discovery of similar nanobacteria-like particles from the stratosphere is discussed in Chapter 3.

The presence of amino acids in the meteorites has been recognised for over 40 years. In the Murchison meteorite, which is a carbonaceous chondrite that fell at Australia in 1969, more than 70 different types of amino acids including some that did not occur in terrestrial life were found (Cooper *et al.*, 2001). In the Orgueil meteorite, glycine and beta-alanine were found (Ehrenfreund *et al.*, 2001). The compositional analysis of these amino acids revealed that they were likely to have been synthesised from components such as hydrogen cyanide, which have been recently observed in comets Hale-Bopp and Hyakutake. This shows that the Orgueil meteorite was possibly derived from the comet, and if it is so, these amino acids might be break down products of remnants of cometary bacteria (such as Hoover's fossilised cyanobacteria).

Dust Particles and Microorganisms in Atmosphere

Dust particles that enter the Earth's atmosphere without melting (micrometeorites) are normally referred to as Brownlee particles or interplanetary dust particles (IDPs). Brownlee *et al.* (1976a) collected many IDPs from the stratosphere by using U-2 aircraft since 1974. He found some that have chondritic abundance (within a factor of 3) for the 12 most abundant elements, as well as some that do not. Their extraterrestrial nature was proved by the detection of solar flare tracks in mineral

grains (Bradley *et al.*, 1984) and the presence of the presolar grains as well as the large D/H enrichments (Zinner *et al.*, 1983). Brownlee classified these particles into several groups, which are discussed in Chapter 2.

While meteoritic dust particles have been identified in the atmosphere, microorganisms that might arrive within the dust have also been sought at altitudes free from terrestrial contamination. Although there were some reports of isolated microorganisms in 1960's and 1970's, these were criticised because of the primitive nature of the sterilization procedures. The newly invented cryogenic sampler used in Indian balloon-borne investigation from 2001 is capable of overcoming these problems. Identification of IDPs and the microorganisms from this experiment is discussed in Chapters 3 and 4.

1.8 Extremophiles

An extremophile is an organism that can survive in intolerably hostile or extreme environments. The study of extremophiles is particularly interesting to astrobiologists since their discovery points to the extraordinary adaptability of primitive life-forms which are capable of surviving in conditions similar to those known to exist on other planets, or in space.

At present, many extremophiles are categorised by degrees of tolerance to various hostile environments. Hyperthermophiles can grow in high temperature conditions, for example, the archaea *Pyrolobus fumarii* (Strain 121) survives at 121°C. Kashefi *et al.* (2003) showed the survival of Strain 121 at 130°C for 2 hours in the laboratory. Psychrophiles can live in extreme low temperature conditions such as the bacterium *Colwellia psychrerythraea* (Strain 34H) surviving at -2°C to -20°C in arctic wintertime sea ice (Junge *et al.*, 2004). Junge *et al.* (2006) also detected the survival of the same bacterium in the liquid nitrogen at -196°C. Halophiles can survive in extreme salinity such as the archaea *Haloarcula marismortui* surviving at 2-5M of NaCl. This halophile was discovered to produce a specialised protein, which protects from the

effect of salt (Paul *et al.*, 2008). Since the surface of Mars contains a high salt concentration, any microbes surviving on Mars may have to be similar to this terrestrial halophile.

Piezophiles can survive in extreme high pressure such as a microbe surviving at 130 Mpa. Sharma (2002) show the survival of *Shewanella oneidensis* and *Escherichia coli* at 1600 Mpa in the laboratory. A chemoautotroph gains its energy by oxidising inorganic chemicals such as *Thiobacillus neapolitanus* which oxidises sulfur to sulfuric acid. The bacterium *Deinococcus radiodurans* found within the cores of nuclear reactors can survive about 2000 times the dose of ionising radiation that would kill a human, making it the most radiation-resistant organism known (Secker *et al.*, 1994).

Such types of extremophiles are the best candidates for surviving in space. In 2001, the red rain phenomenon that occurred in India involved red-coloured unidentified microorganisms that fell with the rain over the Kerala. Louis *et al.* (2003) who collected a sample showed survival of these organisms at 300°C in the laboratory. Our study of red rain cells is discussed in Chapter 5.

CHAPTER 2

Techniques Used to Collect Cosmic Dust Particles

2.1 Space Collections

2.1.1 Cosmic Dust Detector

The *in situ* study of cosmic dust in space began with the non-recoverable cosmic dust detector of the Pioneer 8 mission in 1967. Since then, recoverable detectors have been flown on orbiting satellites. The craters of dust particles formed by their impact on the exposed surface of the collectors are analysed in the laboratory. This approach, however, yields little material because most of the dust particles impacting at high velocities (typically 20-30 km/s) are partially or totally destroyed. In laboratory simulation experiments using iron micrometre-sized projectiles impacting a metal target, it has been shown that particles with impacting velocity up to 13 km/s can survive (Dietzel *et al.*, 1972). From the contamination point of view, contaminants of orbital debris with their low velocities will blow to the side of the exposed surface or do not produce the craters, therefore they are distinguishable. They are also distinguished by their chemical signatures.

Skylab Mission

The first recoverable micrometeoroid collector (S-149) was deployed during the second manned Skylab missions in 1973 (apoapsis 442 km) and many micrometeoroid craters were reported (Hallgren and Hemenway, 1976a). By using the energy-dispersive X-ray analysis in a scanning electron microscope (SEM-EDX), most of the craters were found to be high in aluminium. Many of them were pure aluminium in their composition, and since the most solid-fuel rockets produce pure aluminium oxide spheres as exhaust, they were more likely to be contaminants. Hemenway (1976) then found new submicrometre craters containing the compositions of Mg, Si and Fe with ratios consistent with a chondritic meteorite.

An unrelated Skylab experiments (S-228) provided unexpected two additional micrometeoroid craters on its pure Al cover (30 μm and 110 μm). The smaller crater contained an iron-sulfur residue with minor amounts of nickel and magnesium, and

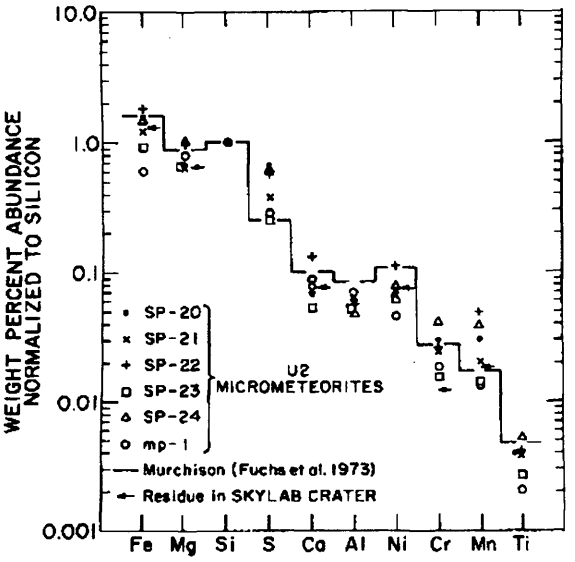

Figure 2-1: Elemental abundance ratio. Six chondritic aggregate micrometeorites collected with U2 aircraft and meteoroid residue found in a 110 μm diameter micrometeorite crater found on Skylab. The results are compared with the Murchison carbonaceous chondrite meteorite. (Brownlee *et al.*, 1982)

the larger crater contained a large quantity of meteoroid residue that very closely matched cosmic abundances for Fe, Mg, S, Si, Ca, Ni, Cr, and Mn (Brownlee *et al.*, 1974) **(Fig. 2-1)**.

Long Duration Exposure Facility (LDEF)

To overcome the partial or total destruction of the dust particles requires the collection of reasonable-sized (10 μm or more) particles. In order to do that it is necessary to collect the grains on a longer time scale. In 1984, LDEF was launched and orbited in a Low-Earth Orbit (LEO) at an altitude of 483 km for 5.7 years. The LDEF contained 57 individual experiment trays from many different investigation groups, and they were analysed after the recovery in 1990. See *et al.*, (1991) counted most of impact features found with the naked eye on the entire LDEF, which were approximately 35,000. The impact features on the different target materials such as the glass fabric cover and the Mylar foils were also investigated (Mandeville, 1991). In the case of the glass fibre cover, the damage consists of both brittle fibre fracture and fibre melting. The Mylar foil, which was located under the glass fabric cover, became very brittle and was badly damaged upon impact due to the long exposure to the UV irradiation.

Although the flux of dust particles detected by their craters was increased, the target materials were now in need for serious reconsideration.

Two complementary experiments followed. In 1992, the European Retrievable Carrier (EURECA) was launched and put into an orbit at an altitude of 508 km for 1 year. Another one called Geostationary Orbit Impact Detector (GORID) was launched in 1996 and orbited around LEO at an altitude of 600 km for 5.7 years. The cumulative impact flux distribution of EURECA was similar to that of LDEF (Wright *et al.*, 1995) and the flux of dust particles of GORID was also reasonably similar (Graps *et al.*, 2006). In every case, the number of well defined dust particles was counted.

2.1.2 Microdust Analysis from Comet

Vega 1 and 2, and Giotto Mission

Scientists have long been interested in investigating comets as solar system bodies. It is commonly assumed that they are pristine bodies which contain relatively unaltered material from the beginning of our solar system. Three missions were sent to study Halley's comet in 1986, Vega 1 and 2 by the Soviet Union and Giotto by the European Space Agency. Impact ionisation time-of-flight mass spectrometers were used for the dust analysis including the Particulate Impact Analyser (PIA) and the Dust Impact Mass Analyzer (PUMA). The bulk composition of Halley's dust contained 25% of refractory components (rich in H, C, N, and O) called CHON particles, 25% of the rock-forming components (such as Fe-poor Mg-silicates, Fe-sulfide, and rarely Fe metal) called ROCK particles, and 50% of mixed particles (Jessberger, 1999). The presence of high-temperature minerals like Mg-rich silicates and Fe-sulfides is evidence that equilibration at low temperature is a too slow a process to have affected these dust particles in their formation environment. Therefore it suggests that most of the particulate mineral materials were formed in high temperature regions close to the protosun and later transported outward to the comet-forming regions of the solar nebula.

Stardust Mission

Stardust spacecraft was launched in 1999 and encountered Comet Wild 2 in 2004. It passed through the comet's coma at speed of ~6.1 km/s, trapping microdust particles from the comet in an exposed silica aerogel. The samples were brought back in 2006 and analysed by SEM-EDX and time-of-flight mass spectrometry. First report showed the finding of very high-temperature minerals such as olivine and Mg components which were rich in Ca, Al, and Ti (Jeffs, 2006). In a recent report, the finding of similar mineral compositions from Halley's comet such as Fe-poor Mg-rich silicate (probably forsterite), Fe-sulfides and Fe-oxide haematite were shown (Bridges *et al.*, 2008). Haematite could be derived from the oxidation of magnetite which was precipitated from the low temperature hydrothermal fluids on a comet, showing the possible evidence for low temperature activity at some point in the history of the comet nucleus.

The mean refractory element abundance pattern of Wild 2 particles is similar to that in anhydrous, porous interplanetary dust particles (IDPs) and not to carbonaceous CI-group meteorites, suggesting that, if Wild 2 dust preserves the original composition of the solar nebula, the porous IDPs may best reflect the solar nebula abundances (Flynn, 2008).

Deep Impact Mission

Deep Impact is a NASA space probe launched in 2005 and the primary objective was to collide the impactor onto the comet Tempel 1 nucleus, excavating debris from the interior of the nucleus. The images and the infrared spectra were taken before and after the impact. The results show that the comet's outer layer is more dusty (1~100 μm fine particles) and much less icy than expected. The spectral analysis of preimpact material shows the emission of H_2O, CO_2 and organic features such as formaldehyde and methanol. However, postimpact spectra show very strong organic features despite the fact that changes in CO_2 relative to H_2O were small (A'Hearn *et al.*, 2005). This suggests that the strong C-H features arose from impact-vaporised organic materials that would not normally be vaporised in comets, or that the organic materials

vaporised by impact are normally released as CHON particles which cannot be observed in the preimpact spectra.

2.2 Atmospheric Collections

2.2.1 Earth's Atmosphere

The Earth's mesosphere and stratosphere **(Fig. 2-2)** are also suitable environments for the collection of interplanetary dust particles (IDPs). IDPs enter in the Earth's atmosphere at very high velocities but soon slow down under atmospheric friction to much lower settling velocities, for example 10 μm particles fall at ~ 1 cm per second at 30 km altitude (Kasten, 1968), and they can easily be collected by non-destructive techniques. Contamination from the troposphere decreases with altitude, therefore the higher the altitude of collection, the less likely to get any terrestrial particles.

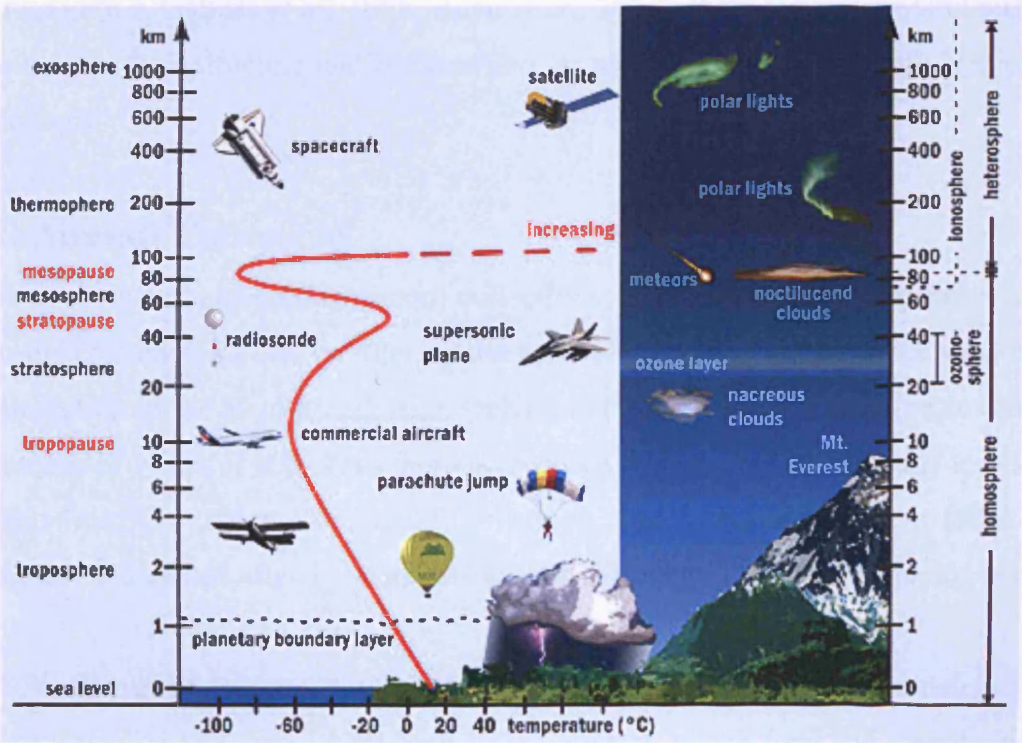

Figure 2-2: Typical diagram of Earth's atmosphere with the graph of altitude against temperature. ©kowoma

2.2.2 Rocket Collections

A typical sounding rocket can reach the mesosphere and the particles are collected by inertial impaction at below 100 km. Dust particles collected at altitudes above 120 km still have very high velocities and are mainly destroyed on impact. Since the first cosmic dust collector was flown into the mesosphere by the Venus Flytrap experiment in 1961 (Hemenway and Soberman, 1962), many have followed with improved contamination controls. The results were, however, doubted due to relatively high particle fluxes.

The most recent rocket collections have been targeted to collect particles at ~80 km in noctilucent clouds. Noctilucent clouds are thin clouds which are usually seen only at high latitudes and at the times when the sun is below the horizon. A number of attempts have been made to collect these particles by the groups like the Dusty Plasma Group and the MISU Middle Atmosphere Group. However, though there are many successful measurements of charged particles, presumably meteoric smoke in this region (e.g. Gelinas *et al.*, 1998; Rapp *et al.*, 2005), there is no successful attempt to determine their structure and composition, or any relation to the noctilucent cloud phenomena.

2.2.3 Aircraft Collections

There are two methods used in aircraft collections: either smashing the particles in the air to the collection surface or filtering the particles from the air. In either way, there is a limitation to the aircraft collection technique in that usually it must be conducted at altitudes of 20 km or less. Thus there is always a serious risk of collecting terrestrial aerosols from this region. The aircraft collection, which was started from 1958, was practically abandoned after 10 years due to this difficulty in the contamination control.

In 1974, Brownlee began a programme of aircraft collection again. He enlisted the help of one of NASA's U-2 ultra-high flying aircraft, which flew and stayed aloft at around 20 km for hours (Brownlee, 1976a). By exposing the glass plates coated with

sticky oil outside the aircraft, Brownlee managed to recover micron-sized and larger particles. Particles in the 3 μm to 35 μm size range were analysed for elemental abundances by using an energy-dispersive X-ray spectroscopy (EDX). About 90 percent of the particles in the range of 3 μm to 8 μm were aluminium oxide spheres (AOS) similar to those found from the solid-fuel rockets exhaust (Brownlee *et al.*, 1976b) **(Fig. 2-4)**. Of the particles did not have high aluminium content, over half were identified as extraterrestrial because of their closely matched elemental abundances to that of chondritic meteorites **(Fig. 2-3)** or minerals in carbonaceous chondritic meteorites.

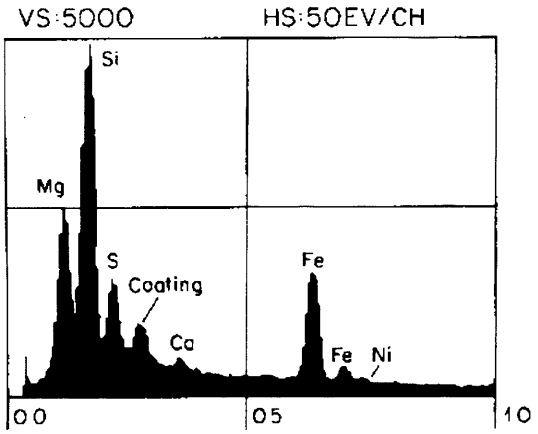

Figure 2-3: Typical spectrum of a chondritic meteorite as observed with a solid-state X-ray detector in an SEM operating at 20 kV. (Brownlee *et al.*, 1982)

After several attempts of aircraft collection, Brownlee *et al.* (1982) separated the collected particles into two main morphological groups. One group has porous, aggregate morphology **(Fig. 2-5)**, and the other group has a smooth morphology **(Fig. 2-6)**. By the elemental abundance, the particles can be classified into several groups (Brownlee, 1985). The chondritic group comprises particles which typically have chondritic abundances (within a factor of 3) for the 12 most abundant elements. Iron-Sulfur-Nickel-rich (FSN) group comprises particles made of smooth sulfide spheres composed of magnetite and pyrrhotite with Ni **(Fig. 2-7)**. The Calcium-Aluminium-Titanium-rich (CAT) group comprises particles in the form of a silicate sphere, depleted in Fe and enriched in Ca, Al, and Ti relative to chondritic abundance.

Magnesium-Iron-rich (mafic) group **(Fig. 2-9)** is a silicate mineral with Mg and Fe such as olivine and pyroxene in a crystal, whisker, ribbon or platelet form **(Fig. 2-10)**. Metal mound silicate (MMS) group is comprised of spheroidal silicates covered with small mounds of taenite (FeNi metal) **(Fig. 2-8)**. Infrared transmission spectroscopy has shown the presence of layer-lattice silicate (Sandford, 1983) and phyllosilicates probably a clay mineral (Fraundorf, 1980).

After Brownlee's success in aircraft collection, NASA has started collecting IDPs in the lower stratosphere since the beginning of 1981, employing U-2, ER-2 and WB-57 aircraft. These flights have ranged over most of the USA (as far north as Alaska) and Central America. The samples are distributed to many interested scientists. Recent researches on these collections have concentrated in finding presolar grains by using nanoSIMS.

Although the aircraft collection technique successfully found many interplanetary dust particles, the samples also contained particles of tropospheric origin. The aircraft, which was flying at 200 miles per hour, was however destructive for the fragile and smaller particles on impact. Due to effect the collections excluded the smaller fraction (<few μm) in the population of stratospheric dust.

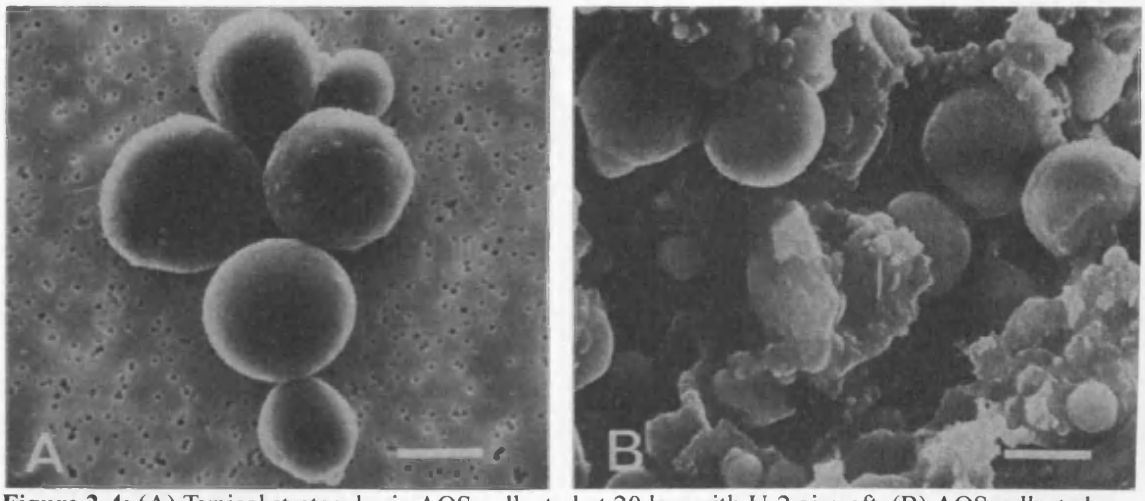

Figure 2-4: (A) Typical stratospheric AOS collected at 20 km with U-2 aircraft. (B) AOS collected from the smoke plume of a Titan III rocket. The spheres are from the rocket and the other material is filter paper ash. (scale bar - 5 μm) (Brownlee *et al.*, 1976b)

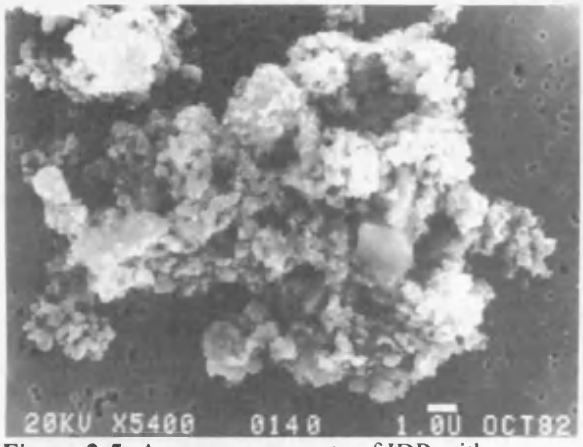

Figure 2-5: A porous aggregate of IDP with chondritic composition. (scale bar - 1 μm) (Brownlee, 1985)

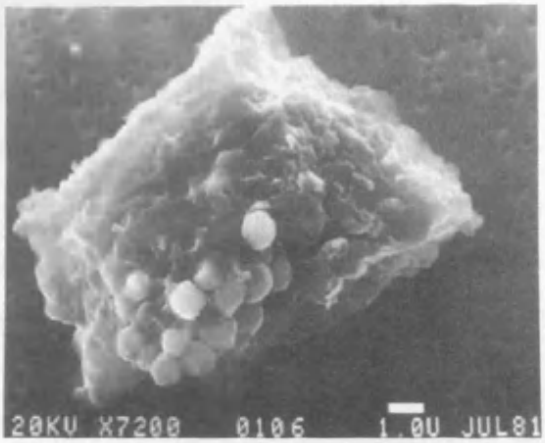

Figure 2-6: A smooth chondritic IDP with 1 μm grains of magnetite attached. (scale bar - 1 μm) (Brownlee, 1985)

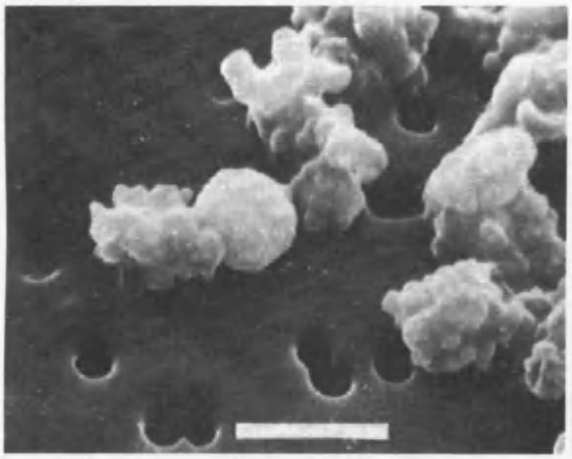

Figure 2-7: A rounded FSN (FeS + Ni) particle (centre) surrounded by chondritic aggregate material. (scale bar - 1 μm) (Brownlee *et al.*, 1982)

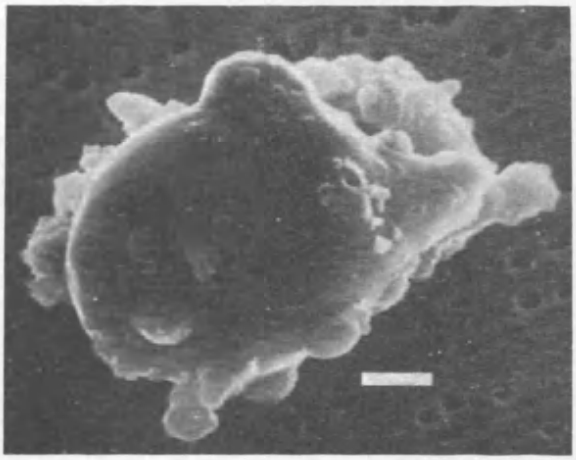

Figure 2-8: A glassy chondritic particle covered with Nickel-iron mounds. (scale bar - 1 μm) (Brownlee *et al.*, 1982)

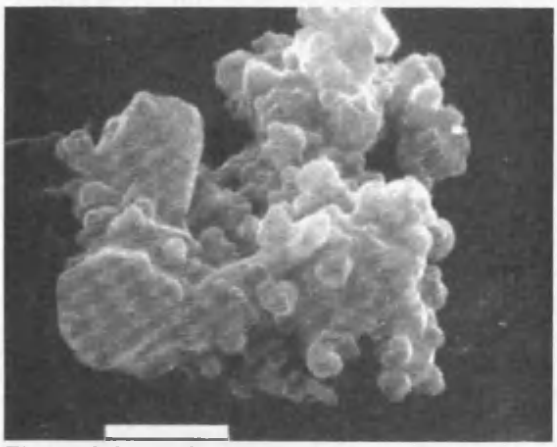

Figure 2-9: A micrometeorite consisting of chondritic aggregate material on the right and a smooth transparent olivine grain on the left. (scale bar - 1 μm) (Brownlee *et al.*, 1982)

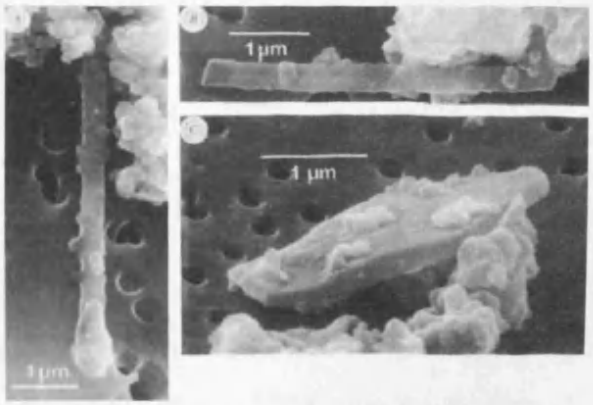

Figure 2-10: Collected at 20 km with U-2 aircraft. (A) An enstatite rod. (B) An enstatite ribbon. (C) An enstatite platelet. (Bradley *et al.*, 1983)

2.2.4 Balloon Collections

Balloon-borne collection techniques are thought to be best suited for dust collection in the stratosphere. They overcome the problem of contamination from the troposphere since it is able to ascend much higher than the 20 km aircraft altitudes, far into the upper stratosphere. It also can stay aloft in the stratosphere for a longer period of time increasing the flux of collected dust particles. The cost for carrying out experiments by this method is also reasonable.

Many different collectors were invented and tried out in the balloon collection techniques. In 1963 and 1964 during different meteor showers, many balloons were flown by Dudley Observatory using the Sesame collector (Hemenway *et al.*, 1967). It consisted of a rugged anodised aluminium box, with two cassettes each containing collecting slides. The box was placed on top of the balloon, and opened at around 35 km for 5 to 35 hours depending on the flights. The recovered particles in these flights were analysed by x-ray diffraction, and thirteen particles longer than 20 μm were found to be the extraterrestrial particles without crystalline structures. Electron-beam probe experiments had shown the presence of iron and found to be magnetic.

In 1970 a high-volume air-sampling system called the Vacuum Monster was flown (Brownlee and Hodge, 1973), which sampled 10^4 m^3 of air during two collection flights at 35 km. Elemental abundance analysis on the recovered particles showed the presence of eight extraterrestrial particles similar to chondritic particles, FSN particles and a Fe-Ni particle. This technique, however, used a large hydrazine rocket-fuelled air ejector pump, which ejected the air at 200 m s^{-1} to the target material, to collect the particles by inertial impaction. This actually did not constitute an improvement on the destructive nature of aircraft collection technique.

More ambitious collectors were tried out but were unsuccessful in finding cosmic particles, for example a collector used by Bhandari *et al.* (1968) and co-workers. It consisted of a 280 μm monofilament nylon fibre screen (10 m^2 size), which was suspended at 2 km below the balloon, and during its 8 hours exposure at 22 km, an

estimated 10^6 m^3 of ambient air was filtered. Analysis of the filter for particles after the flight, however, was unable to distinguish dust particles and it was suggested that most of the air blew around the screen-filter. Another example was the Magellan balloon experiment, which was designed to collect ≥50 μm particles (Wlochwicz *et al.*, 1976). A collector consisted of a large cone-shaped funnel with 40 m^2 aperture of an open end pointing upward, and suspended 300 m below a balloon. The larger particles were expected to simply fall into it and the smaller particles were expected not to roll down the sides of the funnel during its flight at 25 km. The main flight lasted 210 days, but unfortunately the collector was not recovered (Hallgren *et al.*, 1976b).

Since 1980's, the balloon collection technique was used mainly in noctilucent cloud studies (e.g. Miloshevich *et al.*, 1997). However in 2001, Indian Space Research Organisation launched a balloon carrying a prototype cryogenic sampler above Hydrabad in India for purpose of finding IDPs and the aerosols with the biological origin. Aseptic cylinders were taken up to 41 km and the air was sucked in by powerful cryopump. This technique was designed to collect the fragile fluffy particles in a gentle manner thus the smaller fractions of IDPs were obtainable. The non-destructive nature of this technique is also ideal for collecting the microbiological cells, which had been excluded in many other techniques.

In Chapter 3, we discuss the methods of 2001 balloon-borne experiment and the results of particles collected, which were compared with the IDPs and the cometary particles discovered from the previous studies. In Chapter 4, the investigation of biology from those samples is discussed.

CHAPTER 3

Studies of Dust Particles from Stratosphere

3.1 Introduction

3.1.1 General Introduction

Earth's atmosphere, especially the stratosphere and mesosphere, is the best location to study any extraterrestrial materials coming into Earth. It is known that about 20,000 tons of the interplanetary dust particles (IDPs) enter Earth's atmosphere per year (Love and Brownlee, 1993). Since the first study of such particles in atmosphere by the Venus Flytrap experiment in 1961, a significant number of experiments have followed using various techniques. The natures of IDPs collected have been thoroughly investigated, and an amazing correlation between them, meteorites and cometary dust particles has been found. Some of these particles contained pristine material going back before the formation of the solar system. Particles comprised of different refractory minerals can tell the history and the mechanisms of formation of their parental bodies.

The various techniques used for collecting particles, however, are not ideal for the collection of smaller fragile particles. Therefore a new design of collector was made, which can overcome this disadvantage. In this Chapter, we discuss a new type of balloon collection technique, and discuss the results of the IDPs collected. The analysis used scanning electron microscopy and energy-dispersive X-ray spectroscopy (SEM-EDX) to obtain high resolution images and the elemental compositions of the particles, which can be compared with results for other dust particles from the past research.

3.1.2 Balloon-borne Collection of Aerosols in Stratosphere

In the early hours on 21 January 2001, Indian Space Research Organisation (ISRO), Inter-University Centre for Astronomy and Astrophysics (IUCAA), Tata Institute of Fundamental Research (TIFR) and Centre for Astrobiology Cardiff University have collaborated to launch a balloon carrying the scientific payload from the National Scientific Balloon Facility of TIFR at Hyderabad, India (lat 17^0 28' 20", long 78^0 34' 48").

The payload included a cryosampler manifold with sixteen fully sterilised evacuated stainless steel cylinders (SS 304L) each with 0.35 litre capacity and capable of withstanding a pressure in the range of 10^{-6} mbar to 600 bar **(Fig 3-1)**. The sterilisation methods used and the technical specifications of the instrumentation are described elsewhere (Shayamlal *et al.*, 1996). During the flight the cylinders were immersed in liquid Ne, which were cooled to under 25°K, thus producing a powerful cryopump. In all more than a hundred STP litres of air (and aerosols) was sucked into each cylinder through fully sterilised valves fitted so as to be opened at pre-determined heights in the range of 20 – 41 km and frozen *in situ*. Four cylinders were opened at every different height. One cylinder from each height was brought back to Cardiff University and stored at -70°C until the laboratory analysis work began. The details of the probes we obtained are listed below:

Probe	Collection height range (Km)	Collected NTP volume (litres)
A	19.28 – 20.32	81.0
B	24.36 – 27.97	70.5
C	28.47 – 39.05	38.4
D	39.75 – 41.06	18.5

Table 3-1: The details of probes brought back to Cardiff University from India for analysis.

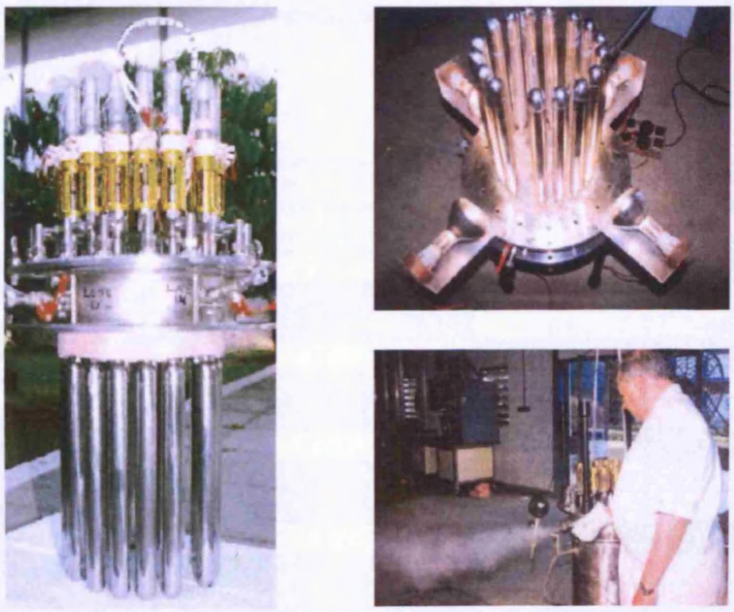

Figure 3-1: Evacuated and sterilised cryoprobes: Left: Assembled in a manifold ready for immersion in liquid Ne for launch. Top Right: Heat sterilisation under vacuum in an infrared setup at 140°C. Bottom Right: Steam sterilisation procedure.

3.1.3 Extraction of Aerosols from the Air Sample

After the cylinders were brought back to Cardiff, the aerosols in those probes were extracted aseptically in two procedures:

Procedure 1: From each of the 4 probes the air was passed in a sterile system in a laminar flow chamber sequentially through a 0.45 μm and a 0.22 μm micropore cellulose acetate filter (47 mm in diameter). 8 filters were thus obtained plus 2 different pore-size filters without air going through as the negative controls **(Table 3-2)**. These filters were stored at -70°C until further experiments.

Procedure 2: Following the completion of procedure 1, the cylinders were injected with sterile phosphate buffer pH7.3 solution, left for several hours on a shaker to dislodge particles adhered to the wall, and the liquid syringed out and passed sequentially through a 0.7 μm glass microfiber filter, a 0.45 μm and a 0.22 μm cellulose nitrate filter. The cylinders were then injected with sterile phosphate buffer pH7.3 solution with micro-sized glass beads to remove any remaining particles. The liquid was extracted same way as before. 24 filters were thus obtained plus 3 different filters without buffer injection as the negative controls **(Table 3-2)**. All the filters were stored at -70°C until further experiments. Some of these filters were sent to Sheffield University for analysis.

Probe	Procedure		Cellulose acetate filter (0.45 μm)	Cellulose acetate filter (0.22 μm)	Glass microfiber filter (0.7 μm)	Cellulose nitrate filter (0.45 μm)	Cellulose nitrate filter (0.22 μm)
A (~ 20 km)	Passing Air only		A1	A2			
	Wash with Phosphate buffer solution	GB			A3	A5	A7
		No GB			A4	A6	A8
B (~ 27 km)	Passing Air only		B1	B2			
	Wash with Phosphate buffer solution	GB			B3	B5	B7
		No GB			B4	B6	B8
C (~ 39 km)	Passing Air only		C1	C2			
	Wash with Phosphate buffer solution	GB			C3	C5	C7
		No GB			C4	C6	C8
D (~ 41 km)	Passing Air only		D1	D2			
	Wash with Phosphate buffer solution	GB			D3	D5	D7
		No GB			D4	D6	D8
Control	Unused filter		E1	E2	E3	E4	E5

Table 3-2: The code of the filters produced from four probes. GB = Shaken with glass beads.

3.1.4 Previous Study by SEM Analysis

Wallis and Al-Mufti *et al.* (2002) started with the analysis of dust particles as soon as the sample filters were obtained. 0.45 μm micropore filter at 41 km (D1) was aseptically cut into 25 mm^2 size pieces, which were then mounted onto aluminium stubs. The stubs were stabilised by gold sputter-coatings, and observed under the scanning electron microscopy (SEM - Philips XL-20) at 7 x 10^{-9} bar vacuum.

Wallis and Al-Mufti *et al.* (2002) had identified several interesting particles on the stubs. Figure 3-2 and 3-3 show 20 μm-sized cylinder with submicron rod particles. These particles were first thought to be the broken bits of diatoms. However, further analysis and spectroscopy were required. Particles which are analogous to Brownlee's IDPs were observed such as the fluffy aggregate particles **(Fig. 3-4)** and a crystalline IDP, fragile enough to break into two on the filter **(Fig. 3-5)**. The most interesting finding was those diverse spore-like particles, often in association with other materials **(Fig. 3-6)**. Figure 3-7 could represent another spore-like particle, but it has a similar morphology to those aluminium oxide spheres, therefore spectroscopic analysis was required.

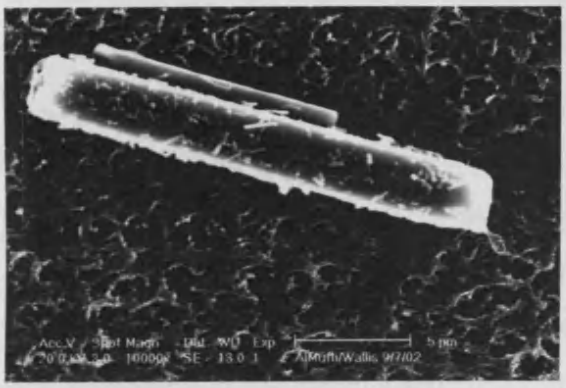

Figure 3-2: 20 μm cylinder with submicron rod particles.

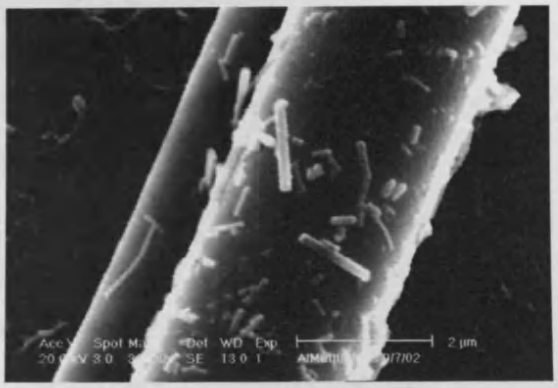

Figure 3-3: Enlarged image of submicron rod particles.

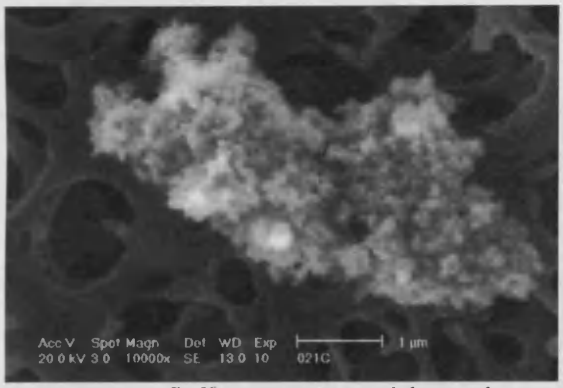

Figure 3-4: A fluffy aggregate particles analogous to Brownlee's IDP.

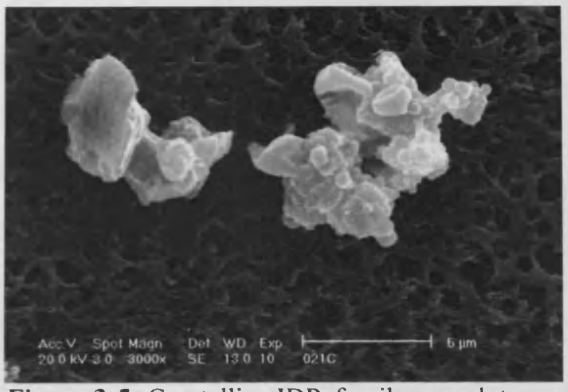

Figure 3-5: Crystalline IDP, fragile enough to break into two on the filter.

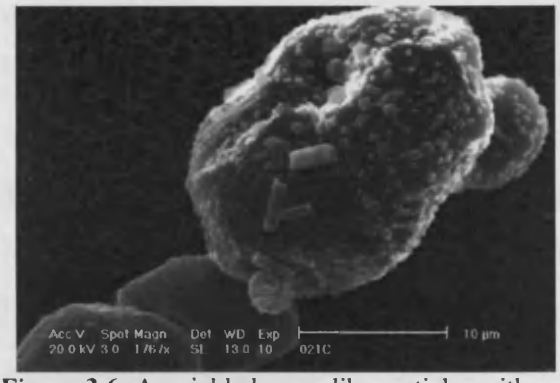

Figure 3.6: A wrinkled spore-like particles with spots and rods.

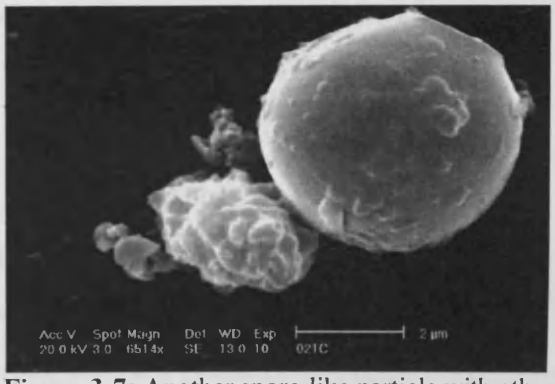

Figure 3-7: Another spore-like particle with other materials. Morphologically similar to AOS.

3.2 Materials & Methods

In this section, the procedures used for the analysis of stratospheric air sample are explained. Scanning Electron Microscopy (SEM) and Energy Dispersive X-ray analysis (EDX) were used (**Fig 3-8** Philips XL30 ESEM FEG). SEM is a type of electron microscope capable of producing high-resolution images of a sample surface. A SEM image has a characteristic three-dimensional appearance and is ideal for visualising the surface structure of the sample. X-rays, which are produced by the interaction of electrons with the sample, are measured by a detector within the SEM and analysed. Due to the fundamental principle of each element of the periodic table having unique electronic structures, a unique response to the incident electron beam can be detected by EDX.

In this study, EDX analyses were carried out under vacuum pressure of 7×10^{-9} bar. This method adopted was suited to imaging bacteria because bacterial cell walls would not collapse or explode during the exposure under the electron beam. An energy range of 10 – 20 keV of the electron beam was used. The lower voltage allowed the images to have high resolution, and the higher voltage increased the range of spectra and the count rates. The aperture of the gun used was 40 – 50 microns. Each spectrum was taken for an average of 10 seconds.

All preparation procedures were carried out in an aseptic environment with fully sterilised tools to avoid any cross-contamination. Negative controls were introduced to confirm the contamination-free procedures.

3.2.1 Preparation of Stubs with the Sample Filter for SEM Analysis

As in the previous study (Wallis and Al-Mufti *et al.*, 2002), a 0.45 μm acetate filter from 41 km (D1) was used. Approximately 25 mm^2 of the filter was aseptically cut using a sterile scalpel blade. An aluminium stub (12 mm in diameter) was sequentially washed in 90% ethanol for 5 minutes and in running distilled water for 5 minutes to remove the excess ethanol. The surface of the stub was dried by 'Dust Off' (Falcon),

and a circular carbon tape (12 mm in diameter) was placed on the stub. The sample filter was then attached to the stub, followed by gold sputter-coating at 40mA to stabilize. A new acetate filter (E1) was also cut and attached to the stub as a negative control.

3.2.2 Preparation of Stubs with Silicon Wafer containing Electrostatically and Vibrationally transferred Aerosols from the Sample Filter

An aluminium stub was washed with ethanol and distilled water and dried as before. The carbon tape was cut into small square-sized pieces (0.2~0.3cm) to take care of the smaller size of silicon wafer, which can increase the detection of anything outside the wafer by EDX. The 4mm^2 silicon wafer was then carefully attached on top. From here, two different procedures were carried out **(Fig. 3-9)**.

Procedure 1: Electrostatic Particle Transfer

The stub with wafer was first gold sputter-coated to increase the electrical conductivity. An approximately 25 mm^2 of 0.7 μm glass microfiber filter from 41 km (D3) was aseptically cut by a sterile scalpel blade. Then it was placed upside down on the gold-coated silicon wafer so that the particles trapped side were touching the surface of wafer. The particles were electrostatically transferred to the silica wafer by attaching a 9 volt battery. The negative end of the battery was attached to the bottom of the stub, and the positive end was attached to the nearby sink. After 15 minutes, the sample filter was removed and the stub was gold coated again at 40mA.

Procedure 2: Vibrational Particle Transfer

0.7 μm glass microfiber filters from 41 km (D3 and D4) and a 0.45 μm cellulose nitrate filter from 39 km (C5) were used. An approximately 25 mm^2 of the filter was aseptically cut by a sterile scalpel blade. It was then placed upside down on the non-gold coated silicon wafer. The aerosols were transferred to the silica wafer by tapping

the stub holder very gently. After 15 minutes, the filter was removed and the stub was goal coated at 40mA.

To increase the probability of finding aerosols, two stubs were prepared for each sample filters in both procedures. The removed filters were attached to the other sterilised stubs and kept as the positive controls. The original filters (E3 and E4) were also subjected to the same procedures as the negative controls. The original silicon wafer was also kept as a negative control. From both procedures, a total of 19 stubs were thus obtained **(Table 3-3)**.

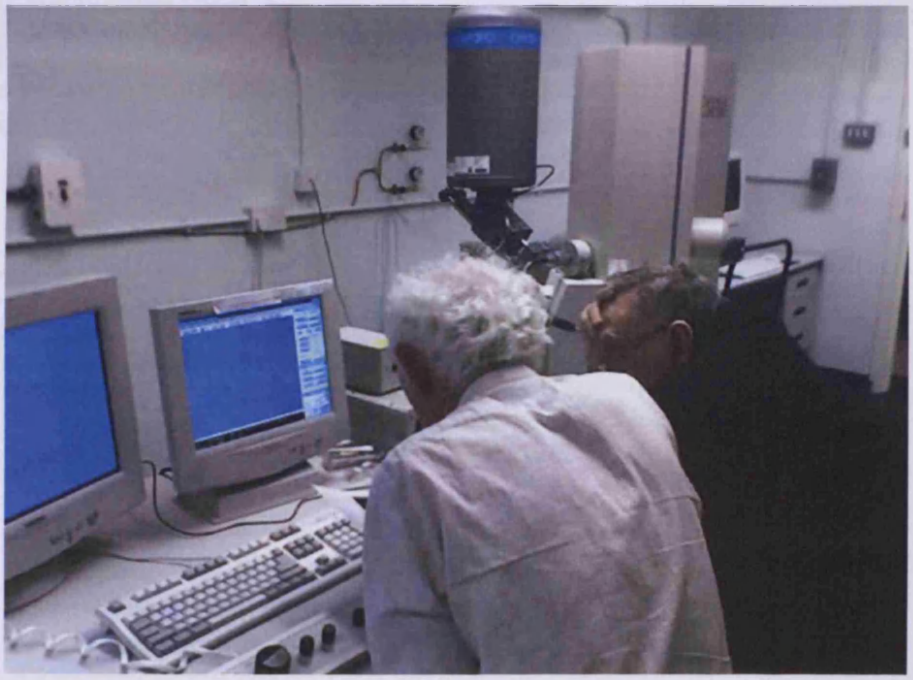

Figure 3-8: SEM-EDX used in Earth Science Faculty, Cardiff University (Philips XL30 ESEM FEG). Dr. Wallis (left) and Dr. Al-Mufti (right) investigating the stratospheric IDPs.

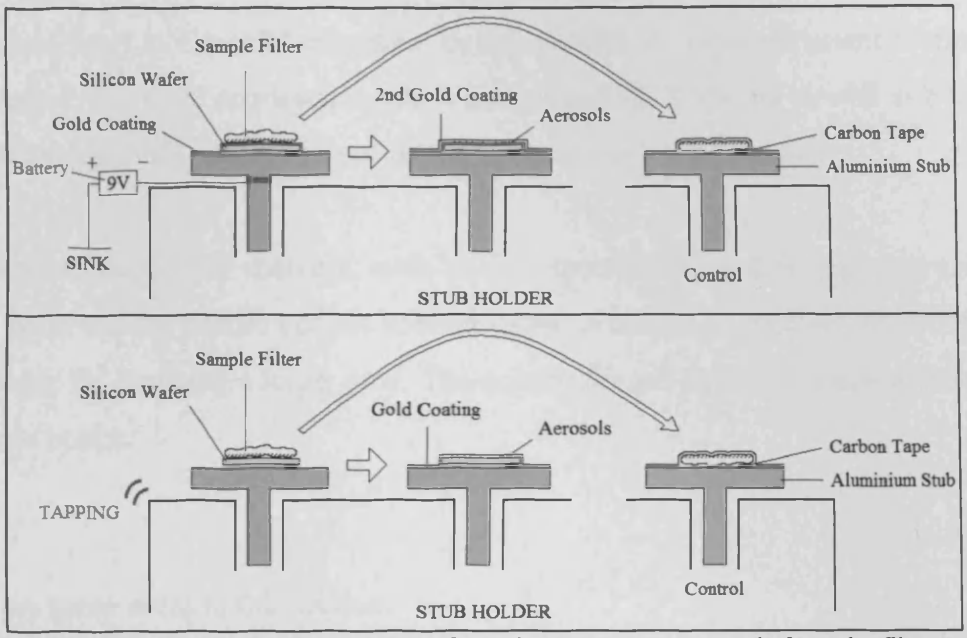

Figure 3-9: Diagram showing the Particle Transfer techniques. Top: Aerosols from the filter were electrostatically transferred to silicon wafer by using 9V battery. Bottom: Aerosols from the filter were transferred by tapping the stub holder to give some vibrational effect.

Sample Filter	Transfer Methods	Sample Filter after transfer (+ve control)	Silicon Wafer with transferred Aerosols	–ve Control
	Silicon wafer only			Stub Q
D3	**Vibrational**	Stub A	Stub C	**E3** Stub R
		Stub B	Stub D	
	Electrostatic	Stub E	Stub G	
		Stub F	Stub H	
D4	**Vibrational**	Stub I	Stub K	
		Stub J	Stub L	
	Electrostatic			
C5	**Vibrational**	Stub M	Stub O	**E4** Stub S
		Stub N	Stub P	
	Electrostatic			

Table 3-3: 19 stubs prepared from the particle transfer methods. **D3** – 0.7 µm glass microfiber filter from Phosphate buffer plus glass beads washout of 41 km probe; **D4** – 0.7 µm glass microfiber filter from Phosphate buffer washout of 41 km probe; **C5** – 0.45 µm cellulose nitrate filter from Phosphate buffer plus glass beads washout of 39 km probe; **E3** – Original 0.7 µm glass microfiber filter; **E4** – Original 0.45 µm cellulose nitrate filter.

3.3 Results

All the SEM and EDX data of identified aerosol particles are archived at the Centre for Astrobiology in Cardiff University. In this section, the most important findings are summarised. They are displayed in SEM images and EDX spectra as well as a table of quantitative analysis of elements of the aerosols **(Table 3-4, 3-5 and 3-6)**.

The images contain the markers, such as S1 (spectrum 1) and S2 (spectrum 2) etc, which point out the position of the spectra taken. It can be a single dot shown by + or a rectangle for scanning a larger area. The colour of each marker is same as that in the spectrum image.

There are some notes to this section:

Note 1: The spectra were taken in optimum conditions (high vacuum pressure – 7 × 10^{-9} bar, close working distance – 10 mm, high accelerating voltage – 10~20 kV) for the most precise readings. The backscattered X-rays come from an area of order 1 μm in size of the target (http://www.tsl-oim.com/applications/vip.cfm).

Note 2: The quantity of element is written in percentage of total weight.

Note 3: In sample D1, quantity of carbon and oxygen are uncertain since part of the signal can be picked up from the background acetate filter.

Note 4: In sample D3, D4 and C5, quantity of silicon is uncertain since signal can be picked up from the background silicon wafer.

Note 5: If the spectrum was taken at the edge of the sample filter or silicon wafer, part of the aluminium signal may be from the stub. (e.g. D3-103H)

Note 6: In Table 3-4 and 3-5, the stubs were gold coated therefore the quantity of Ag was excluded by EDX.

Note 7: In Table 3-6, the stubs were gold-palladium coated therefore Ag and Pd spectra were excluded by EDX.

3.3.1 Aerosols found in D1 (0.45 μm acetate filter, probe from 41 km)

Confirmation of 'ROCK' particles:

D1-404: Composite of ~0.1 μm 'grape'-like particles (**Fig. 3-10**). It is very fragile and seems to have fallen apart on the filter. It has a very high Fe (~22.29%) and O (~28.57%). Content is therefore possibly an aggregate of magnetite grains. It also contains P (~6.71%), Na (~5.26%), Ca (~2.28%) and Cl (~1.18%).

D1-512: 7~8 μm smooth crystalline particle with low porosity (**Fig. 3-11**). It looks like an aggregate of particles melted by sudden increase in temperature. Its composition shows enrichment in Cr (~8.69%), Fe (~42.67%) and O (~28.96%) supporting the subhedral iron chromite, which is normally found in a layered ultramafic rock (lacks Si). Therefore those small grains attached could be magnetite or FeNi metals, Ni (~0.54%).

D1-519: 9~10 μm porous particle (**Fig. 3-12**). It is based with silicate (~3.46%) and contains rich Ca (~19.81%) minerals. It has a signature of mafic group, such as olivine, pyroxene and spinel. The presence of high Fe (~2.56%) and Al (~2.31%) compare to Mg (~0.98%) shows possibly a mixture of fayalite or ferrosite with spinel.

D1-901: 3~4 μm aggregate of platelet-like particles (**Fig. 3-13**). It contains relatively higher abundance of Mg (~3.25%) and Fe (~9.53%) than *D1-519*. However, a particle at S1 contains higher Al (~10.07%), Si (~22.75%) and O (~44.66%) showing possible mixture with pyrophyllite.

D1-908: 4~5 μm particle with very low porosity (**Fig. 3-14**). It contains both FSN and MMS group features. It is mainly Fe (~8.15%) and Si (~2.87%) with some S (~0.57%) and Ni (~1.41%). The particle seems to originally consisted of a mixture of small grains which underwent some condensation process.

D1-912: 9~10 μm classic high-temperature lattice silicate mineral particle **(Fig. 3-15)**. Its composition is enriching in Si (~10.97%), Al (~10.72%) and O (~34.71%) showing the presence of clay mineral. It has an embedded 0.5 × 2 μm Ti-rich crystal. This crystal contains ~4.07% of Ti which is about 60-70% of Si. It is presumably a high temperature condensate of titanium nitride indicating its parental body to be cometary such as Tempel 1 (known to contain clay material).

Confirmation of particles with the whiskers:

D1-213: A single glassy whisker with 1 μm in diameter and 5 μm in length **(Fig. 3-16)**. This is similar to the one found earlier (Wallis and Al-Mufti *et al.*, 2002). While no quantitative analysis was obtained, the spectrum shows enrichment in Si and O indicating that it is probably a siliceous fibre. It also has a submicron organic rod attached.

D1-410: 4~8 μm particle covered with many submicron crystals **(Fig. 3-17)**. It contains high Fe (~32.98%) and O (~29.58%) indicating the presence of magnetite. It has an embedded glassy whisker, which is 0.3~0.5 μm in diameter and 4~5 μm in length. Since it contains Si (~12.38%) and Fe (~18.24%), it can be a ferrosilite having a whisker growth pattern.

Confirmation of 'CHON' particles

D1-517: 3~8 μm cluster of fluffy smoke-like particles **(Fig. 2-18)**. Its composition shows high C (~58.70%), O (~14.90%) and N (~20.44%). Apart from having a low amount of salt, it is a classic example of a 'CHON' particle.

D1-702: 9~10 μm near-spherical particle with continent-like coating **(Fig. 3-19)**. The carbon fraction of particle is slightly lower (~62.47%) compared to that of the background (~86.27%) but as the C (particle)/C (background) ratio is very high compare to others, there is no doubt of highly carbonaceous and also oxidised (~11.77%) material. The coating has Na

(~7.75%) and Cl (~4.62%) as well as some S (~1.00%), Si (~0.43%) and K (~0.30) but in less than stoichiometric amounts. It could be an acritarch with fossilised fragella, however, it requires a further testing for confirmation of the biological origin.

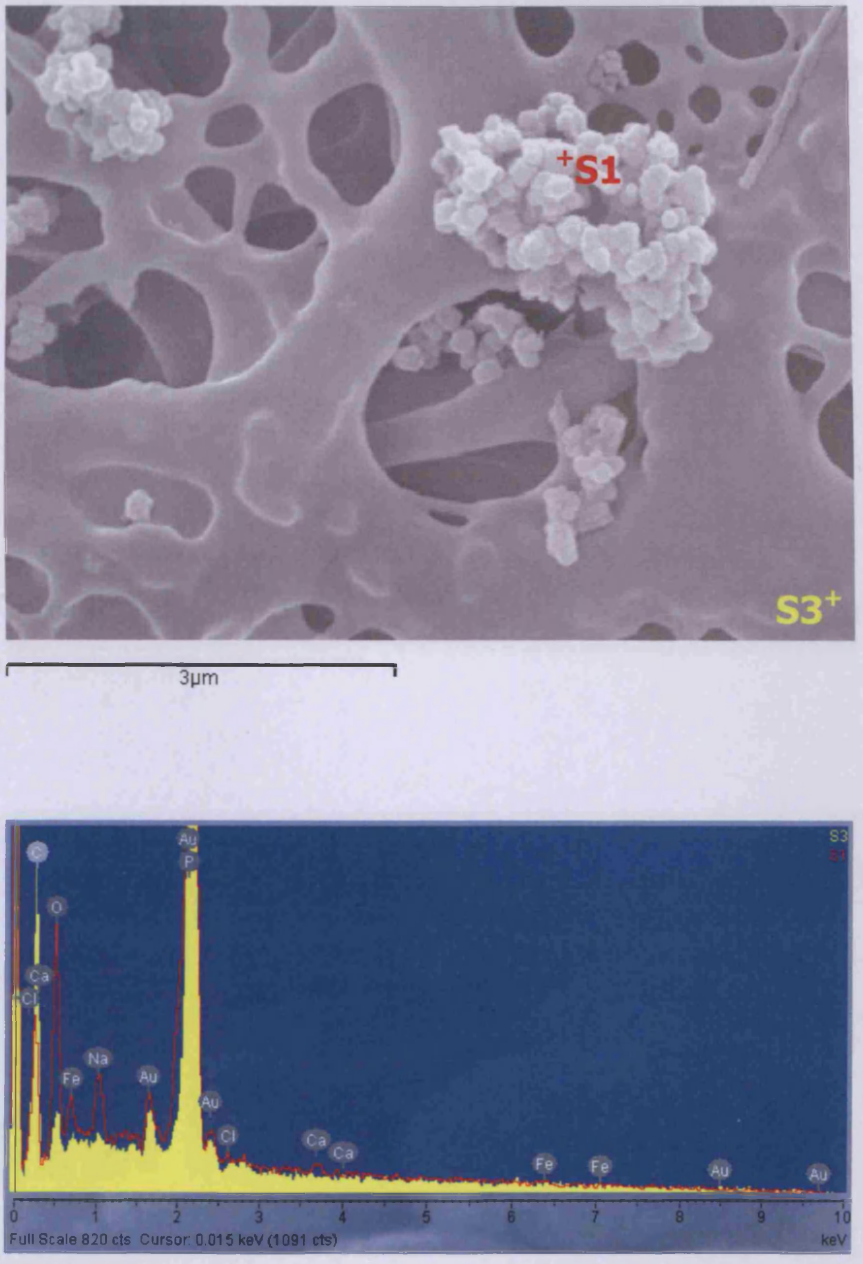

Figure 3-10: D1-404 sample from 41 km on 0.45 µm acetate filter.
Top: SEM image showing a Composite of ~0.1 µm 'grape'-like particles. Bottom: Spectrum showing the sign of magnetite. (red – S1, yellow – background spectrum S3)
(The methods for sample preparation and taking images are described in section 3.2)

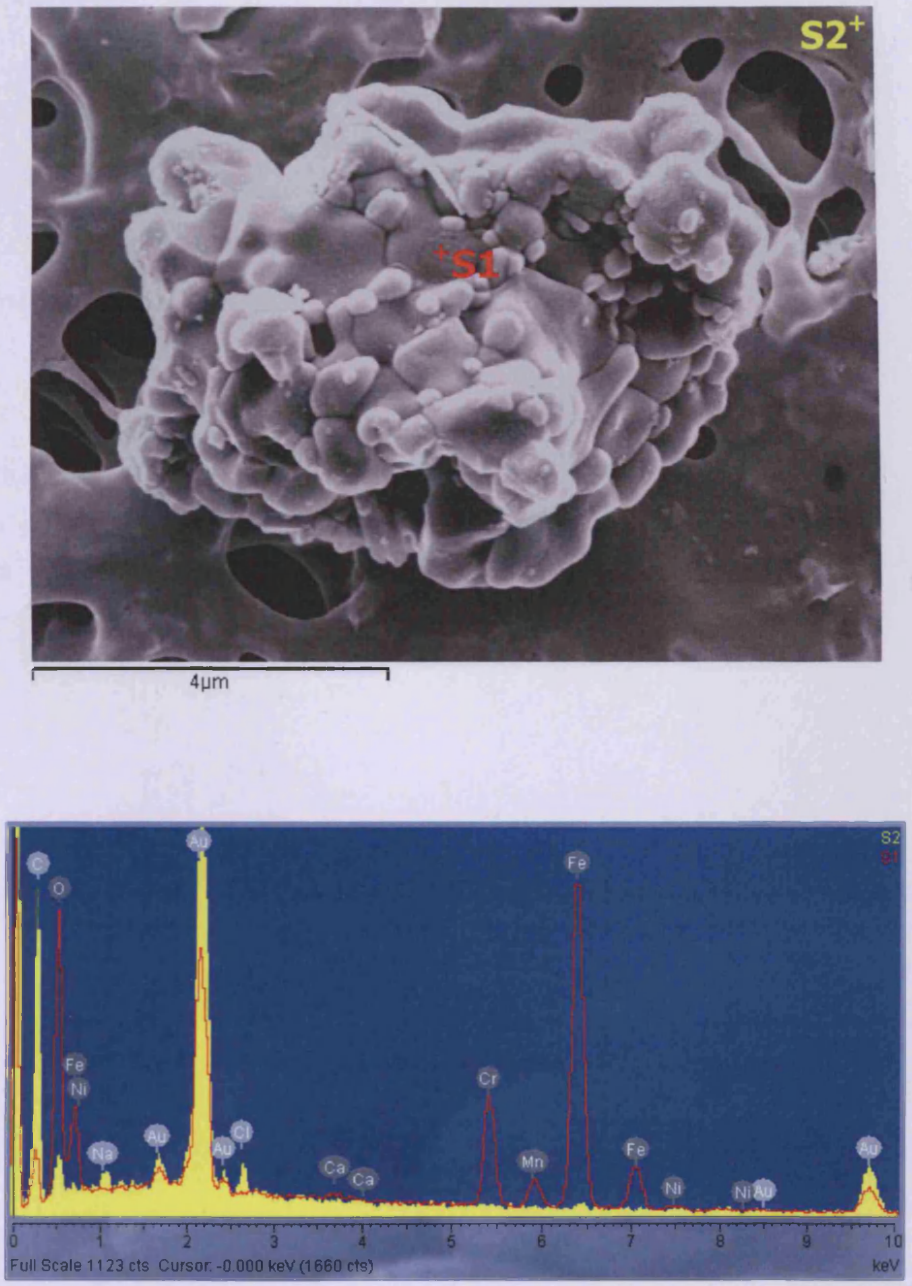

Figure 3-11: D1-512 sample from 41 km on 0.45 µm acetate filter.
Top: SEM image showing a 7~8 µm smooth crystalline particle with low porousity and has many submicron grains attached. Bottom: Spectrum showing the 'ROCK' components of subhedral chromite (S1) and magnetite (possibly grains). (red – S1, yellow – background spectrum S2)
(The methods for sample preparation and taking images are described in section 3.2)

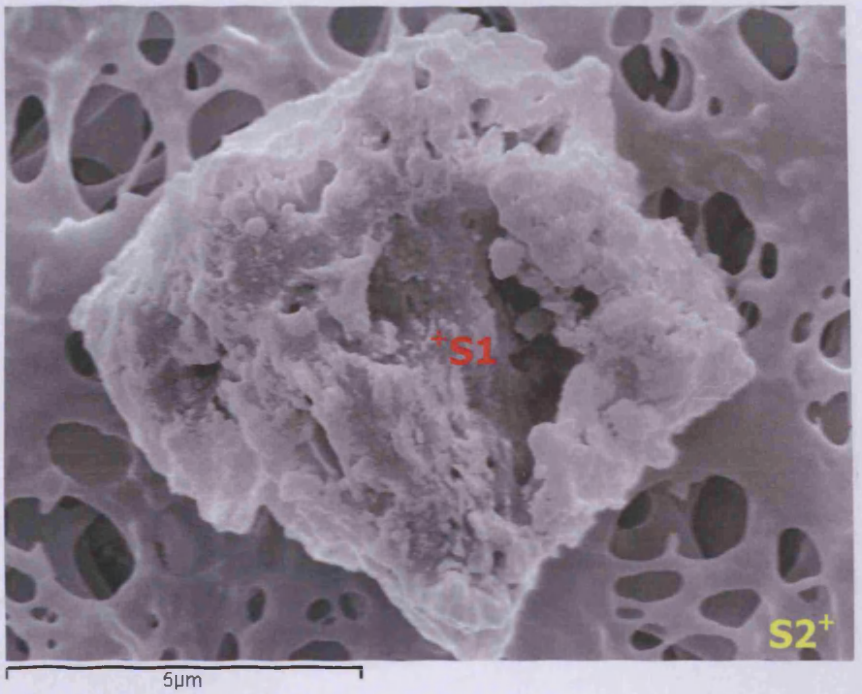

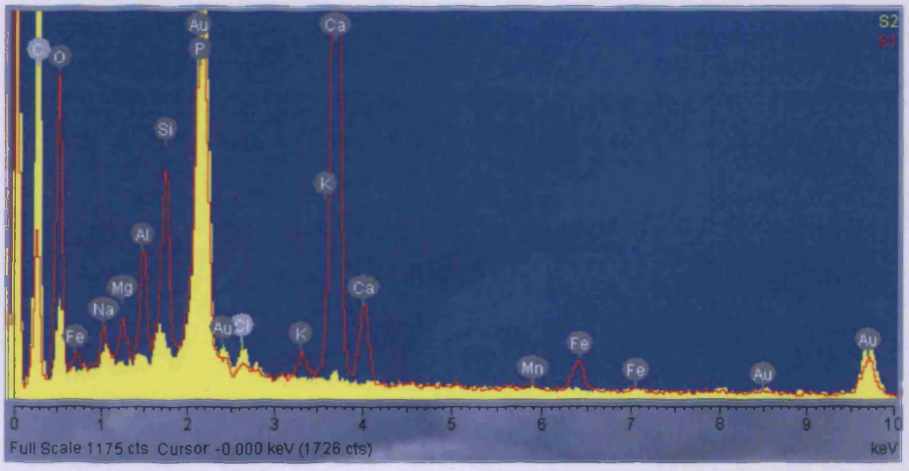

Figure 3-12: D1-519 sample from 41 km on 0.45 µm acetate filter.
Top: SEM image showing a 9~10 µm porous particle. Bottom: Spectrum showing the 'ROCK' components of spinel with fayalite or ferrosilite. (red – S1, yellow – background spectrum S2)
(The methods for sample preparation and taking images are described in section 3.2)

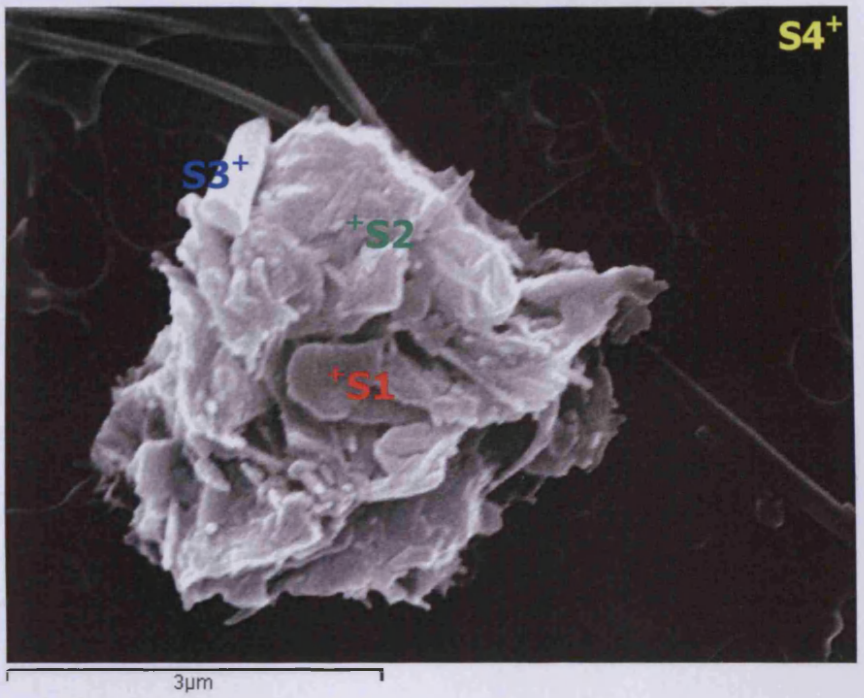

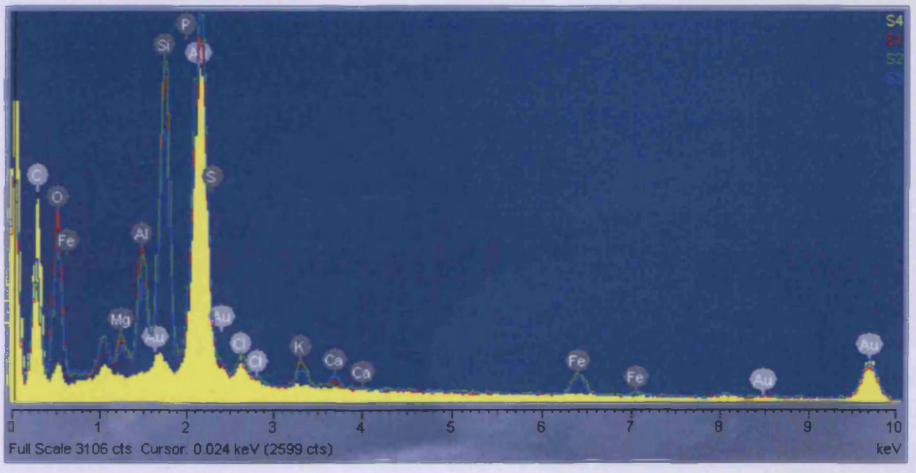

Figure 3-13: D1-901 sample from 41 km on 0.45 µm acetate filter.
Top: SEM image showing a 3~4 µm aggregate of platelet-like particles. Bottom: Spectrum showing the 'ROCK' components with possibly pyrophyllite. (red – S1, green – S2, blue – S3, yellow – background spectrum S4)
(The methods for sample preparation and taking images are described in section 3.2)

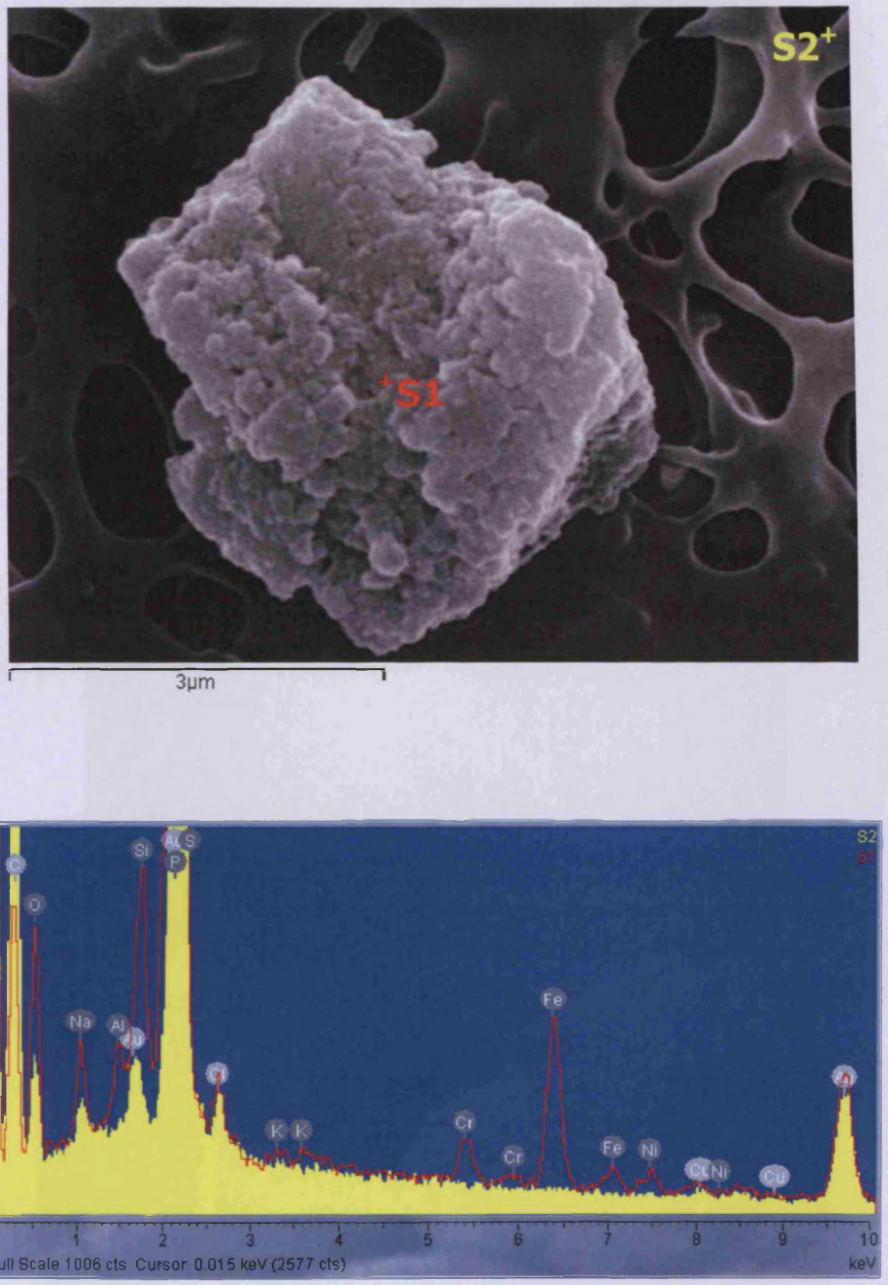

Figure 3-14: D1-908 sample from 41 km on 0.45 µm acetate filter.
Top: SEM image showing a 4~5 µm particle with very low porosity. Bottom: Spectrum showing both FSN and MMS group features. (red – S1, yellow – background spectrum S2)
(The methods for sample preparation and taking images are described in section 3.2)

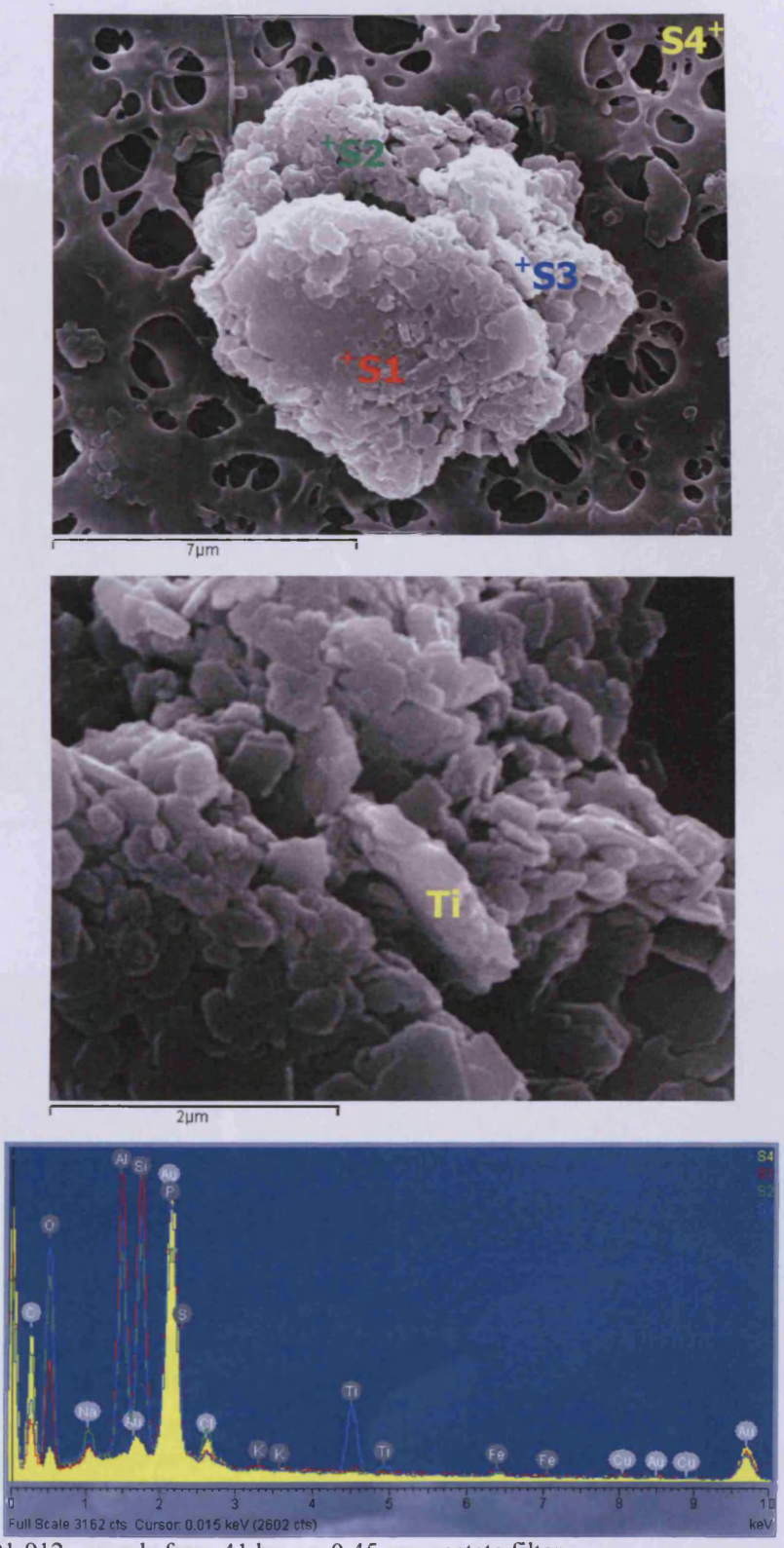

Figure 3-15: D1-912 sample from 41 km on 0.45 µm acetate filter.
Top: SEM image showing a 9~10 µm high-temp lattice silicate mineral particle. Middle: Enlarged image showing a Ti crystal embedded. Bottom: Spectrum confirming a Ti crystal and the presence of clay minerals. (red – S1, green – S2, blue – S3, yellow – background spectrum S4)
(The methods for sample preparation and taking images are described in section 3.2)

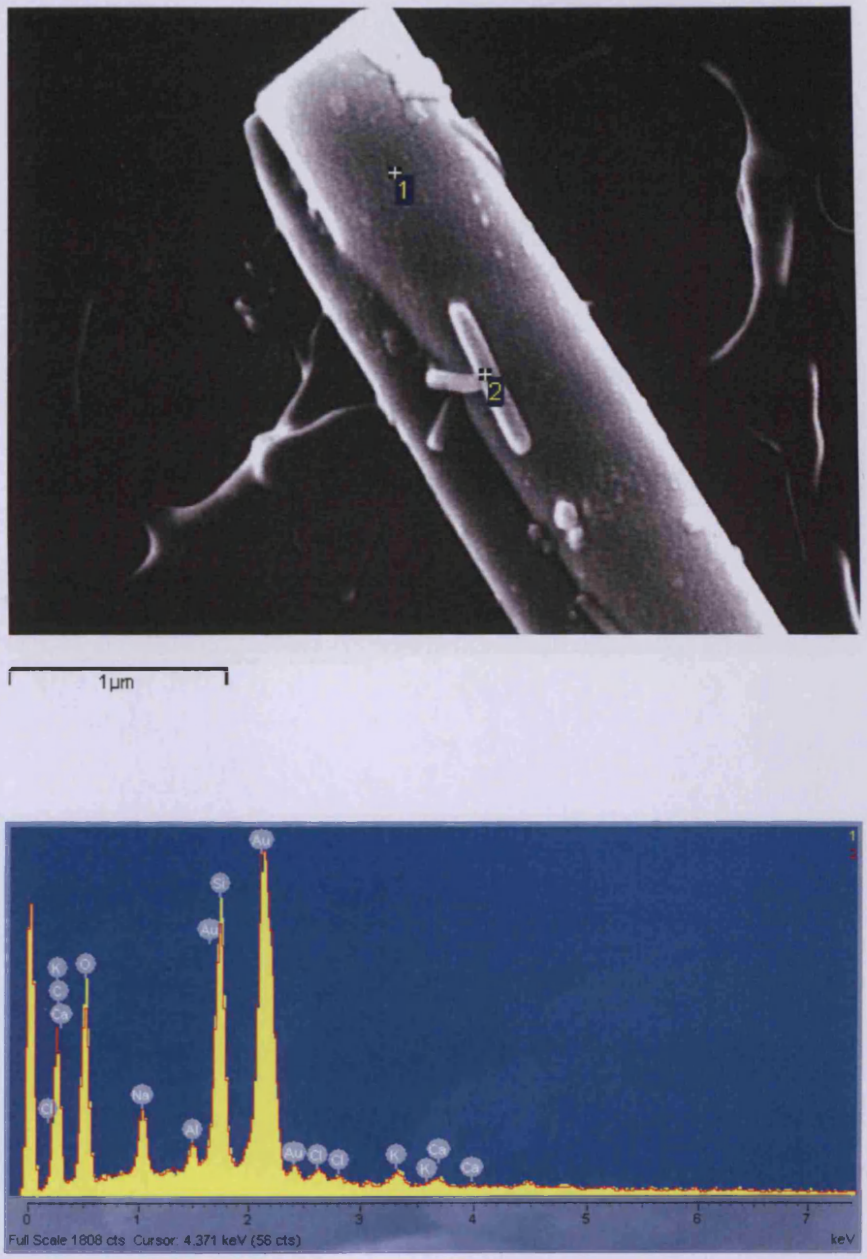

Figure 3-16: D1-213 sample from 41 km on 0.45 µm acetate filter.
Top: SEM image showing a single siliceous fibre (1) with the submicron organic rods (2) attached.
Bottom: Spectrum showing SiO_2 of fibre and C of rod. (yellow – 1, red – 2)
(The methods for sample preparation and taking images are described in section 3.2)

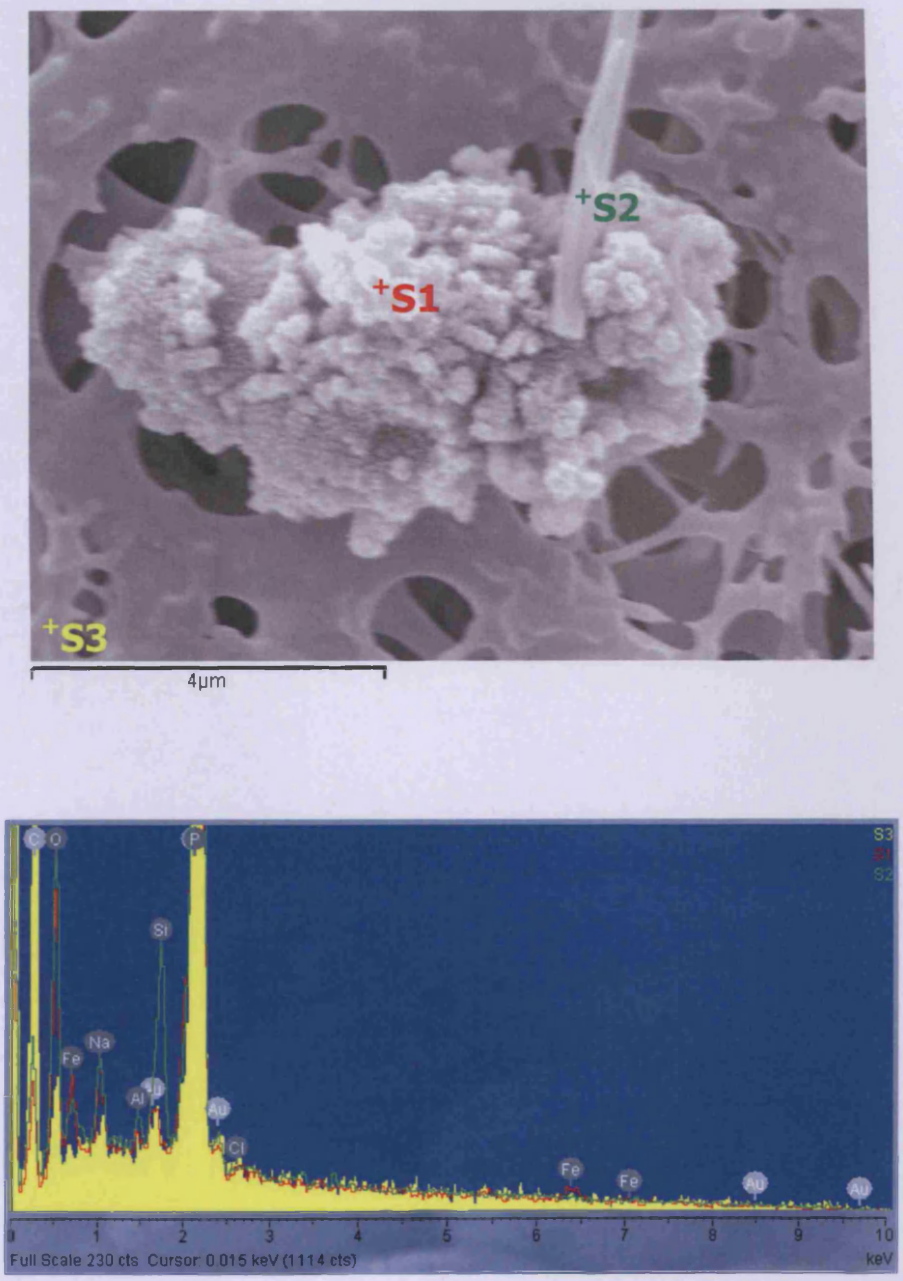

Figure 3-17: D1-410 sample from 41 km on 0.45 µm acetate filter.
Top: SEM image showing a 4~8 µm particle with many submicron crystals attached. It also has an embedded glassy whisker (S2). Bottom: Spectrum showing the 'ROCK' components of magnetite and the whisker made out of ferrosilite. (red – S1, green – S2, yellow – background spectrum S3)
(The methods for sample preparation and taking images are described in section 3.2)

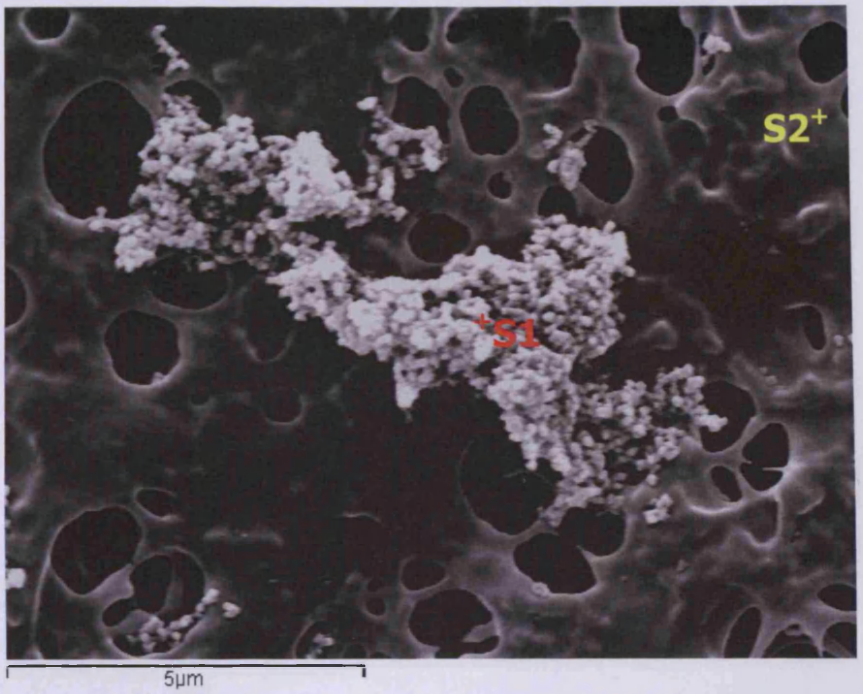

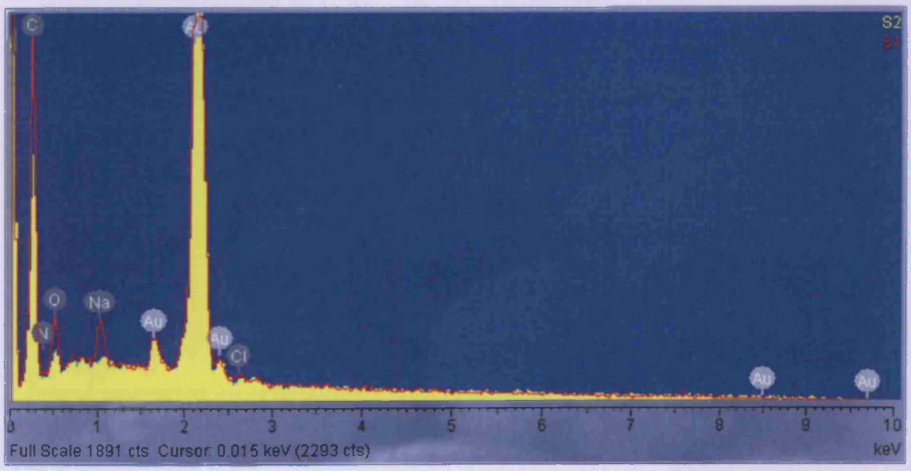

Figure 3-18: D1-517 sample from 41 km on 0.45 µm acetate filter.
Top: SEM image showing a 3~8 µm cluster of fluffy smoke-like particles. Bottom: Spectrum showing the 'CHON' components. (red – S1, yellow – background spectrum S2)
(The methods for sample preparation and taking images are described in section 3.2)

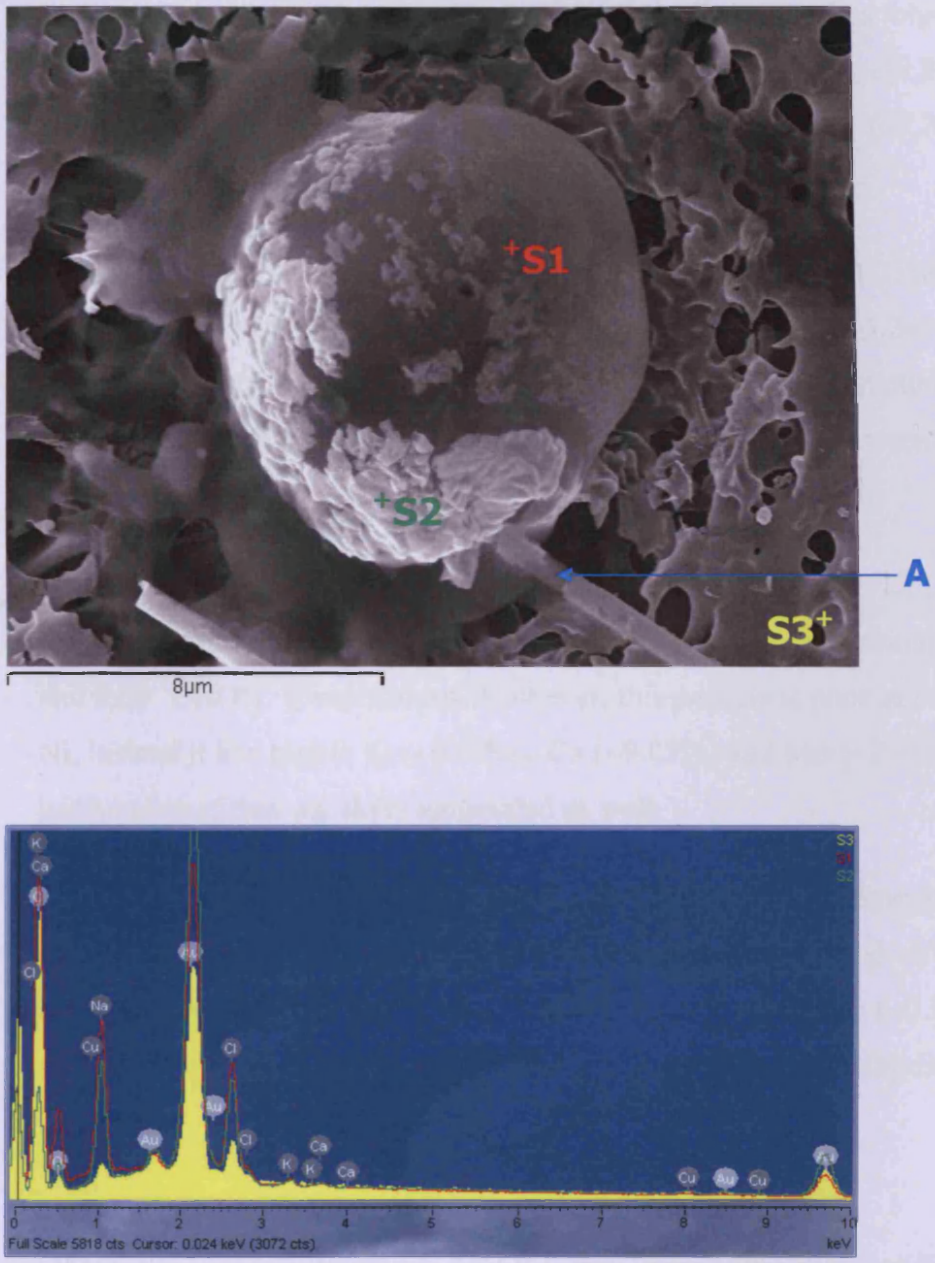

Figure 3-19: D1-702 sample from 41 km on 0.45 µm acetate filter.
Top: SEM image showing a 9~10 µm near-spherical particle (S1) with continent-like coating (S2). There are number of whiskers (A). Bottom: Spectrum showing the organic composition (particle) and the minerals from coating. (red – S1, green – S2, yellow – background spectrum S3)
(The methods for sample preparation and taking images are described in section 3.2)

3.3.2 Vibrationally Transferred Aerosols found in D3

(0.7 μm glass microfiber filter, probe from 41 km washed with buffer and glass beads)

Confirmation of mixture of 'CHON' and 'ROCK' particles:

D3-202C: 3~5 μm particle with very low porosity **(Fig. 3-20)**. It has high C (~23.17%) and Si (~48.90%). It also has Al (~4.39%) and O (~19.24%) showing possible presence of clay minerals. Pure Ti-crystal (~3.20%) might be embedded as *D1-912*.

D3-208C: 20~25 μm carbonaceous particle **(Fig. 3-21)**. It has C (~21.27%), O (~33.16) and P (~4.69%). It has high Fe (~23.20%) with Ni (~3.24%). It is an intimately mixed product of 'CHON' particle with small mounds of FeNi metal such as MMS group. It has number of thin strands of whiskers embedded.

D3-209C: ~20 μm carbonaceous crystalline particle **(Fig. 3-22)**. It has C (~22.14%), O (~40.61) and P (~4.53%). It is similar to D3-208C in morphologically and their 'CHON' compositions. However, this particle is poor in Fe and Ni, instead it has higher Si (~9.59%), Ca (~9.05%) and Mn (~2.91%). It has number of thin whiskers embedded as well.

D3-210C: 5~6 μm smooth crystalline particle **(Fig. 3-23)**. It is carbonaceous (~31.97%) particle with high O (~37.71%) and P (~4.65%). It also includes a relative amount of Si (~5.89%), Fe (~3.12%), Mg (~0.37%) and Al (1.89%), which can be a mafic group of spinel with fayalite or ferrosilite.

Confirmation of 'CHON' particle:

D3-110D: Inhomogeneous combinations of ~0.1 μm 'grape'-like particles and a stem-like material **(Fig. 3-24)**. It has a 'grape'-like morphology as found in D1-404 but with 'stem' that is rich in Ca (~9.43%). The particles are rich in C (~30.84%) and O (~22.96%). The combination of Ca, C and O can also suggest $CaCO_3$, as if this particle has been exposed to a watery environment.

3.3.3 Electrostatically Transferred Aerosols found in D3

(0.7 μm glass microfiber filter, probe from 41 km washed with buffer and glass beads)

Confirmation of possible biological particle:

D3-302H: 5~6 μm spherical carbonaceous particle (**Fig. 3-25**). It has the high compositions of C (~64.05%), N (~10.07%) and O (~14.76%). It has a thin transparent skin peeled off at some parts, which looks very similar to the coccoidal microfossil found in Orgueil meteorite (**Fig. 3-38**: Hoover, 2006).

Confirmation of nano-particles: They are also discussed in Sommer *et al.*, 2004.

D3-103H: An aggregate of 0.5~1 μm particles (**Fig. 3-26**). It is enriched in C (~26.87%), N (~28.37%) and O (~12.17%) with the minerals such as P (~9.37%) and Ca (~17.11%). They have nanobacterial morphology but are enrichment in minerals. Al is detected but it is an overlap reading from the Al stub in background.

D3-104H: An aggregate of 0.3~1 μm particles (**Fig. 3-27**). Closer look of these particles show the nanobacterial morphology. The crack in the particle is a very common event to the nanobacteria in vitro (Sommer *et al.*, 2003) and in vivo (Khullar *et al.*, 2004). It is rich in C (~41.93%) and N (~12.29%). Instead of oxygen, it has F (~13.46%). There is some uncertainty on the quantitative analysis since the particles were so small (over the limit of detecting every possible element with full quantity). By looking at what we got, these particles also could be fluorocarbon.

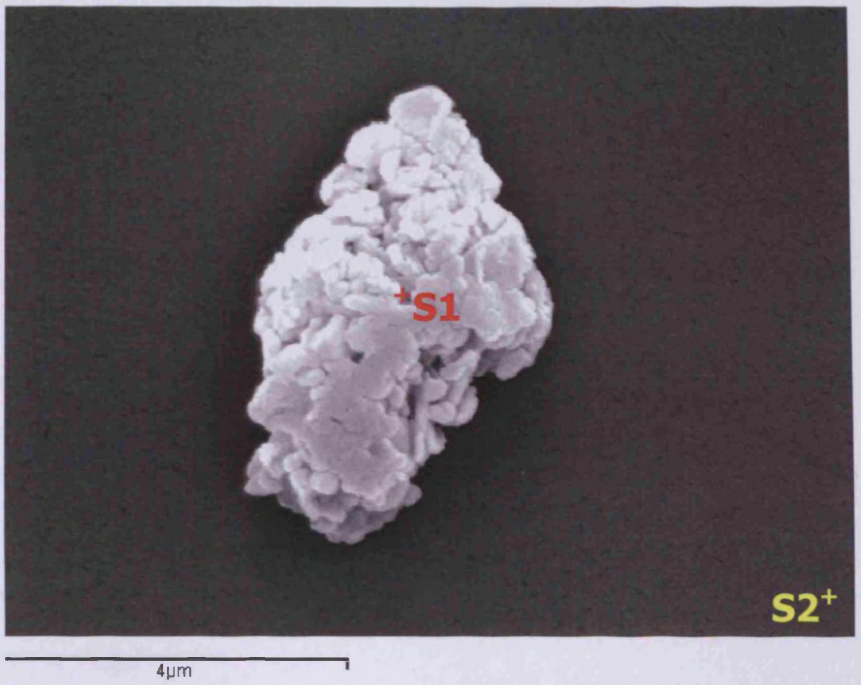

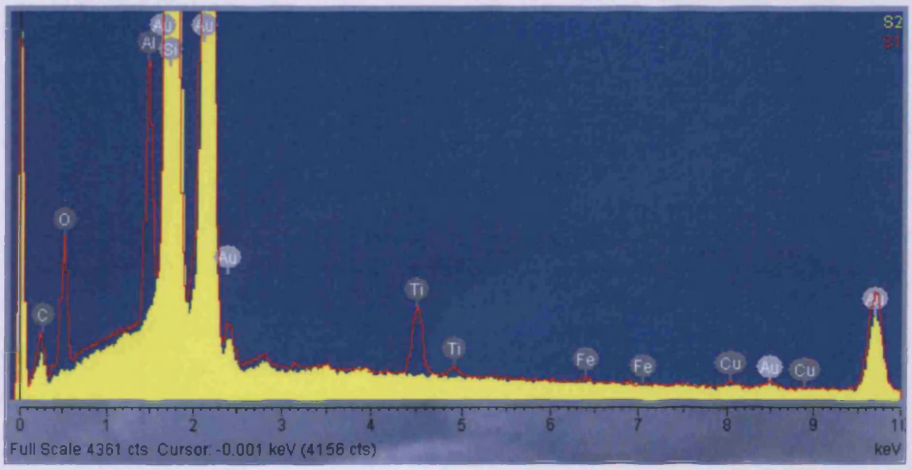

Figure 3-20: D3-202C sample from 41 km on silicon wafer.
Top: SEM image showing a 3~5 µm particle with very low porosity. Bottom: Spectrum showing both 'CHON' components and the 'ROCK' components from several possible sources. Pure Ti-crystal might be embedded as *D1-912*. (red – S1, yellow – background spectrum S2)
(The methods for sample preparation and taking images are described in section 3.2)

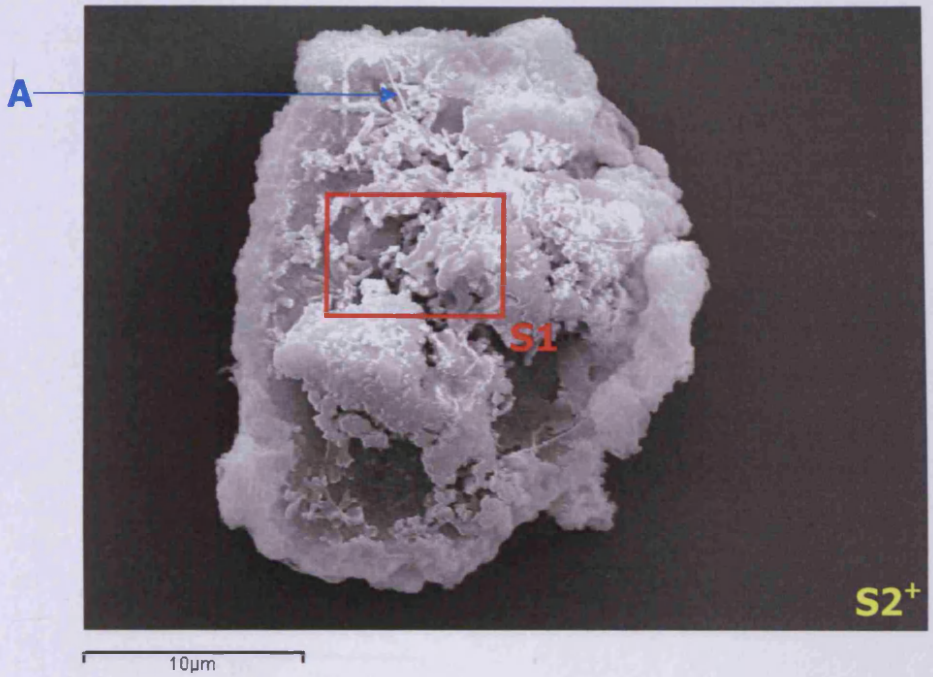

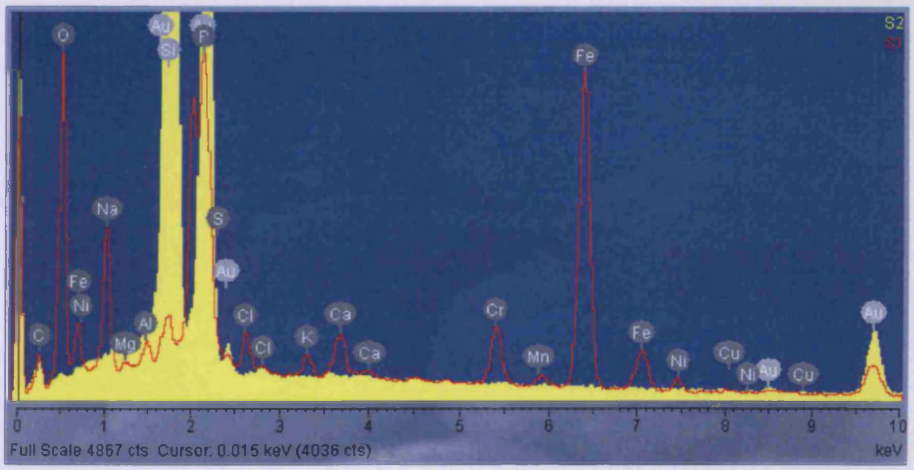

Figure 3-21: D3-208C sample from 41 km on silicon wafer.
Top: SEM image showing a 20~25 µm carbonaceous particle with number of thin whiskers embedded (A). Bottom: Spectrum showing 'CHON' particle with small mounds of FeNi metals. (red – S1, yellow – background spectrum S2)
(The methods for sample preparation and taking images are described in section 3.2)

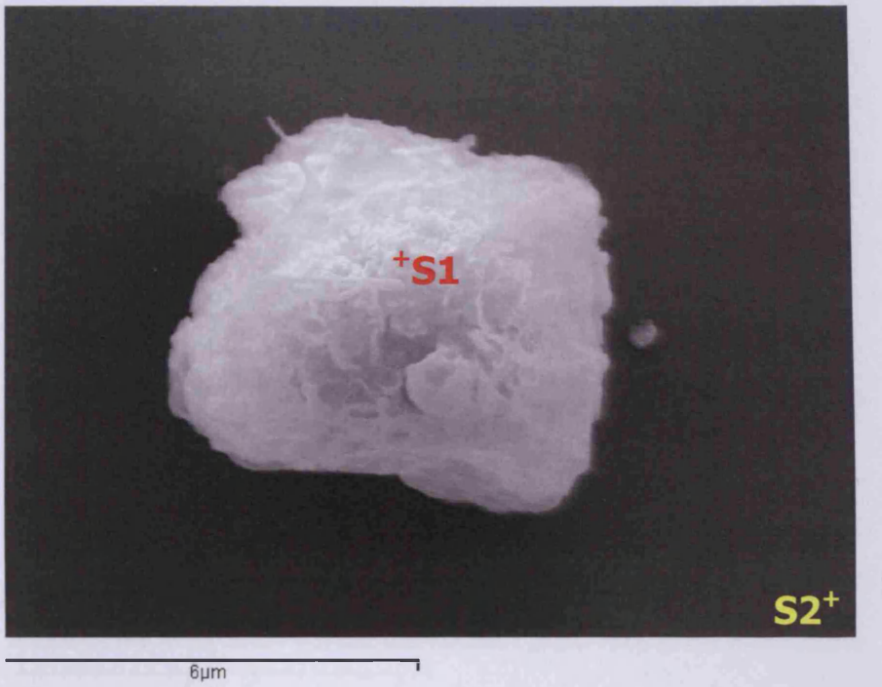

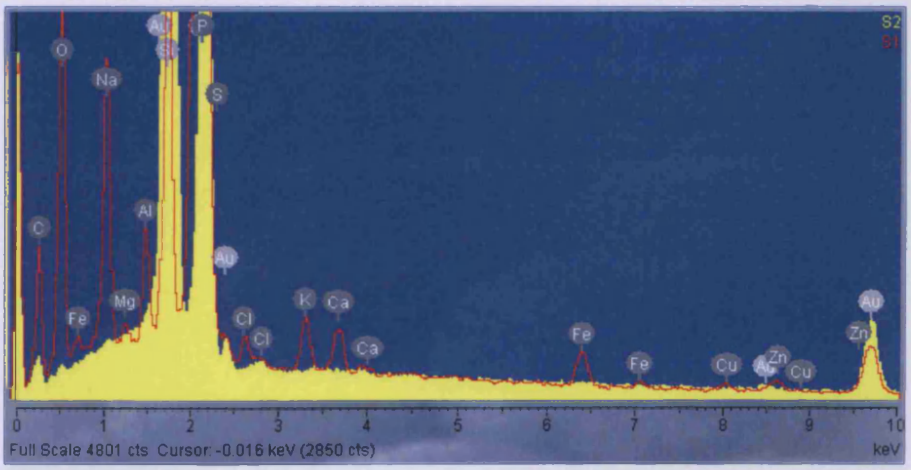

Figure 3-23: D3-210C sample from 41 km on silicon wafer.
Top: SEM image showing a 5~6 µm carbonaceous smooth crystalline particle. Bottom: Spectrum showing both 'CHON' and 'ROCK' components, which are spinel with fayalite or ferrosilite. (red – S1, yellow – background spectrum S2)
(The methods for sample preparation and taking images are described in section 3.2)

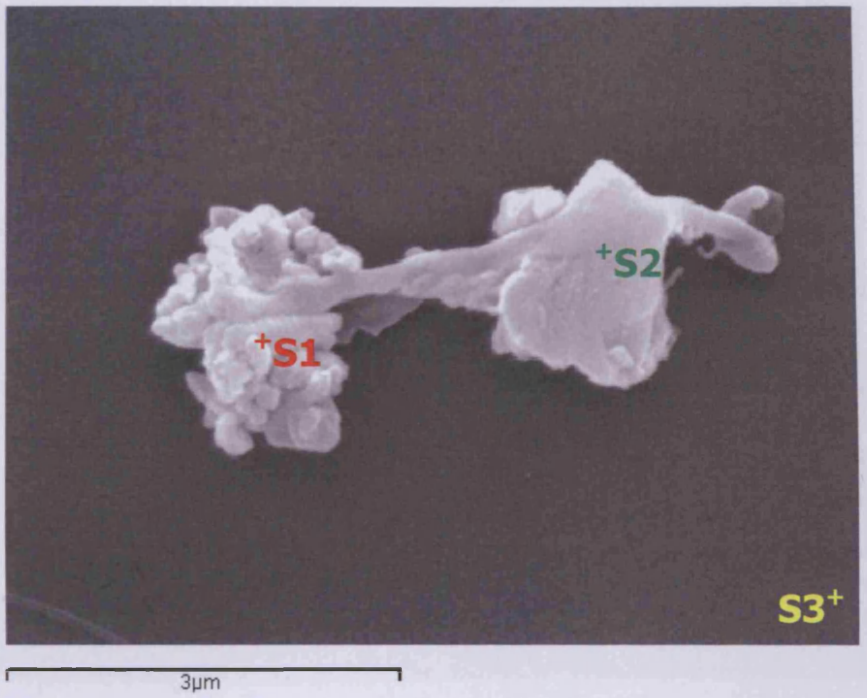

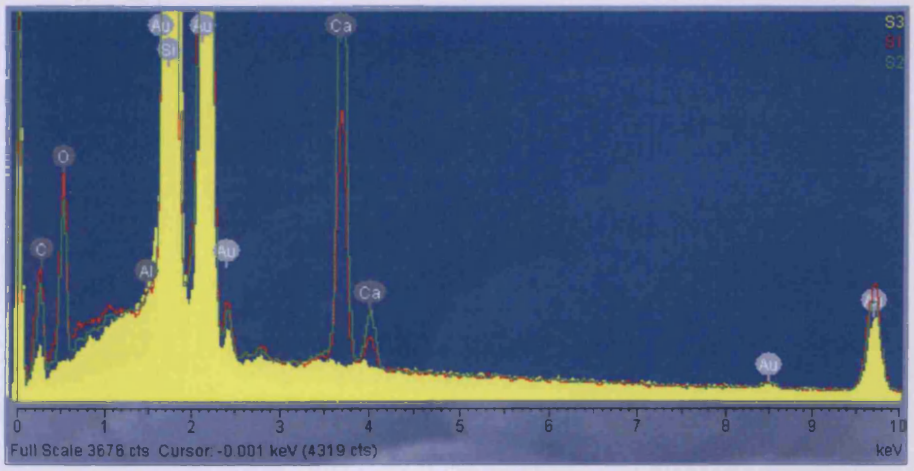

Figure 3-24: D3-110D sample from 41 km on silicon wafer.
Top: SEM image showing the inhomogeneous combinations of ~0.1 µm 'grape'-like particles (S1) and a stem-like material (S2). Bottom: Spectrum showing the 'CHON' components from the 'grapes' and Ca from the 'stem'. (red – S1, green – S2, yellow – background spectrum S3)
(The methods for sample preparation and taking images are described in section 3.2)

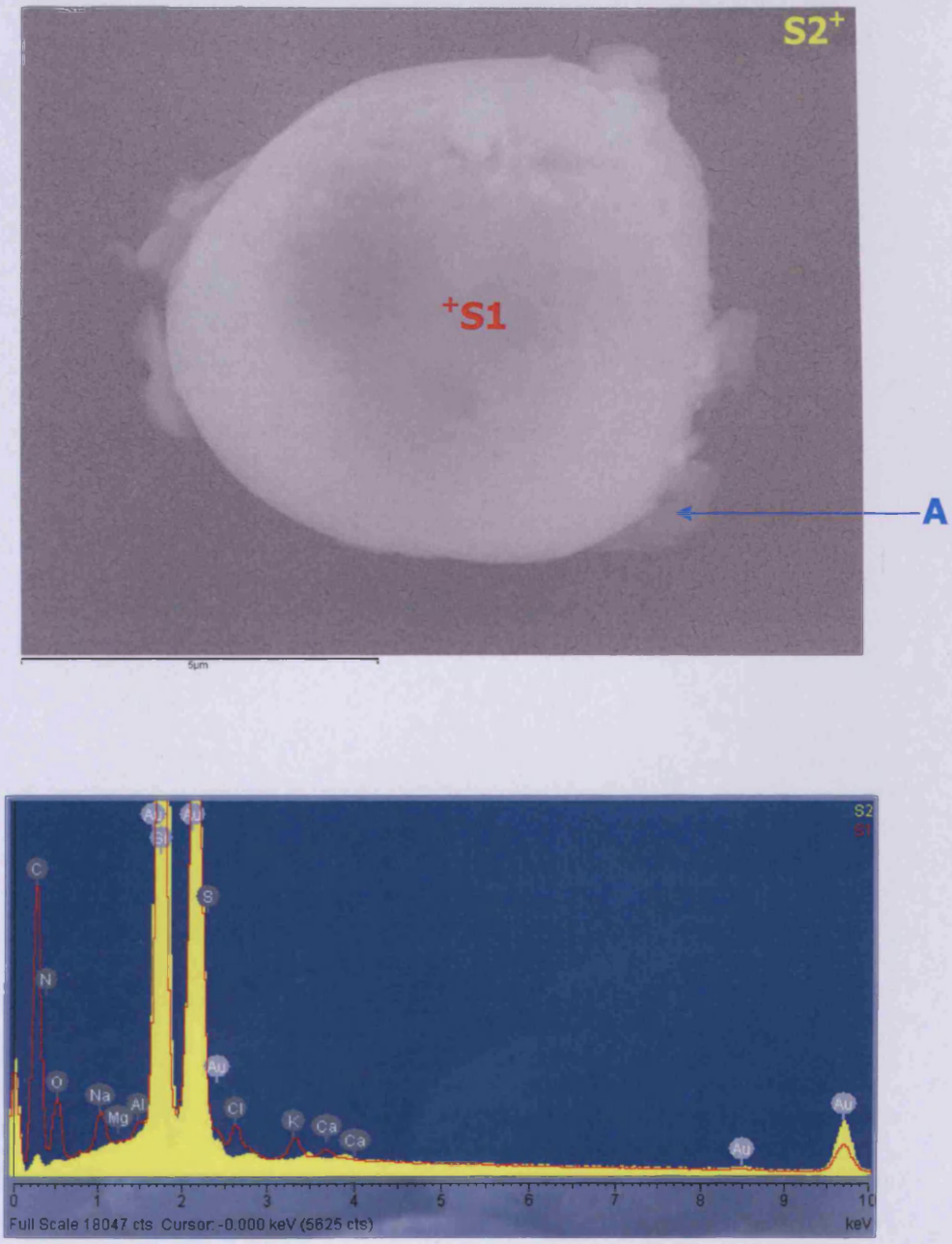

Figure 3-25: D3-302H sample from 41 km on silicon wafer.
Top: SEM image showing a 5~6 µm coccoidal form of particle with very thin envelope or sheath (A).
Bottom: Spectrum showing the organic components with a small amount of minerals. (red – S1, yellow – background spectrum S2)
(The methods for sample preparation and taking images are described in section 3.2)

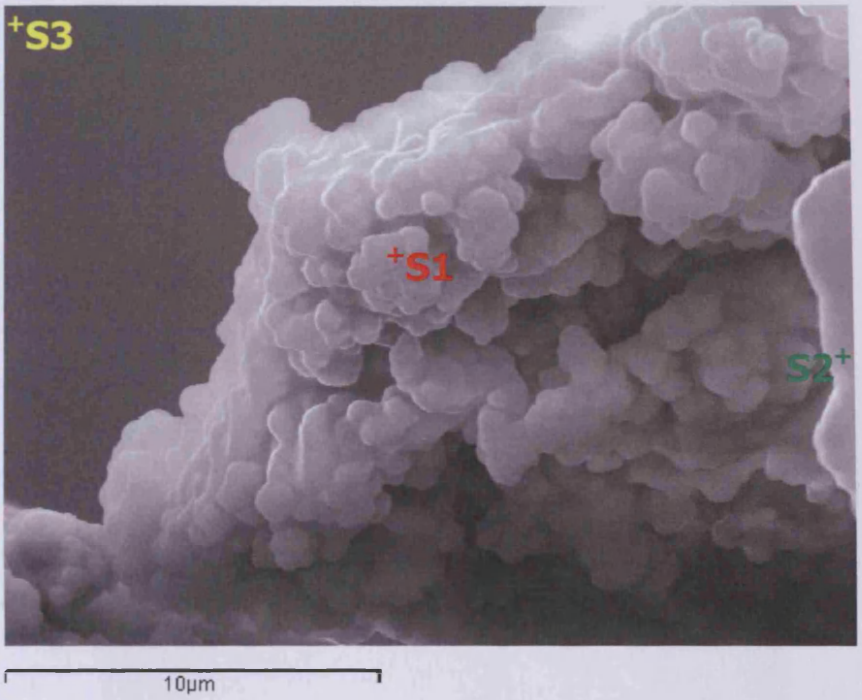

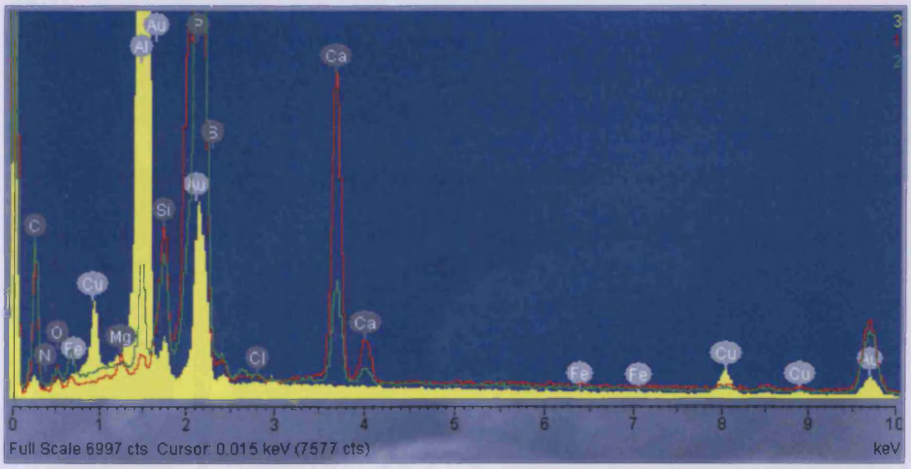

Figure 3-26: D3-103H sample from 41 km on silicon wafer.
Top: SEM image showing an aggregate of 0.5~1 µm particles, which are look like nanobacteria. Bottom: Spectrum showing the organic components with high Ca minerals. Al peak is the background reading from the Al stub. (red – S1, green – S2, yellow – background spectrum S3)
(The methods for sample preparation and taking images are described in section 3.2)

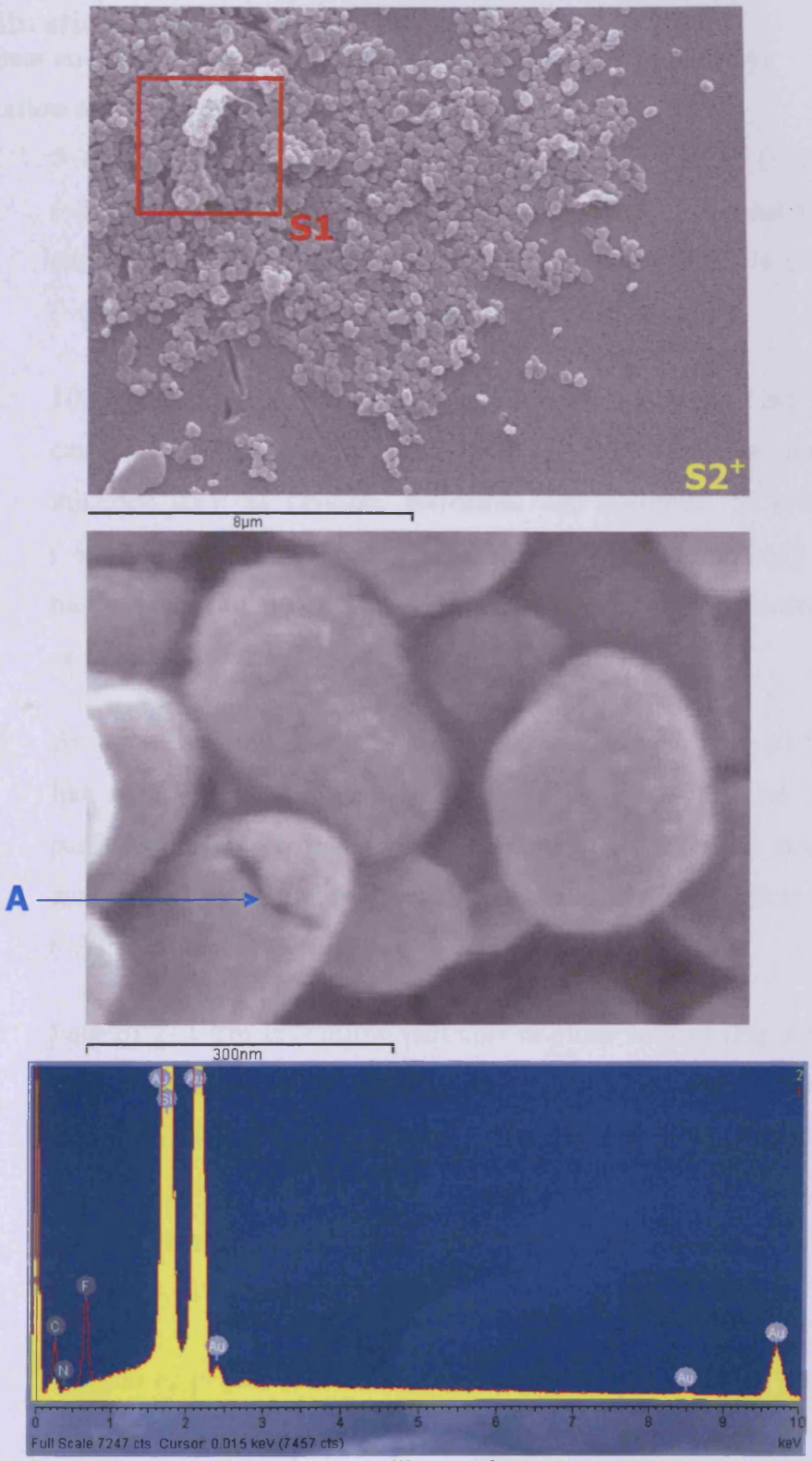

Figure 3-27: D3-104H sample from 41 km on silicon wafer.
Top Left: SEM image showing an aggregate of 0.3~1 µm particles. Top Right: Magnified image of nano-sized particle with a crack (A). Bottom: Spectrum confirming only C, N and F, however, it might have reached a limit to show unambiguous results. (red – S1, yellow – background spectrum S2)
(The methods for sample preparation and taking images are described in section 3.2)

3.3.4 Vibrationally Transferred Aerosols found in D4

(0.7 μm glass microfiber filter, probe from 41 km washed with buffer only)

Confirmation of mixture of 'CHON' and 'ROCK' particles:

D4-105K: 5~6 μm carbonaceous particle **(Fig. 3-28)**. It has C (~19.57%), O (~31.99%) and P (~7.26%). 'ROCK' component of Fe-poor Mg silicate, similar to those found in comet Halley and Wild 2, is present. Mg (~6.68%), Si (~17.01%). Probably forsterite or enstatite.

D4-108K: 10~25 μm particle with many small cavities **(Fig. 3-29)**. It is a mixture of carbonaceous material C (~15.78%), O (~33.93%) and mafic group minerals such as fayalite, ferrosilite and chromite. Si (~9.93%), Fe (~9.24%), Cr (~2.50%) and Mg (~0.73%). The morphology shows the past presence of water within the particle, which was released in space, or pyrolysed at the entrance of the atmosphere.

D4-204K: An aggregate of 0.5~2.0 μm 'grape'-like particles with an 'umbrella'-like particle and a ~3 μm length whisker **(Fig. 3-30)**. The 'grape'-like particles are enrich in Cr (~10.53%) and Fe (~22.52%) suggesting of euhedral chromite and magnetite. An 'umbrella'-like particle contains C (~33.34%) and O (~35.60%).

D4-207K: Four of 2~3 μm crystalline particles in close contact **(Fig. 3-31)**. One of them contains 'CHON' component C (~14.49%) and O (~36.10%). It also contains a silicate (~21.48%) with Mg (~1.51%), Al (~4.91%) and Fe (~15.92%). This is clear indication of mafic group particles of possibly fayalite or ferrosilite with spinel. It also has some minerals such as Na (~3.43%) and K (~2.23%).

D4-405K: 6~7 μm aggregate of carbonaceous particles with medium porosity **(Fig. 3-32)**. It contains high C (~50.19%) and O (~16.48%), and also 'ROCK' components of Cr (~2.91%) and Fe (~3.98%), possibly a mixture of subhedral chromite and pyroxene. There is a ~2 μm salt crystal, which is

embedded so deep that it must have come with the particle, and a short whisker with ~1 μm long.

Confirmation of particles with the whiskers:

D4-202K: 5~7 μm carbonaceous particle with medium porosity **(Fig. 3-33)**. It is highly composed with Fe (~39.43%) and O (~30.38%) showing the presence of magnetite. It contains other minerals such as P (~5.22%) and Ca (~2.58%). Various nano-sized rods and whiskers are embedded, and where they are most embedded has a small amount of Ti (~2.23%).

D4-406K: 4~5 μm platelet silicate with many size-ranged whiskers embedded **(Fig. 3-34)**. Its composition has Mg (~3.31%), Si (~41.70%) and Fe (~0.30%), which shows Fe-poor Mg silicate such as forsterite or enstatite. It is in a form of large platelet as well as those smaller whiskers (~0.1 μm diameter, ~1.5 μm length) and larger whiskers (~0.5 μm diameter, varies from 3~10 μm length). Its enrichment in C (~16.16%) and O (~37.12%) shows that the surface irregularities are 'CHON' particles.

Confirmation of possible biological particles:

D4-404K: ~20 μm long particle with tail-like structure at one end **(Fig. 3-35)**. It has C (~38.12%), N (~10.24%) and O (~25.81%). From its size, it could be a protozoan but further samples and studies are required.

D4-105L: 2~3 μm spore-like particles with intriguing coatings **(Fig. 3-36)**. It is highly carbonaceous (~58.32%), and has N (~11.87%) and O (~4.33%). One image looks like a diplococcus division.

3.3.5 Vibrationally Transferred Aerosols found in C5

(0.45 μm cellulose nitrate filter, probe from 39 km washed with buffer and glass beads)

Confirmation of possible biological particle:

C5-201O: 8~10 μm wrinkled spore-like particle similar to those Wallis and Al-Mufti finding **(Fig. 3-31)**. It has high C (~35.49%), N (~5.63%) and O (~26.77%) with some minerals such as Na (~1.28%), Al (~1.36%), Cl (~1.39%) and Ca (~19.29%).

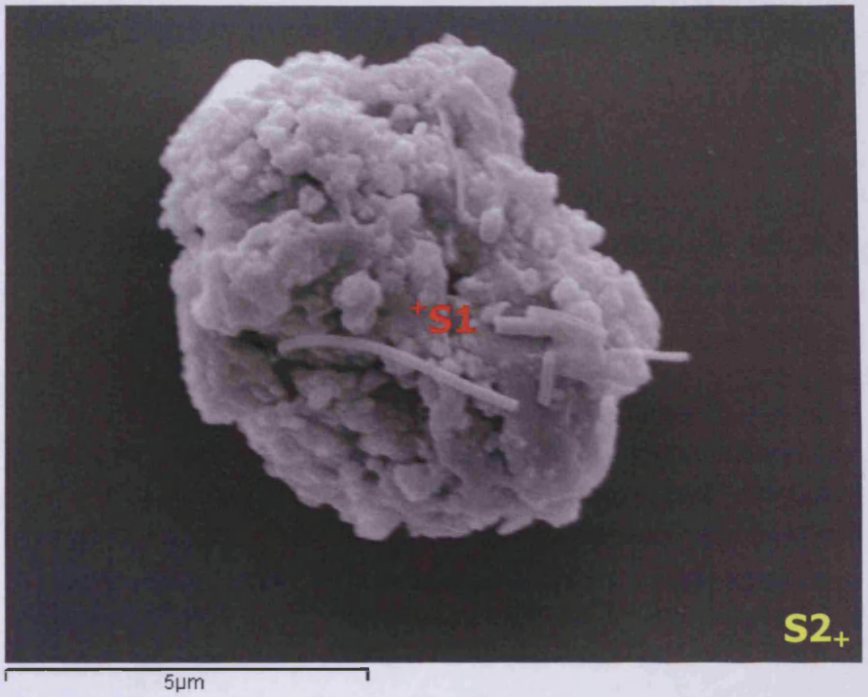

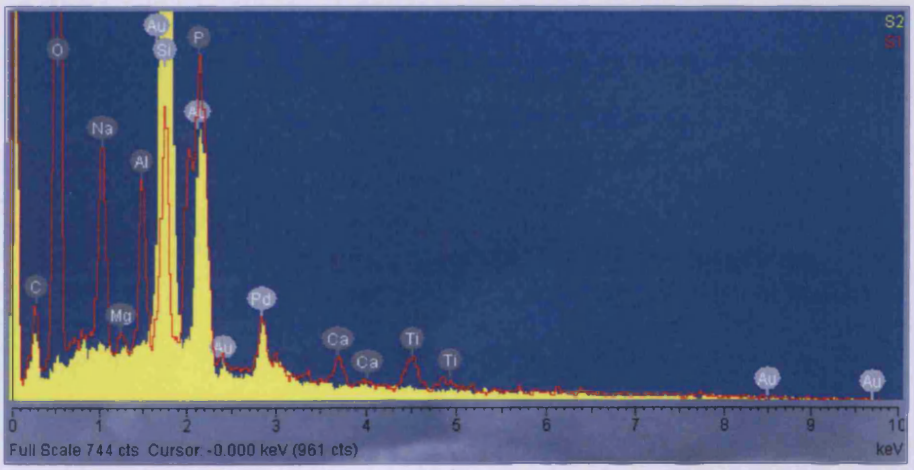

Figure 3-28: D4-105K sample from 41 km on silicon wafer.
Top: SEM image showing a 5~6 µm particle. Bottom: Spectrum showing 'CHON' and 'ROCK' component of Fe-poor Mg silicate, possibly forsterite and enstatite. (red – S1, yellow – background spectrum S2)
(The methods for sample preparation and taking images are described in section 3.2)

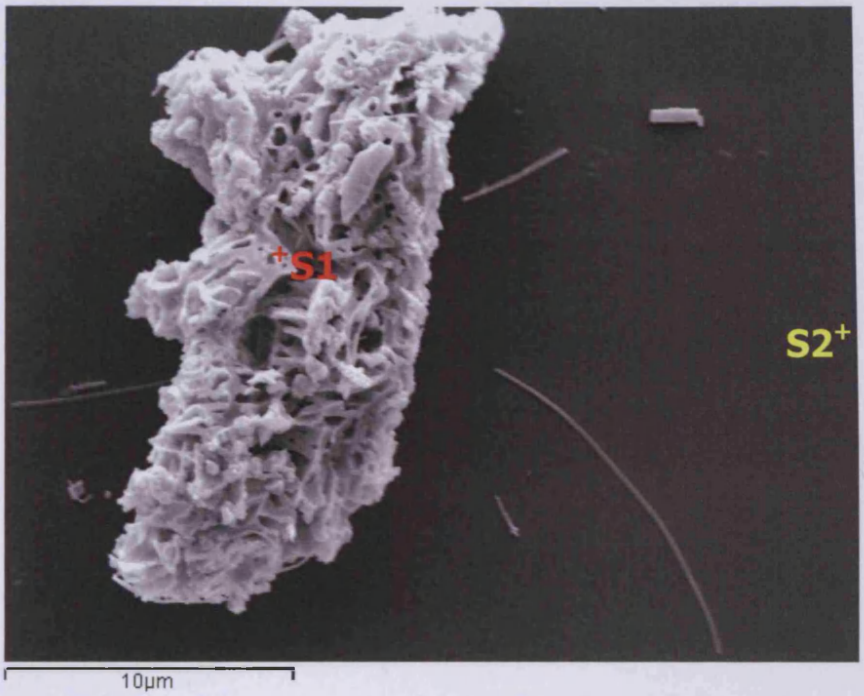

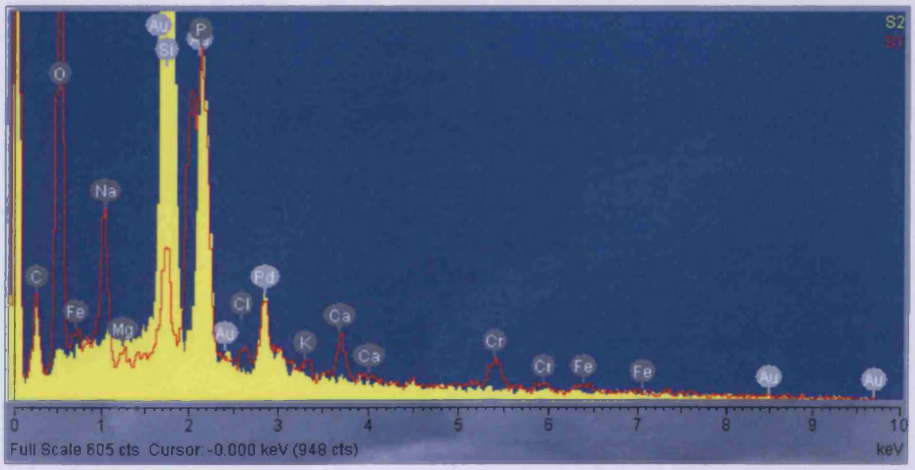

Figure 3-29: D4-108K sample from 41 km on silicon wafer.
Top: SEM image showing a 10~25 µm particle with many small holes. Bottom: Spectrum showing 'CHON' and some minerals as well as the 'ROCK' components such as fayalite, ferrosilite and chromite. (red – S1, yellow – background spectrum S2)
(The methods for sample preparation and taking images are described in section 3.2)

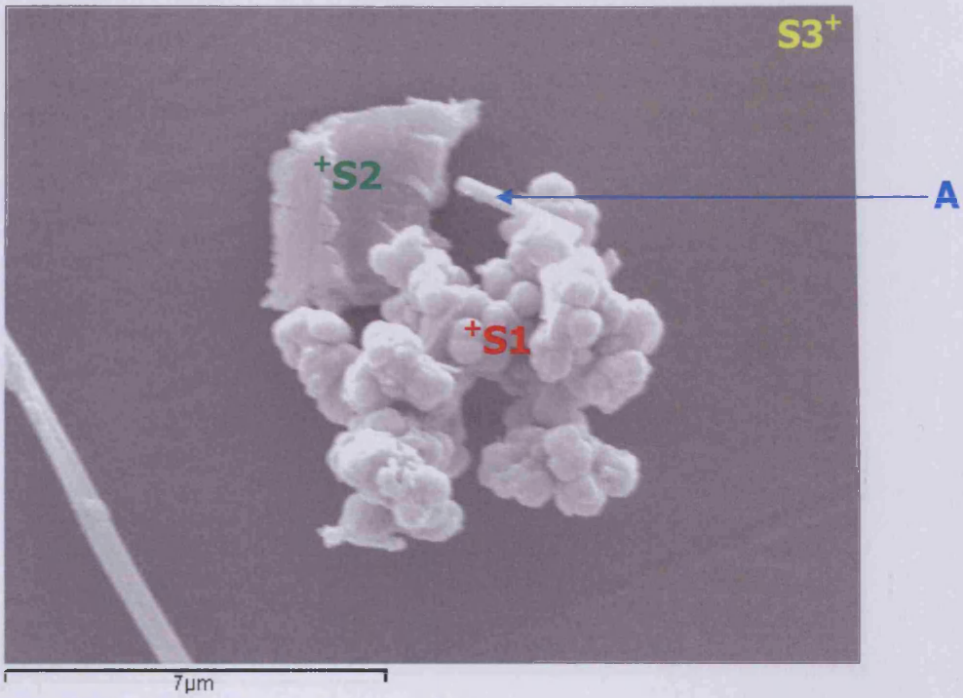

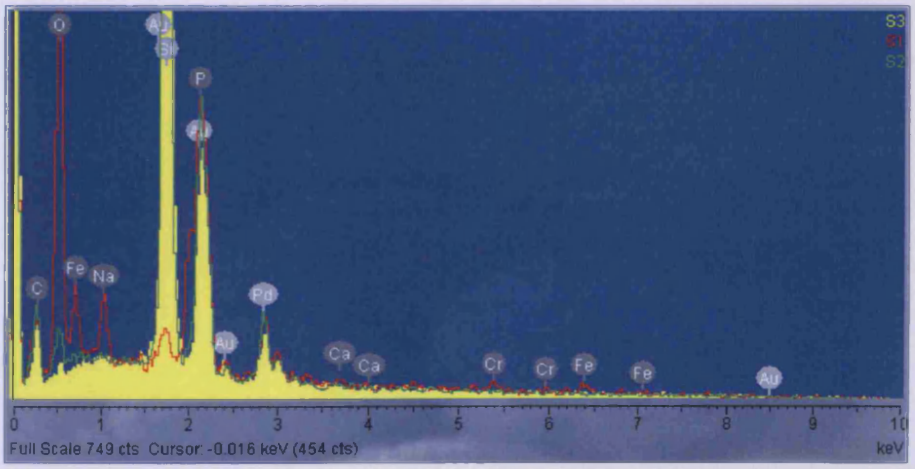

Figure 3-30: D4-204K sample from 41 km on silicon wafer.
Top: SEM image of an aggregate of 0.5~2.0 µm 'grape'-like particles (S1) with an 'umbrella'-like particle (S2) and a whisker (A). Bottom: Spectrum showing the 'ROCK' components of euhedral chromite (particles), magnetite (possibly whisker) and the carbonaceous 'umbrella'. (red – S1, green – S2, yellow – background spectrum S3)
(The methods for sample preparation and taking images are described in section 3.2)

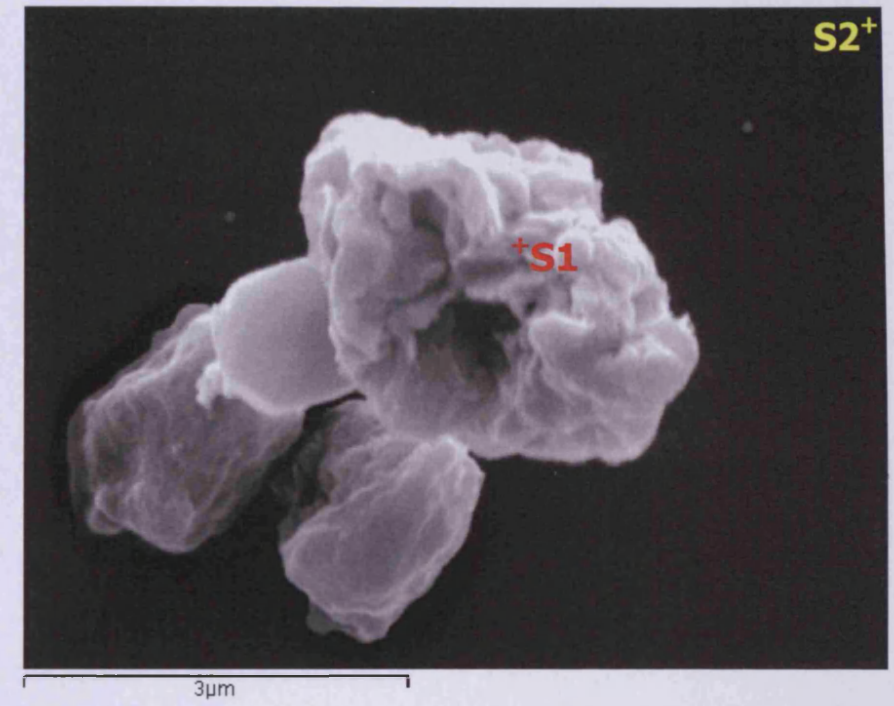

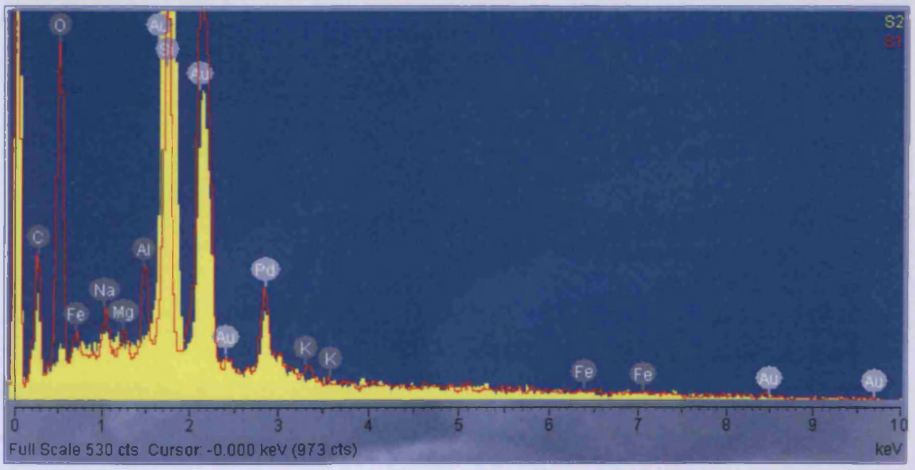

Figure 3-31: D4-207K sample from 41 km on silicon wafer.
Top: SEM image showing four of 2~3 µm crystalline particles in close contact. Bottom: Spectrum showing the 'CHON' and the 'ROCK' components of spinel with fayalite or ferrosilite. (red – S1, yellow – background spectrum S2)
(The methods for sample preparation and taking images are described in section 3.2)

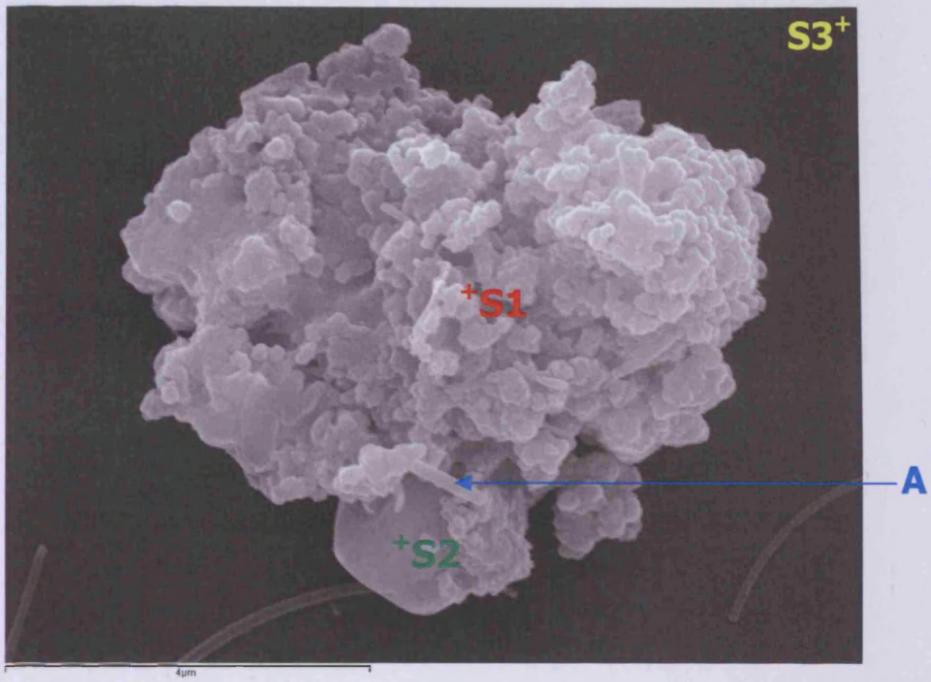

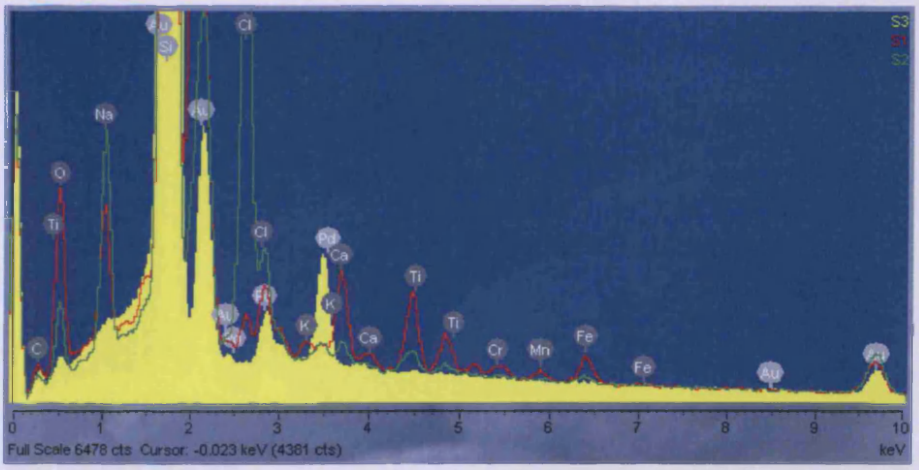

Figure 3-32: D4-405K sample from 41 km on silicon wafer.
Top: SEM image showing a 6~7 µm aggregate of carbonaceous particles with salt crystal (S2) and rod embedded (A). Bottom: Spectrum showing both the 'CHON' and 'ROCK' components, probably a mixture of subhedral chromite and pyroxene. (red – S1, green – S2, yellow – background spectrum S3)
(The methods for sample preparation and taking images are described in section 3.2)

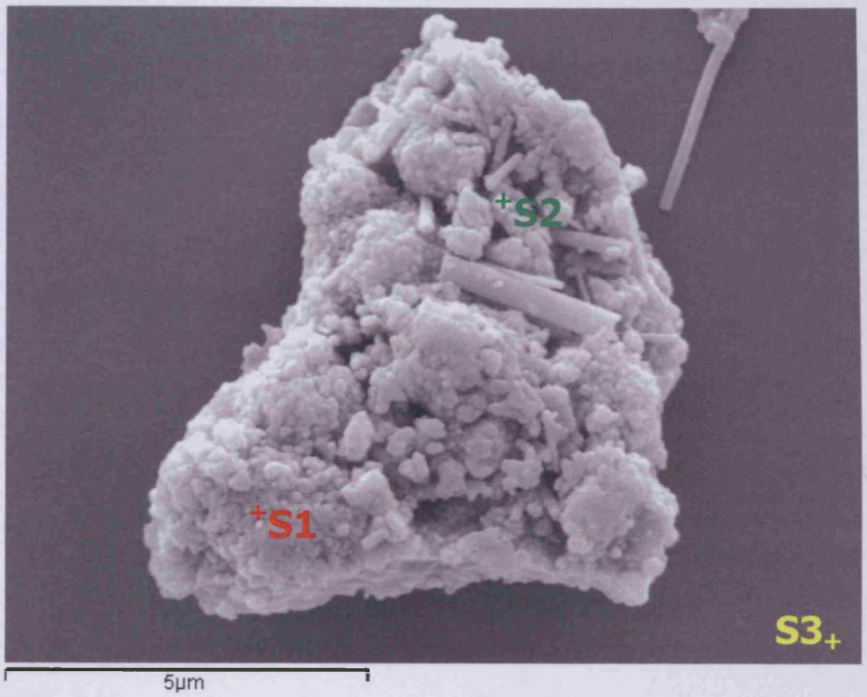

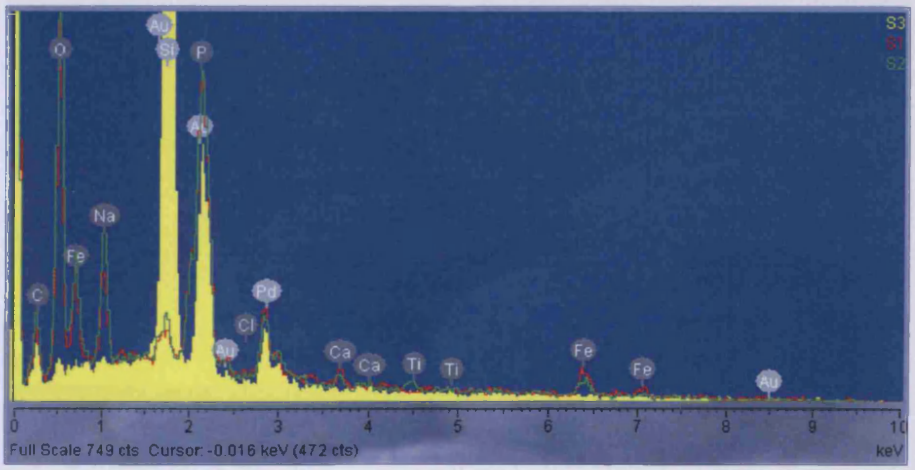

Figure 3-33: D4-202K sample from 41 km on silicon wafer.
Top: SEM image showing a 5~7 µm particle with medium porosity and has many various sized whiskers embedded. Bottom: Spectrum showing both the 'CHON' and 'ROCK' component of magnetite. (red – S1, green – S2, yellow – background spectrum S3)
(The methods for sample preparation and taking images are described in section 3.2)

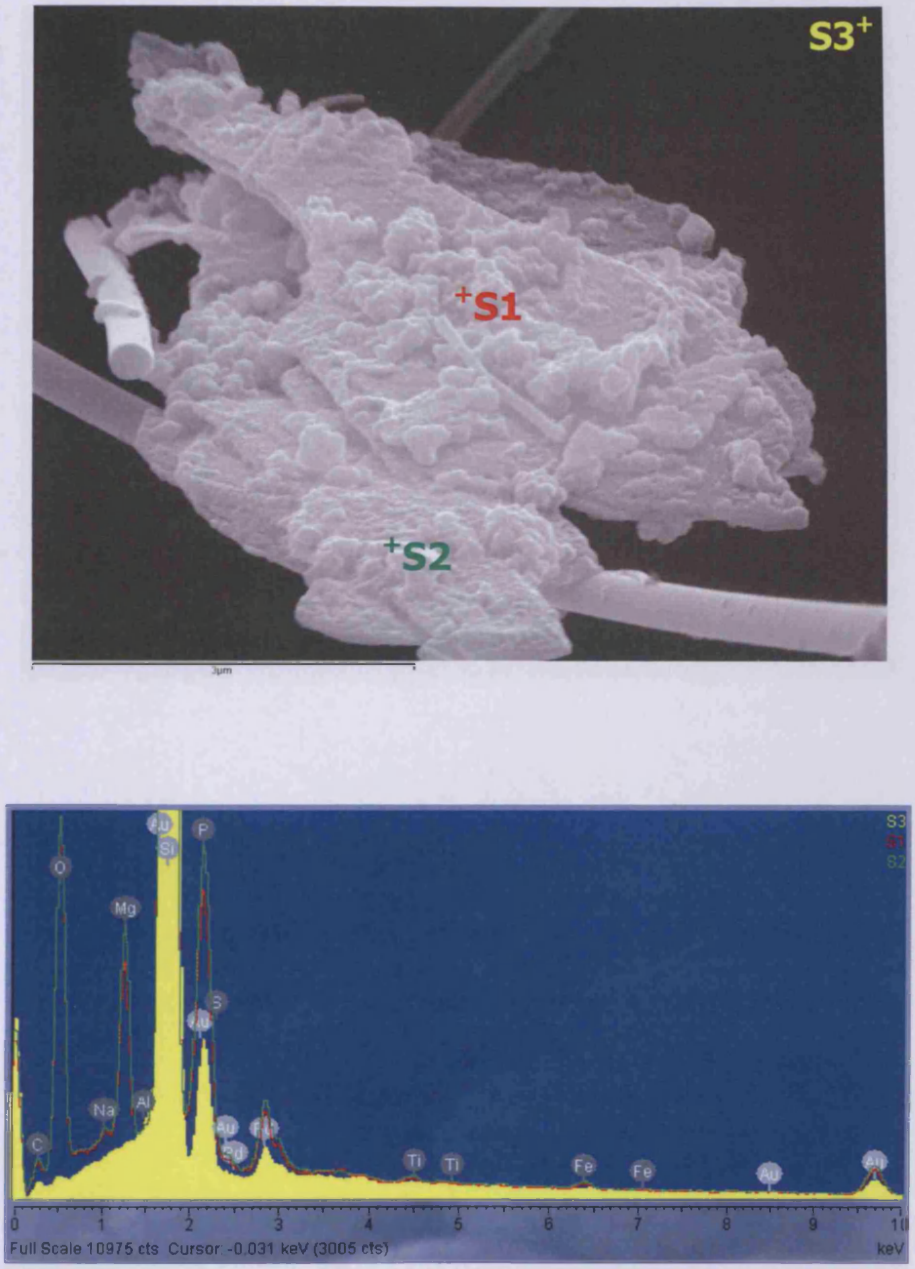

Figure 3-34: D4-406K sample from 41 km on silicon wafer.
Top: SEM image of a 4~5 μm platelet silicate with many size-ranged whiskers embedded. Bottom: Spectrum showing both the 'CHON' components and 'ROCK' components of fosterite and enstatite. (red – S1, green – S2, yellow – background spectrum S3)
(The methods for sample preparation and taking images are described in section 3.2)

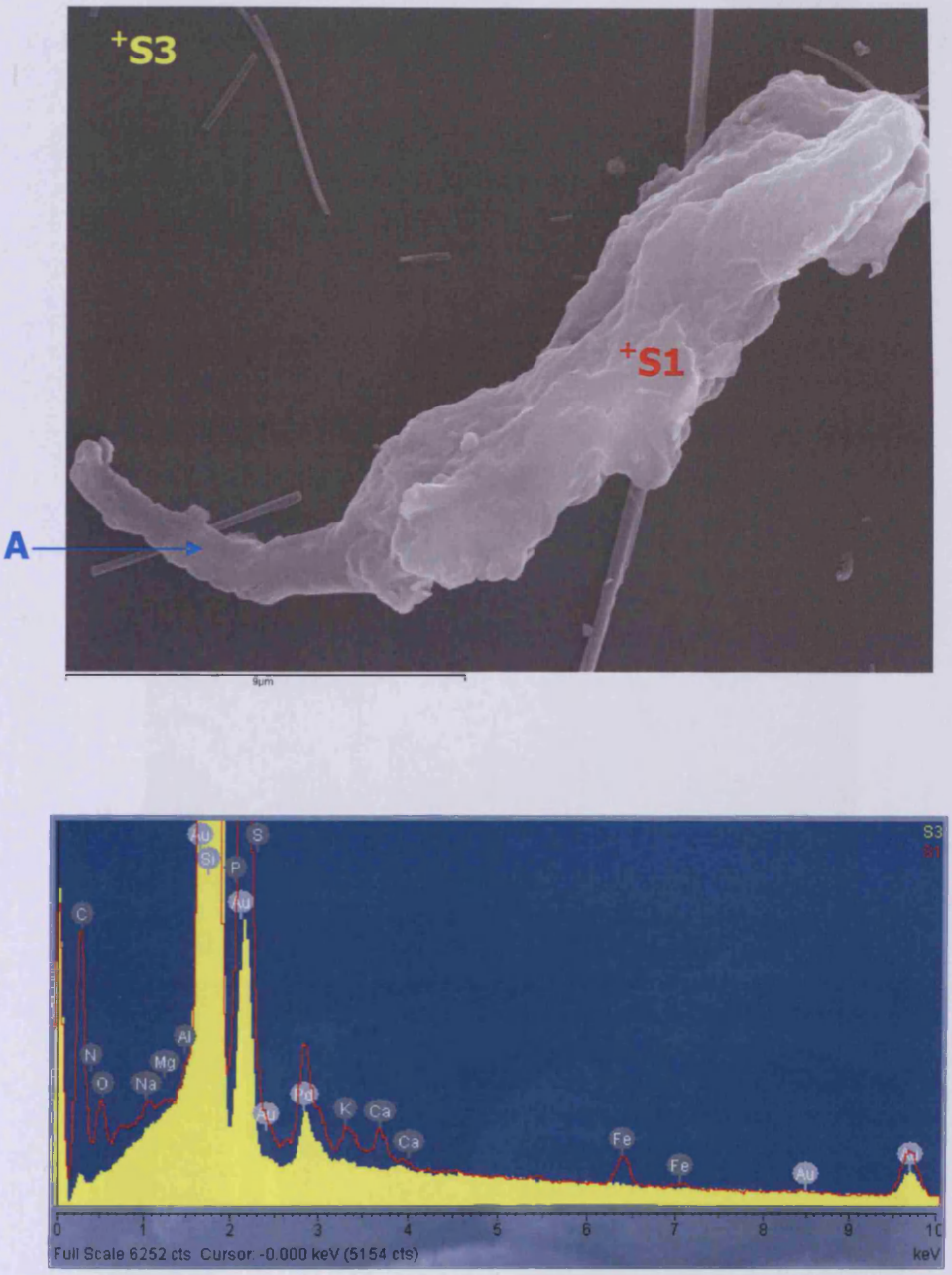

Figure 3-35: D4-404K sample from 41 km on silicon wafer.
Top: SEM image of a ~20 µm long particle with tail-like growth at one end (A). Bottom: Spectrum showing organic components with the small amounts of minerals. (red – S1, yellow – background spectrum S3)
(The methods for sample preparation and taking images are described in section 3.2)

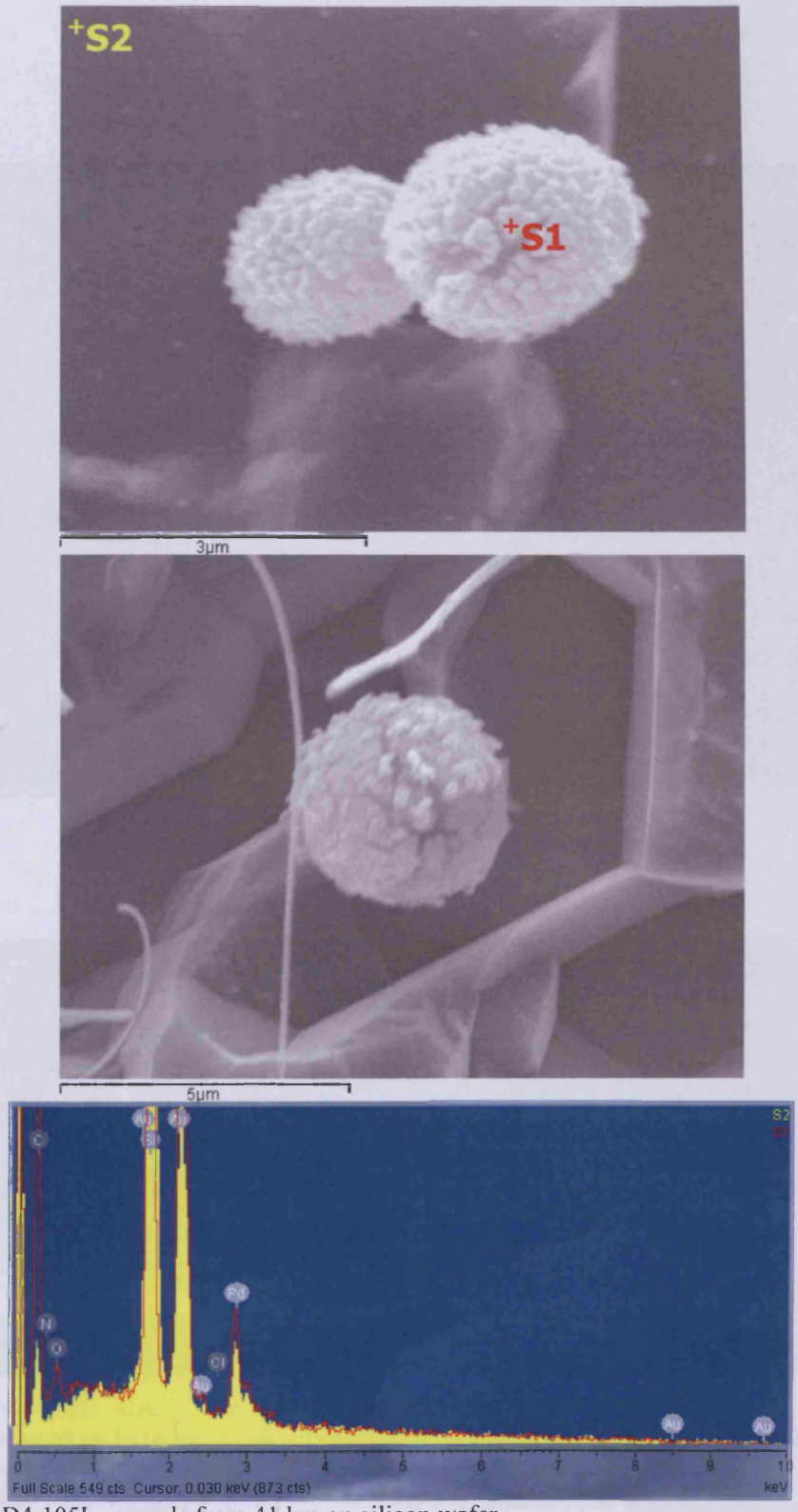

Figure 3-36: D4-105L sample from 41 km on silicon wafer.
Top: A pair of 2~3 µm spore-like particles similar to diplococcus division of bacteria. Middle: A single 3.5~4 µm spore-like particle (D4-108L). Bottom: Spectrum showing the presence of organic components. (red – S1, yellow – background spectrum S2)
(The methods for sample preparation and taking images are described in section 3.2)

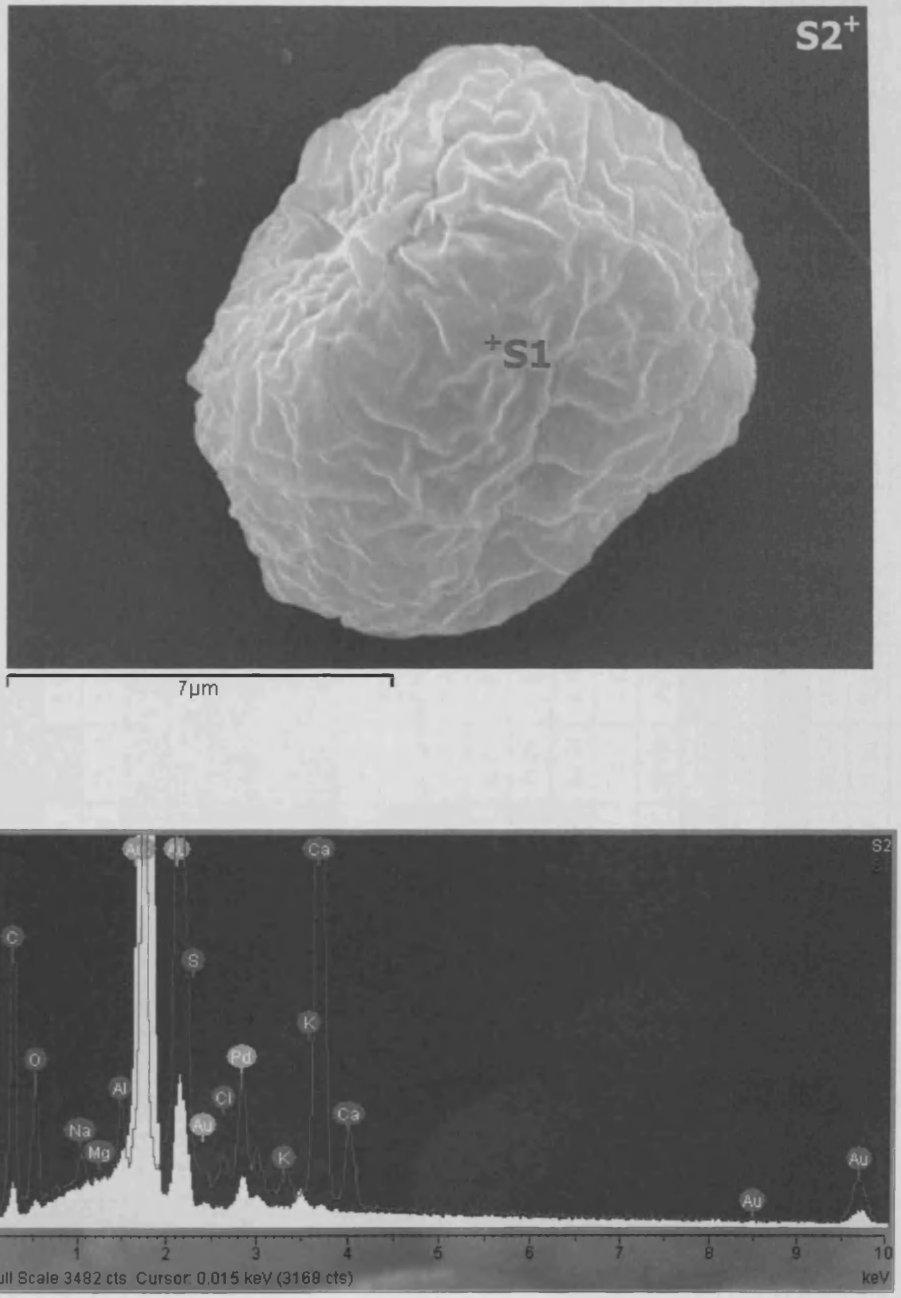

Figure 3-37: C5-201O sample from 39 km on silicon wafer.
Top: SEM image of an 8~10 µm wrinkled spore-like particle. Bottom: Spectrum showing the organic components with some minerals. (red – S1, yellow – background spectrum S2)
(The methods for sample preparation and taking images are described in section 3.2)

NAME	Spec.	C	N	O	F	Na	Mg	Al	Si	P	S	Cl	K	Ca	Ti	Cr	Mn	Fe	Ni	Cu
D1-404	S1	33.71		28.57		5.26				6.71		1.18		2.28				22.29		
	S2	37.05		28.39		5.22				6.87				3.43				19.05		
	S3 (B)	76.38		23.62																
D1-410	S1	20.83		29.58		7.88		1.08		5.92		1.73						32.98		
	S2	24.57		38.01		3.02		1.10	12.38	2.68								18.24		
	S3 (B)	74.56		25.44																
D1-512	S1	17.28		28.96										0.24		8.69	1.63	42.67	0.54	
	S2 (B)	76.51		17.86		1.87						2.52						1.22		
D1-517	S1	58.70	20.44	14.90		4.49						1.48								
	S2 (B)	55.31	25.88	13.26		2.51						1.04								
D1-519	S1	20.61		46.49		1.62	0.98	2.31	3.46	0.82		0.28	0.65	19.81			0.40	2.56		
	S2 (B)	71.03		25.37		1.45			0.36			1.30		0.49						
D1-702	S1	62.47	11.77	17.15		5.05			0.09	0.40	0.39	2.43	0.16	0.09						
	S2	71.06		13.72		7.75		0.10	0.43	0.87	1.00	4.62	0.30	0.15						
	S3 (B)	86.27		9.92		1.28			0.36	0.33		1.83								
D1-901	S1			44.66		4.76	2.97	10.07	22.75	1.57	0.99	2.23	2.85	0.66				7.94		
	S2			44.53		5.16	3.25	8.67	22.32	2.17	1.41	2.67	2.55					9.53		
	S3			43.77		6.48	2.68	8.17	21.52	2.46	1.07	2.50	2.31	1.56				9.36		
	S4 (B)	67.48		23.24					9.28											
D1-908	S1	44.33		31.42		2.96		1.10	2.87	3.24	0.57	1.20	0.28			1.56		8.15	1.41	0.91
	S2 (B)	73.76		22.75		1.08						1.29								1.13
D1-912	S1	39.06		34.71		1.16		10.72	10.97	0.88		0.75	0.17					0.88		0.69
	S2	44.37		40.73		1.76		5.41	5.26	0.32		1.32	0.09		0.10			0.40		0.25
	S3	31.65		47.34		0.99		7.01	6.71	0.44	0.20	0.44			4.07			0.67		0.48
	S4 (B)	74.09		19.68		2.00			0.58			2.16						0.50		0.99

Table 3-4: Quantitative Analysis of Aerosols found in D1. Measured in % of Total Weight. (B) - Background Spectrum.

NAME	Spec.	C	N	O	F	Na	Mg	Al	Si	P	S	Cl	K	Ca	Ti	Cr	Mn	Fe	Ni	Cu
D3-202C	S1	23.17		19.24				4.39	48.90						3.20			0.27		0.84
	S2 (B)							0.14	99.86											
D3-208C	S1	21.27		33.16		6.32	0.20	0.58	0.80	4.69	0.39	0.97	0.63	1.08		2.78	0.30	23.20	3.24	0.38
	S2 (B)								100											
D3-209C	S1	22.14		40.61		3.92	0.43	0.72	9.59	4.53	0.20	0.35	0.46	9.05		0.99	2.91	3.43	0.37	0.30
	S2 (B)								100											
D3-210C	S1	31.97		37.71		8.87	0.37	1.89	5.89	4.65	0.45	0.55	1.14	1.10				3.12		0.82
	S2 (B)								100											
D3-110D	S1	30.84		22.96				0.19	42.74					3.26						
	S2	26.52		19.28					44.77					9.43						
	S3 (B)								100											
D3-103H	S1	26.87	28.37	12.17			0.86	0.61	3.94	9.37	0.50	0.21		17.11						
	S2	33.80	32.04	10.52				4.95	4.67	3.90	1.24	0.73		8.14						
	S3 (B)			0.88				91.45	2.43											
D3-104H2	S1	40.29	7.31		10.61				41.80											
	S2 (B)								100											
D3-302H	S1	64.05	10.07	14.76		1.12	0.04	0.26	8.34		0.13	0.59	0.46	0.18						
	S2 (B)								99.05		0.95									
NC-101Q	S1								100											
	S2 (B)							93.62										0.28		6.09

Table 3-5: Quantitative Analysis of Negative Control (NC) and Aerosols found in D3. Measured in % of Total Weight. (B) - Background Spectrum.

NAME	Spec.	C	N	O	F	Na	Mg	Al	Si	P	S	Cl	K	Ca	Ti	Cr	Mn	Fe	Ni	Cu
D4-105K	S1	19.57		31.99		4.64	6.68	4.84	17.01	7.26				2.61	5.41					
	S2 (B)								100											
D4-108K	S1	15.78		33.93		5.35	0.73		9.93	11.70		2.43	2.00	5.42		2.50		9.24		
	S2 (B)								100											
D4-202K	S1	15.49		30.38		4.39			1.34	5.22		1.17		2.58				39.43		
	S2	23.57		32.28		5.67			2.10	5.34				2.23	2.23			26.57		
	S3 (B)								98.71			1.29								
D4-204K	S1	12.93		38.76		4.77			1.85	7.47				1.16		10.53		22.52		
	S2	33.34		35.60					31.06											
	S3 (B)	7.16		1.78					91.06											
D4-207K	S1	14.49		36.10		3.43	1.51	4.91	21.41				2.23					15.92		
	S2 (B)			2.09					97.91											
D4-404K	S1	38.12	10.24	25.81		0.26	0.06	0.18	23.30		0.49		0.20	0.26				0.98		
	S3 (B)								100											
D4-405K	S1	50.19		16.48		0.92			19.96			0.32	0.08	0.79	4.23	2.91	0.16	3.98		
	S2	15.19		15.78		17.10			29.88			20.48		0.33	0.85			0.39		
	S3 (B)					0.10			99.90											
D4-406K	S1	16.16		37.12		0.44	3.31	0.10	41.70	0.56	0.18				0.13			0.30		
	S2	17.84		37.84		0.48	3.99		38.52	0.56	0.18				0.18			0.41		
	S3 (B)								100											
D4-105L	S1	58.32	11.87	4.33					24.30			1.18								
	S2 (B)								100			0.00								
C5-201O	S1	35.49	5.63	26.77		1.28	0.22	1.36	7.39		0.56	1.39	0.61	19.29						
	S2 (B)			2.01					97.83											

Table 3-6: Quantitative Analysis of Aerosols found in D4 and C5. Measured in % of Total Weight. (B) - Background Spectrum.

3.4 Interpretations

3.4.1 The Flux of IDPs in Stratosphere

I have counted 32 particles, which are 5 μm or smaller in size, from about 1/69 of whole filter with the sample air past through (D1), thus approximately 2208 particles were collected from the ambient air volume of 5.6×10^8 litre at 41 km (P = 290 Pa, T = 253 K; Wickramasinghe *et al.*, 2003), which is calculated to be 3.94×10^{-6} particle per litre. Even though I have discounted those particles adhered to the inner surface of the cylinder, the flux of small fraction collected by this technique is clearly higher than that of aircraft collections (1.07×10^{-6} particle per litre; Brwonlee, 1978).

The particles stuck to the inner surface of the cylinder were washed out by the buffer solution with or without glass beads and filtered through either glass microfiber filter or cellulose nitrate filter **(Table 3-2)**. These particles were then transferred to a silicon wafer to avoid any carbon, nitrogen and oxygen readings from the background and thus we obtain more accurate light element abundances from the EDX analysis. The particles on the glass microfiber filter (D3) were vibrationally or electronstatically transferred to the silicon wafer. The result has shown that the yield of the particles transferred by using the vibrational force was about a double of that by using the electrostatical force, which means that most of the particles were not charged or weakly charged and just can be removed from the filter by tapping force.

The yields of particles from the various wash out techniques are also compared. The wash out without glass beads (D4 filter) gave about 56% more yield than with glass beads (D3 filter), which shows that the particles were loosely adhered to the surface of the inner cylinder and they can be easily removed by ordinal buffer solution. The transfer to the silicon wafer from the cellulose nitrate filter (C5) gave less than a half yield than from the glass microfiber filter (D3). We have identified some particles on C5 filter after the transfer experiment, however they seem stuck to the cellulose nitrate more firmly than they do to the glass microfiber thus gave a less yield. These results can be referenced in the future experiment, which uses the silicon wafer as the

background medium to increase the accuracy of the light element abundance spectra, however, it depletes the accuracy of Si spectrum in exchange. Therefore a consideration on any new background medium is required when both C and Si spectra readings are demanded.

3.4.2 Morphology of Chondritic and Non-chondritic IDPs Collected

As earlier studies of IDPs show (Fraundorf *et al.*, 1981; Brownlee *et al.*, 1982; Sandford, 1983), we have observed the similar morphologies in particles from our samples. Four classes of particles can be defined. They are highly porous (HP), of medium porosity (MP), of low porosity (LP) or smooth (S) particles. The HP morphology comprises aggregates of submicron 'grapes'-like particles, and they are very fragile, so that a number of partially broken bits can be identified. The majority of HP particles had chondritic abundances of magnetite (e.g. **Fig. 3-10**) as those found in FSN group (Brwonlee *et al.*, 1982), and euhedral chromite (e.g. **Fig. 3-30**). However there were also some non-chondritic 'CHON' particles (e.g. **Fig. 3-18**) that were found. The dust analysis of comet Halley (Jessberger, 1999) and Tempel 1 (A'Hearn *et al.*, 2005) show that the cometary dust contains fine grains of 'CHON' particles, which presumably have HP morphology like those we found.

The most of MP particles are made up of both chondritic and non-chondritic components. An example is carbonaceous particle, D4-405K (**Fig. 3-32**), which has the elemental abundances of subhedral chromite and pyroxene. It also contains a salt crystal embedded deep into the particle. Since the past experimental studies of Mars by Viking Lander and the Martian meteorites predicted that the salty water can exist on the surface of Mars (Lane and Christensen, 1998), it is possible that those salt crystals formed on planets are projected into space and collide with the IDPs to form such a particle as D4-405K. However it is more likely that salt crystals form in the primitive or presolar nebula where more debris are available to interact with. The mode of formation of such a large salt crystal (~2 μm) at that time is still uncertain. Another example of MP particle is D4-108K (**Fig. 3-29**). It has a mixture of olivine or pyroxene and chromite with 'CHON' elements. Many cavities in this particle are

probably indicative of the presence of past water. It was established from the study of the comet Halley in 1986 that this comet is made mostly out of water, so D4-405K may originated from a comet, and when it left the cometary body, the water crystals in the particle were dissociated in space and formed many cavities. Another possible reason is the anhydrous pyrolysis of 'CHON' elements at the entrance of the Earth's atmosphere and formed cavities where those elements were located.

We have also identified some LP particles, which can represent 'boulders' between the individual crystals. The chondritic particle D1-512 **(Fig. 3-11)** has a very smooth surface showing the history of high temperature melting at some point to form this LP morphology. This melting could have happened during the entrance to the atmosphere. However, such a small particle (7~8 μm) requires almost a vertical fall with extremely high speed to get sufficiently heated up (Coulson *et al.*, 2003); therefore, it might represent a fragment broken off from a much larger particle during entrance. The reason for the survival of many submicron magnetite grains on the surface is still uncertain. Another example of LP particle is D3-202C **(Fig. 3-20)**. It is a very soft carbonaceous chondritic particle and seems to have been squashed probably during the collection.

In the case of S particles, they can be separated into two groups, with coating and without coating. Most of the possible biological particles, which are discussed later, have both smooth morphology with and are without coatings. An example of non-biological particle with coating is D3-208C **(Fig. 3-21)**, which is an intimately mixed combination of a 'CHON' particle with small mounds of FeNi metal such as are present in the MMS group (Brownlee, 1985). An example of S particle without coating is the carbonaceous particle, D3-210C **(Fig. 3-23)**, which has the chondritic abundances of spinel with the mafic group of olivine or pyroxene.

3.4.3 Elemental Analysis of IDPs Collected

The recent studies of microdust from comet Halley (Jessberger, 1999) and comet Wild 2 (Bridges *et al.*, 2008) show the presence of a 'ROCK' component of Fe-poor Mg-silicate particles. The IDPs collected by Brownlee *et al.* (1982) with such olivine or pyroxene composition is categorised in the mafic group. From our sample, we identified the mafic particles with similar composition (e.g. **Fig. 3-28**), as well as the Mg-poor Fe-silicate particles (e.g. **Fig. 3-12**), which are normally associated with spinel and chromite. Some of the mafic particles were found in a form of whiskers and platelets (e.g. **Fig. 3-24**) as those found in IDPs collected by U-2 aircraft (Bradley *et al.*, 1983).

The microdust from comets also contain Fe-sulfides (pyrrhotite) and Fe metals (magnetite). The Fe-sulfides in our sample are also associated with Ni, (e.g. **Fig. 3-14**) as are the FSN particles found by Brownlee *et al.* (1982). The magnetite particles were normally found as single grains embedded in the IDPs (e.g. **Fig. 3-11**), except one particle, D4-202K (**Fig. 3-33**), which has many short whiskers of magnetite, similar to those found in the ALH84001 Martian meteorite (Bradley *et al.*, 1996). It is possible that magnetite in both cases have a biological origin.

One of the most intriguing particles I found was D1-912 (**Fig. 3-15**), which is a lattice silicate mineral with the presence of pyrophyllite (a clay mineral). Some other particles from our collection also show clay minerals (e.g. **Fig. 3-13**), which had to be formed in presence of liquid water. The recent studies of the Deep Impact mission revealed the presence of pyrophyllite in the comet Tempel 1 (Lisse *et al.*, 2006), indicating possible cometary origin. Possibly our most important discovery was a refractory crystal of Titanium embedded to this particle. This crystal of size 0.5 × 2 μm implies presolar high temperature condensation. Many different presolar grains have been discovered in primitive chondritic meteorites and IDPs. However, this is the first time that a presolar Ti-crystal, presumably titanium nitride, was identified.

3.4.4 Possible Biological Particles Collected

The past studies of our samples from an altitude of 41 km by Wallis and Al-Mufti (2002) identified the diverse spore-like particles, often associated with other materials **(Fig. 3-6)**. We have found a similar 8~10 μm spore-like particle C5-201O **(Fig. 3-37)** but without any other materials. It is highly carbonaceous and mineralized with Ca. The presence of nitrogen provides evidence of recent biological activity. Another carbonaceous particle D1-702 **(Fig. 3-19)** with a similar size is associated with NaCl coating, and depleted in nitrogen. It could be a small organic fossil such as an acritarch, and the whiskers attached to this particle the remains of its flagella, however, it requires a further testing for confirmation of the biological origin. The smaller 2~3 μm sized spore-like particles, D4-105L and D4-108L **(Fig.3-36)**, were also found. They are rich in C, N and O, and have very intriguing coatings. A pair of particles in D4-105L is very similar to the division of diplococcus **(Fig. 3-38)**. The relatively high carbon contents from all three particles are indicative of biogenicity.

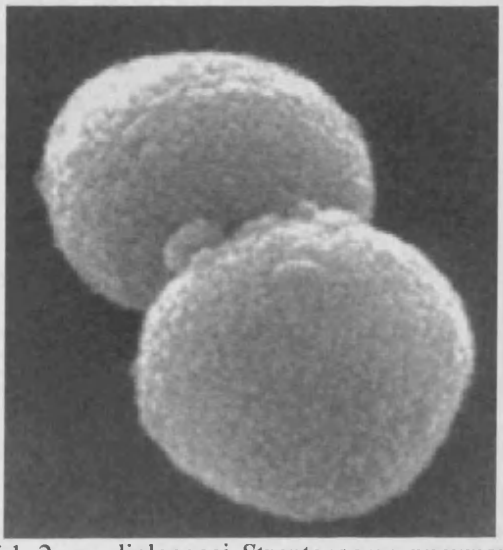

Figure 3-38: SEM image of 1~2 μm diplococci *Streptococcus pneumoniae*. © 2005 Kenneth Todar University of Wisconsin-Madison Department of Bacteriology

We have also identified the particles similar to some of the microfossils reported in carbonaceous meteorites. The 5~6 μm sized carbonaceous particle D3-302H **(Fig. 3-25)** is very similar to 5.2 μm coccoidal microfossils in Orgueil meteorite (**Fig. 3-39**: Hoover,

2006). They have very thin partially broken away sheath-like envelopes. Although the coccoid structure in the meteorite is mineralised and shows no recent evidence of biologenecity, D3-302H is highly carbonaceous and has relatively high nitrogen (compared to the meteoritic), indicating its recent biological viability in space.

The nanobacteria-like particles, similar to the microfossils discovered in the Martian meteorite ALH84001 (**Fig. 3-40**: McKey *et al.*, 1996), were also found. The recent studies of terrestrial nanobacteria show their pathogenic function of extraskeletal calcification (Cisar *et al.*, 2000) and the protein-based slime production (Sommer *et al.*, 2004) causing a number of severe diseases. An aggregate of nanoparticles D3-103H **(Fig. 3-26)** contains high C, N and O with minerals such as P and Ca. This result implies the biogenecity of nanoparticles and induced biomineralization. Another example of the nanoparticle D3-104H **(Fig. 3-27)** had a poor quantitative analysis due to its small particle size. However, we detected fluorine which probably indicates the presence of fluorocarbon. Fluorocarbon is commonly known as a man-made terrestrial contaminant. However, some microorganisms such as the bacterium *Streptomyces cattleya* can biosynthesise organofluorine compounds as a means of pathogen repellant (Hagen *et al*, 1999; Murphy *et al.*, 2002). Natural organoflurine compounds were also found in igneous and metamorphic rocks as well (Harnish *et al.*, 2000).

Earlier studies of the same sample by Harris *et al.* (2002) show a ~1 μm sized cocci-like particle with ~1 μm long and ~0.5 μm wide elongated pilus. We have found a much larger (~12 × 4 μm) protozoan-like particle D4-404K **(Fig. 3-35)** with ~8 μm long and ~2 μm wide tail-like growth at one end, indicating a possibly viable cell. The distortion of the surface of the cell is presumably the result of extreme conditions in space or in upper atmosphere.

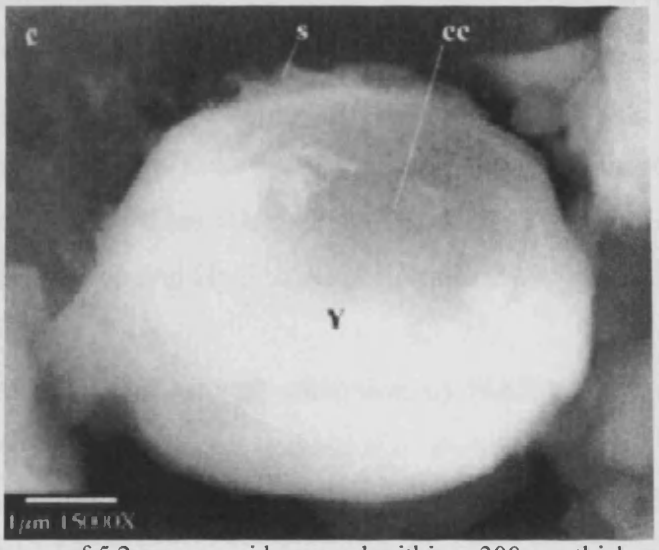

Figure 3-39: ESEM image of 5.2 μm coccoid encased within a 300 nm thick carbonaceous envelope. (Hoover, 2006)

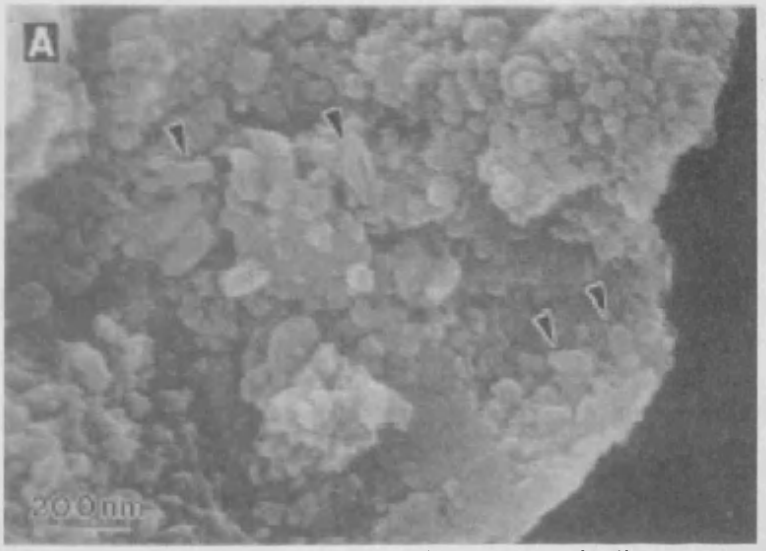

Figure 3-40: SEM image showing numerous ovoids, about 100 nm in diameter (arrows), and tubular-shaped bodies (arrows) associated with ALH84001 carbonate globules. Smaller angular grains may be the magnetite and pyrrhotite. (McKay *et al.*, 1996)

3.4 Discussion

The study of meteorites and Interplanetary Dust Particles (IDPs) is of much topical interest since their morphology and elemental abundances can have a bearing on the nature of their parent bodies – comets or asteroids. The IDPs collected by Brownlee (1976a) using U-2 aircraft flown at an altitude of ~20 km had contained similar elemental abundances to those of carbonaceous chondritic meteorites. Recent studies of some carbonaceous meteorites (Orgueil and Lvuna) revealed that they originated from comets like Hale-Bopp and Hyakutake (Ehrenfreund *et al.*, 2001).

Since 1981, many attempts of aircraft collection by NASA had successfully yielded different IDPs, which include non-chondritic dust particles (Brownlee, 1985). However, the aircraft collection technique undercounted the smaller fraction (<few μm) due to its high velocity upon collection destroying the fragile particles. Our results show that the cryogenic sampler carried by balloon in India, 2001, successfully collected many smaller and more fragile particles from an altitude of 41 km.

Our morphological and elemental abundance analysis of the IDPs collected using the balloon-borne cryosampler shows amazing similarities with the IDPs previously collected by U-2 aircraft (Brownlee, 1985; Bradley *et al.*, 1983) and with the nature of comets that have recently been established (Jessberger, 1999; A'Hearn *et al.*, 2005; Bridges *et al.*, 2008; Flynn, 2008). These correspondences effectively prove their extraterrestrial origin. This conclusion is further supported by our discovery of a presolar crystal of Titanium embedded in one of the particle that was examined.

We identified many particles that had the characteristics of microbiological life-forms. Our collection includes particles similar to many microfossils discovered within the carbonaceous meteorites (McKay *et al.*, 1996; Hoover *et al.*, 2004, 2006), and also those bacterial spore-like particles with one of them forming a pilus. These discoveries support the Hoyle and Wickramasinghe's cometary panspermia (1978),

where a small fraction of microorganisms in the interstellar cloud was incorporated within comets, amplified and delivered to the habitable planets like Earth.

However, the analysis of only morphology and the elemental abundances of the primitive organisms leave some degree of uncertainty as to their viability in space. Further biological analyse are therefore required to reveal the answer to questions relating to the survival of microorganisms in the extreme conditions such as in space and the Earth's upper atmosphere. The analysis in the next chapter deals with some of these questions.

CHAPTER 4

Investigation of Biological Material in the Stratosphere

4.1 Introduction

4.1.1 General Introduction

It has long been known that extremophiles thrive in the extreme boundaries of life. Such microorganisms can survive in extreme temperatures, pH, salinity, and even in environments with high radiation levels. Relating to the question concerning the upper boundary of the biosphere, research had been done many decades ago. Early experiments go as far back as 1934 where the balloon Explorer II was launched in The United States to search for life in an altitude of as high as 20 km. The payload of a metal cylinder containing a parachute and a sampling device was thrown down from the balloon gondola at the target height. This experiment led to the successful collection of a terrestrial bacterium and microscopic fungi from the lower stratosphere (Rogers *et al.*, 1936).

In the 1960's and 1970's, while many space projects were being carried out focussing people's attention on space, upper atmospheric research were also done with the aim of detecting extraterrestrial life (Bruch, 1967). In 1967, Russian scientists, Imshenetsky and Lysenko *et al.* (1978), used rocket probes to obtain aerosol samples. They claimed to isolate four fungi and two bacterial species from the mesosphere at an altitude of 48 to 77 km. Although the techniques for conducting such experiments aseptically at the time were inadequate, the result came with an indication that they were introduced from outside. This work could have been a major support for the theory of Panspermia. However, it was difficult to defend this claim against the possibility of contamination on account of the limited sterilization procedures that were used.

The evolution of new techniques, which can minimise these problems, became available in the late 1990's (Shayamlal *et al.*, 1996). A prototype cryogenic sampler was first tested for its feasibility at the range of 10-36 km in 1999. The unpublished results showed the isolation of *Pseudomonas stutzeri*. However, due to the low altitude of collection, it was still arguable that it was a terrestrial contamination. To

avoid any cross-contamination from terrestrial environment, this cryogenic sampler had to be taken above the upper boundary of the biosphere.

In 2001, Indian Space Research Organisation collaborated with others and launched a balloon-borne experiment carrying this new cryogenic sampler to the altitude of 41 km. The methods used for the collection and the extraction of air sample are explained in chapter 3. Those samples are tested for any sign of biology of extraterrestrial origin.

4.1.2 Previous Studies of Biological Analysis

After the recovery of air samples from the balloon experiment, Harris and Wainwright had studied these samples. Harris *et al.* (2002) used 0.45 μm micropore filter since this size was expected to have trapped microbial sized particles. The filter was aseptically cut to 4 mm^2 squares and treated with either a fluorescent cationic carbocyanine dye, which detects the cell membranes of viable cells, but not of dead cells, or an acridine orange, which stains the nucleic acid. The techniques of those dyes are explained elsewhere (Lloyd and Hayes, 1995; Lopez-Amoros *et al.*, 1995).

The dye-treated samples were observed under a fluorescence microscope and the expectation was that any microorganisms present would fluoresce under ultraviolet light. Figure 4-2 was one of the images taken from the 20 km altitude filter (A1) and shows clearly the form of clumps of 0.3-1 μm sized cells, the clumps themselves measuring 5-15 μm across. The filter from 41 km altitude (D1) also trapped clumps of cells **(Fig. 4-1)**. Wallis and Al-Mufti *et al.* (2002) with their SEM images had detected the morphologically similar clumps of cells from 41 km **(Fig. 4-2)**. Since every procedure was carried out with maximum care possible and none of the fluoresced cells were found in the controls, there was little doubt that the fluorescent dye had detected the living cells from the stratosphere.

Wainwright *et al.* (2003) used many different media to culture any viable cells from 41 km sample filter. After 4 days incubation of a soft potato dextrose agar medium (PDA) at 25°C, although no cultures grew, some bacteria were observed under the

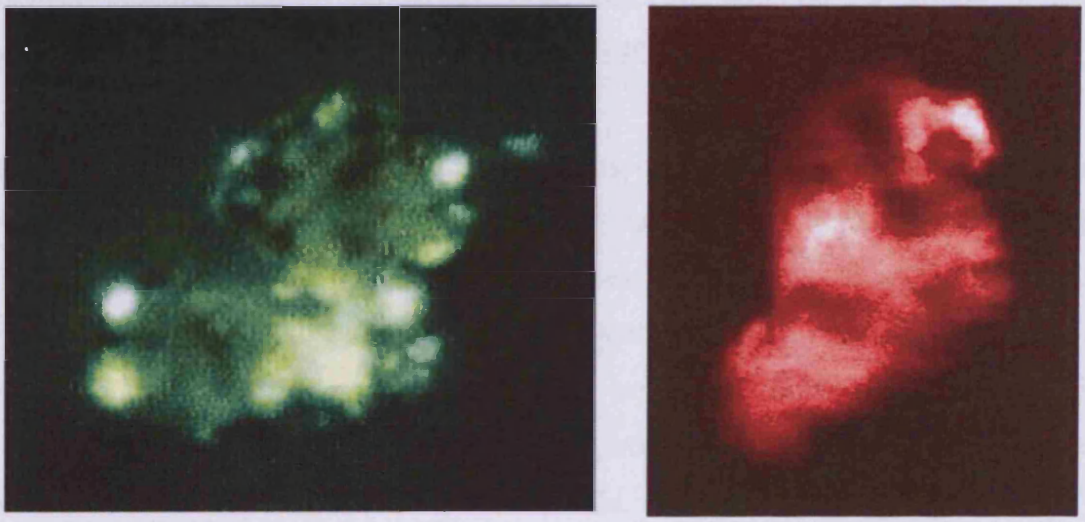

Figure 4-1: (Left) Clumps of cells from 20 km fluorescing after staining with carbocyanine dye. (Right) Clumps of the cells from 39 km fluorescing after staining with acridine orange. The former detecting membrane potential of viable cells, the latter the presence of nucleic acid (Harris *et al.*, 2002)

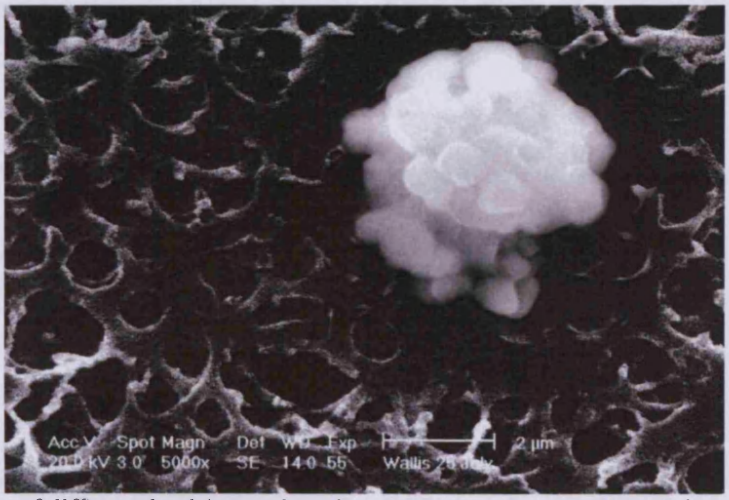

Figure 4-2: Clump of diffuse-edged (non-mineral) 0.6-0.8 µm spheres collected from 41 km. Morphologically similar to those clumps of cells stained with carbocyanine dye (Wallis and Al-Mufti *et al.*, 2002)

optical microscope. The surface medium of the PDA plates was then aseptically transferred to L-broth medium (LB) and incubated for further 2 days at 30°C. Two bacteria species were isolated namely *Staphylococcus pasteuri* (99.9% similarity) and *Bacillus simplex* (100% similarity) **(Fig. 4-3)**. In addition, a single fungus, *Engyodontium album*, was also isolated from the PDA plates.

These results show that viable microorganisms do exist in the upper stratosphere where there is little chance that terrestrial life can reach. A further experiment by Wainwright *et al.* (2004) managed to identify the similar clumps of cells as previously reported by Harris *et al.* (2002) using Live/Dead stains. However, no colonies of microorganisms were isolated from the same sample by using the growth media. Wainwright proposed that most of the stratospheric bacteria present on the sample filters are viable but non-culturable (VBNC) cells.

In this Chapter, I demonstrate the direct 16S rRNA gene analysis from the bulk sample filter. The aim is to identify any VBNC cells from those filters.

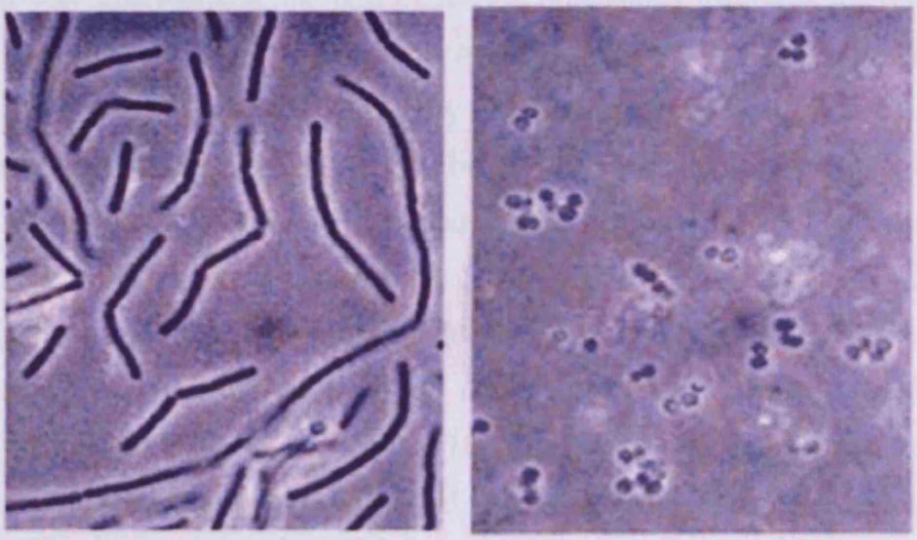

Figure 4-3: Cultures of *B. simplex* (Left) and *S. pasteuri* (Right) grown on LB medium after isolation using soft PDA from stratospheric samples at 41 km. (x1000 using phase contrast microscope) (Wainwright *et al.*, 2003)

4.2 Materials & Methods

In this section, the procedures used for DNA isolation and amplification from the stratospheric air sample filter are explained. If there are VBNC cells on the sample filter, they would be identified by isolating their DNA directly from the bulk filter and comparing them with bacterial gene sequences in the data bank of known microorganisms. The procedures were carefully carried out in a sterile laminar flow chamber with fully sterilised tools to avoid any cross contamination. Negative controls were introduced to confirm the contamination free procedures.

4.2.1 Isolation of DNA from the Bulk Filter

Solutions used in this experiment were supplied in the FastDNA® SPIN Kit for Soil (Bio101® Systems). All tools such as tips and pipettes were autoclaved and/or UV sterilised in the CL-1000 Ultraviolet crosslinker for 5 minutes. The environment was maintained as RNase and DNase free conditions at all times.

Methodological comparisons of different DNA extraction techniques including our kit were studied before (Webster *et al.*, 2003). Since our sample filter was expected to contain a very low biomass, the best extraction procedures from this reference were used to obtain the maximum DNA yield. A half section of 0.45 μm cellulose nitrate filter from 41 km (D6) was cut aseptically into smaller pieces using a sterile scalpel blade and added into Lysing Matrix E Tube. A 900 μl volume of Sodium Phosphate buffer and 120 μl MT buffer were added into the tube. The tube was secured in FastPrep® Instrument and processed for 30 seconds at speed 5.5. The tube was centrifuged at 14,000 rpm for 8 minutes. 800 μl supernatant was transferred to a clean silicanised 1.5 ml volume tube then 250 μl PPS reagent was added and mixed by shaking the tube by hand for 10 minutes. The tube was centrifuged at 14,000 rpm for 5 minutes. The supernatant was transferred to another clean silicanised 15 ml volume tube. Binding Matrix (1 ml) Suspension was added to the supernatant, and the tube repeatedly inverted by hand for 2 minutes. The tube was then placed in a rack for 30 minutes and the silica matrix allowed to settle. A 500 μl volume of supernatant was

carefully removed to avoid disturbing Binding Matrix. The Binding Matrix and the remaining supernatant were resuspended and this mixture was transferred to a SPIN™ Filter. After the centrifuging of the tube at 14,000 rpm for 1 minute, the catch tube was emptied, and then 500 µl SEWS-M was added to the SPIN™ Filter, which was sequentially centrifuged at 14,000 rpm for 1 minute and discarding the flow-through for a couple of times to dry the matrix. A 100 µl volume of DES was added and gently flipped the tube by finger to resuspend the matrix. After leaving the SPIN™ Filter for 20 minutes, the SPIN™ Filter was centrifuged at 14,000 rpm for 2 minutes to transfer eluted DNA to catch tube. The catch tube and the SPIN™ Filter were stored at -40°C.

The same protocols were repeated with the control filter (E4), which was an identical 0.45 µm cellulose nitrate filter but without having the air passing through. Also the same protocols were carried out without any filters for a blank control. To quantify DNA yield, the extracts were examined by agarose (1.2% w/v) gel electrophoresis, stained with 0.5 µg/ml ethidium bromide and compared with HyperLadder I DNA quantification marker (Bioline).

4.2.2 Polymerase Chain Reaction (PCR) Amplification of 16S rRNA Gene Sequences

16S rRNA genes were amplified by the combinations of 27F-907R, 27F-1492R and 357F-GC-518R using PCR.

Primer	Sequence (5'-3')	Reference
27F	AGA GTT TGA TCA TGG CTC AG	DeLong, 1992
907R	CCG TCA ATT CAT TTG AGT TT	DeLong, 1992
1492R	GGT TAC CTT GTT ACG ACT T	DeLong, 1992
357F*	CCT ACG GGA GGC AGCAG	Muyzer *et al.*, 1993
518R	ATT ACC GCG GCT GCTGG	Muyzer *et al.*, 1993

Table 4-1: Details of the primers used. *For DGGE this primer has the GC-clamp at the 5' end, CGCCCGCCGCGCGCGGCGGGCGGGGCGGGGGCACGGGGGG (Muyzer *et al.*, 1993)

Primary Annealing:

Both 27F-907R and 27F-1492R primers were used for the primary amplification reactions. The DNA templates prepared were those from the DNA extraction method as well as the 1 µl of DNase/RNase free water for the negative control and 1 µl of known bacterial DNA (*Bacillus thuringiensis*) for the positive control. To increase the accuracy, two replicate reactions were prepared for each sample (except –ve and +ve controls) thus in total of 16 reactions were carried out as shown below:

No.	Primer 27F-907R	No.	Primer 27F-1492R
1	Air Sample filter 1	9	Air Sample filter 1
2	Air Sample filter 2	10	Air Sample filter 2
3	Control filter 1	11	Control filter 1
4	Control filter 2	12	Control filter 2
5	DNA Blank Control 1	13	DNA Blank Control 1
6	DNA Blank Control 2	14	DNA Blank Control 2
7	PCR -ve Control	15	PCR -ve Control
15	+ve Control (Bacteria)	16	+ve Control (Bacteria)

Table 4-2: The samples prepared for primary annealing. **Air Sample filter** – Stratospheric air plus nitrate membrane filter plus DNA extraction solution; **Control filter** – Nitrate membrane filter plus DNA extraction solution; **DNA Blank Control** – DNA extraction solution only; **PCR -ve Control** – Without any previous solution; **+ve Control** – known Bacteria plus DNA extraction solution.

The reagents for PCR reaction were added in the following order:

Reagents	Amount
1x reaction buffer (Bioline)	0.5 µl
Forward Primer 27F (50µg/ml)	0.5 µl
Reverse Primer 907R or 1492R (50µg/ml)	0.5 µl
0.25mM dNTP (Bioline)	0.5 µl
1.5mM $MgCl_2$ (Bioline)	1.5 µl
1.5 U Biotaq DNA polymerase (Bioline)	0.25 µl
DNA template	1 µl
DNase and RNase free water (Bioline)	25.25 µl
Total	50 µl

Table 4-3: Amounts of the reagents used for the preparation of primary PCR reaction.

The PCR reaction was carried out in a DNA Engine Dyad Thermal Cycler (MWG AG BIOTECH Primus 96 ^{PLUS}, MJ Rsearch, Boston, MA, USA) according to the following sequences:

1. Held at 95°C for 2 minutes
2. 30 cycles of 94°C for 30 seconds → 52°C for 30 seconds → 72°C for 90 seconds plus 1 second per cycle
3. Final extension step at 72°C for 5 minutes

Secondary annealing:

357F-GC-518R primer was used for the secondary amplification reactions. For the DNA templates, the primary PCR products of the sample filters, the control filters, the blank controls and the negative controls were prepared. 1 µl of known bacterial DNA (*Bacillus thuringiensis*) was used as the positive control, not those from the first reactions, thus in total of 15 reactions were carried out as shown below:

No.	27F-907R and 357F-518R	No.	27F-1492R and 357F-518R
1	Air Sample filter 1	8	Air Sample filter 1
2	Air Sample filter 2	9	Air Sample filter 2
3	Control filter 1	10	Control filter 1
4	Control filter 2	11	Control filter 2
5	Blank Control 1	12	Blank Control 1
6	Blank Control 2	13	Blank Control 2
7	-ve Control	14	-ve Control
15	Only secondary annealing by 357F-518R: +ve Control (Bacteria)		

Table 4-4: The samples prepared for secondary annealing. **Air Sample filter** – Stratospheric air plus nitrate membrane filter plus DNA extraction solution; **Control filter** – Nitrate membrane filter plus DNA extraction solution; **Blank Control** – DNA extraction solution only; **-ve Control** – Without any previous solution; **+ve Control** – known Bacteria plus DNA extraction solution.

The reagents for PCR reaction were added in the following order:

Reagents	Amount
1x reaction buffer (Bioline)	5 µl
Forward Primer 357F (50µg/ml)	0.5 µl
Reverse Primer 518R (50µg/ml)	0.5 µl
0.25mM dNTP (Bioline)	0.5 µl
1.5mM $MgCl_2$ (Bioline)	1.5 µl
1.5 U Biotaq DNA polymerase (Bioline)	0.25 µl
DNA temperate	1 µl
DNase and RNase free water (Bioline)	40.75 µl
Total	50 µl

Table 4-5: Amounts of the reagents used for the preparation of secondary PCR reaction

The PCR reaction was carried out in the same sequences as shown in the *primary annealing*.

4.2.3 Denaturing Gradient Gel-Electrophoresis (DGGE) Analysis

DGGE was carried out on the secondary PCR products to analyse the bacterial community of the stratospheric air sample. The basic protocols for construction and running of the DGGE kit in this experiment were explained in Zwart *et al.* (2004).

Glass plates of the gelchamber and the gradient maker were cleaned with detergents and rinsed with ionised water thoroughly and dried with Watman paper. The gelchamber was constructed, and the pump was connected to the gradient maker. The pump tube was emptied and the pipette tip at the outlet tube was attached to the top-middle of the gelchamber with tape. Both 4 µl TEMED and 40 µl APS were added to 4 ml of 0% denaturant solution (100% denaturant is defined as 7 M urea with 40% [vol/vol] formamide). This mixture (1 ml) was poured between the glasses of the gelchamber evenly to check for any leakage. Denaturant solution acrylamide was prepared with a final volume of 12 ml of acrylamide solution with the highest denaturant concentration (60% denaturant, 12% acrylamide gel) and 12 ml of acrylamide solution with the lowest denaturant concentration (30% denaturant, 8%

acrylamide gel). Both 6 µl TEMED and 60 µl APS were added to 60% and 30% acryl-denaturant, and mixed well immediately. They were poured into the designated slot of the gradient maker. The pump was started at 5 ml/min and filled the gelchamber slowly. After all the solutions were poured, a few ml of water-saturated butanol was added on top of the gelchamber to obtain a straight surface. The gelchamber was then sealed with cling film and left overnight to let the gel polymerise.

After the polymerisation, the butanol was washed out well with de-ionized water. The comb was placed and filled up the gelchamber with a 0% denaturant solution, 8 µl TEMED and 80 µl APS. The gelchamber was sealed with cling film again and left to polymerise for a few hours. Meanwhile The DGGE tank was filled with 7 litres of 1 x TAE buffer. The circulation of the tank was started and left until the temperature reached 65°C.

Figure 4-4: Image of DGGE analysis apparatus

After the gel was polymerised, the comb was removed, and the empty slots were flushed and filled with the buffer. Each PCR products (10 µl) were mixed with 2 µl loading dye and they were loaded by using the gel-saver-tips. For +ve control, only 5 µl was loaded since it will appear brighter than others. A 10 µl volume of the marker was loaded as well. The gelchamber was placed in the tank slowly, and then the circulation was restarted at 60°C. The gel was run at 80V for 10 minutes followed by 200V for 5 hours **(Fig. 4-4)**. When the circulation was ended, the gel was taken out from the gelchamber and stained with SYBRGold nucleic acid gel stain (Molecular Probes) for 20 minutes. The gel was imaged and captured with a Gene Genius Bio Imaging System (Syngene).

4.2.4 Re-amplification and Sequencing of the Target Genes

The target bands from the DGGE gel were excised with sterile scalpel blade and placed in 0.5 ml tube. They were washed with 50 µl of DEPC treated Nuclease free water (Seven Biotech Ltd.) for 10 minutes, and then the water was removed. They were air dried for 10 minutes and crushed with a clean sterile tip. A 10 µl volume of sterile distilled water was added to the each tube and centrifuged for 30 seconds so that all samples were at the bottom of the tube. They were left for overnight at 4°C (Webster *et al.*, 2006, 2007). 1 µl of the crushed band solution was used as DNA template and re-amplified by using the same technique as the *secondary annealing*. The concentrations of re-amplified products were calculated and they were sequenced directly with 518R primer using an ABI PRISM 3100-Genetic Analyzer (Applied Bio-systems, Foster City, CA, USA). Samples run on a 50 cm capillary array using pop7 performance optimized polymer. Sequenced partial 16S genes were subjected to a NCBI BLASTN (http://www.ncbi.nlm.nih.gov/blast/) search to identify sequences with highest similarity.

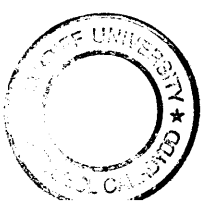

4.3 Results

4.3.1 Determination of DGGE Profile and Sequences of Excised Band

A half section of 0.45 μm cellulose nitrate filter from 41 km (D6) was aseptically crushed by the mixture of ceramic and silica particles supplied in FastDNA® SPIN Kit for Soil (Bio101® Systems), which are designed to efficiently lyse all microorganisms. Bacterial 16S rRNA genes were then amplified using nested PCR with the combination of 27F-907R or 27F-1492R and 357F-GC-518R primers **(Table 4-1)**. Nested PCR products were subjected to DGGE analysis, where individual bacterial 16S rRNA genes were separated using 8% (w/v) polyacrylamide gels with a denaturant gradient between 30% and 60%.

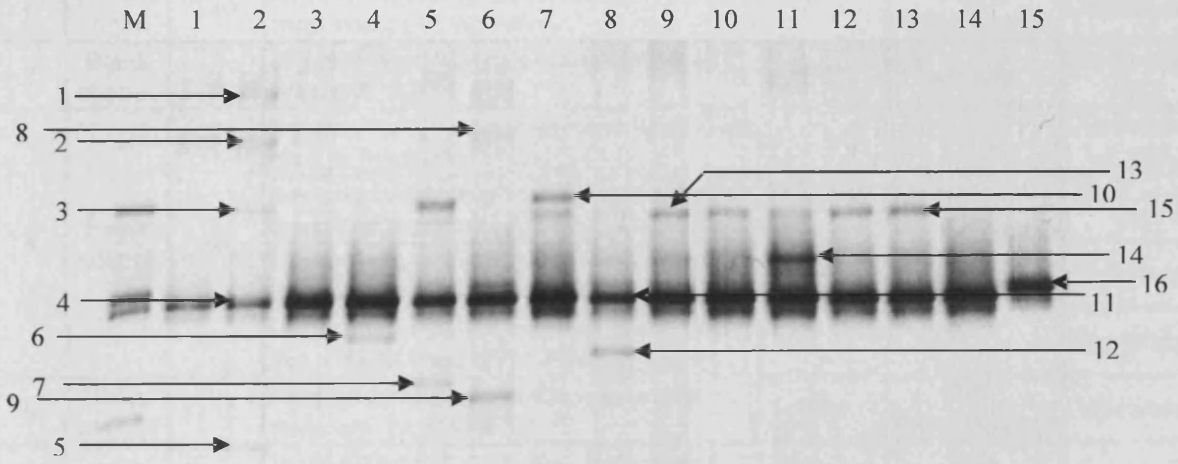

Figure 4-5: DGGE profile delivered from the stratospheric air sample collected at 41 km. **Lane M** – Marker; **Lane 1-7** – Annealing by 27F-907R and 357F-GC-518R primers; **Lane 8-15** – Annealing by 27F-1492R and 357F-GC-518R primers; **Lane 1, 2, 8, 9** – sample filter; **Lane 3, 4, 10, 11** – control filter; **Lane 5, 6, 12, 13** – blank control; **Lane 7, 14** – -V control; **Lane 15** – +V control (*B. thuringiensis*)

Analysis of DGGE profiles **(Fig. 4-5)** identified a number of separated bands demonstrating a number of possible bacterial species present. Each band on the gel is assumed to be representative of one distinct species (Webster *et al.*, 2002), which was proved upon sequencing of the band. Nineteen DGGE bands were targeted. They were excised with sterile scalpel blade, which were then extracted and re-amplified. After careful purification of the target DNA, they were sequenced directly with the 518R primer and sequences identified here using BLASTN with highest similarities in the DNA data bank **(Table 4-6)**.

Band No.	Origin	Length (bp)	Closest Relative by BLASTN analysis	Similarity	Phylogenetic Family	Reference
1	Sample	193	Biphenyl-utilizing bacteria from contaminated pine root zone (EF507033.1)	96%	Actinobacteria	Leigh *et al.* 2007
			Jiangella gansuensis from a desert soil north-west China (AY631071.1)			Song *et al.*, 2005
2	Sample	130	Biphenyl-utilizing bacteria from contaminated pine root zone (EF507033.1)	96%	Actinobacteria	Leigh *et al.* 2007
			Jiangella gansuensis from a desert soil north-west China (AY631071.1)			Song *et al.*, 2005
3	Sample	72	Bacteria from a plague-like diseased region of Caribbean coral (AF544953.1)	100%	Alpha Proteobacteria	Pantos *et al* 2003
4	Sample	200	*Burkholderia sp.* from the weathering feldspars (EU876657.1)	95%	Beta Proteobacteria	Unpublishe
5	Sample	21	*Thermococcus sp.* from mid-Atlantic deep sea vent. DGGE band T31 (AJ874321.1)	100%	Thermotogae	Postec *et al.* 2005
6	Control filter	140	Hexane-degrading bacteria from consortium (AY903892.1)	97%	Alpha Proteobacteria	Unpublishe
7	Blank control	21	18S rDNA of *Xenopus laevis* similar to yeast (X02995.1)	100%	Metazoa	Salim *et al.* 1981
8	Blank control	86	Bacterium in kerosene-based drilling fluid used in Antarctica (DQ422867.1)	94%	Alpha Proteobacteria	Alekhina *et al.*, 2007
			Bacterium from methane hydrate deep marine sediments near Japan (AY093470.1)			Reed *et al.*, 2002
			Bacterium associated with corals from Bermuda and Panama (AF365515.1)			Unpublishe
			Bacterium in marine aerosols in the East Sea. DGGE band ES01-E26 (AY436581.1)			Unpublishe
9	Blank control	173	*Burkholderia sp.* from the weathering feldspars (EU876657.1)	96%	Beta Proteobacteria	Unpublishe
10	–ve control	199	*Burkholderia sp.* from the weathering feldspars (EU876657.1)	95%	Beta Proteobacteria	Unpublishe
11	Sample	200	*Burkholderia sp.* from the weathering feldspars (EU876657.1)	95%	Beta Proteobacteria	Unpublishe
12	Sample	201	*Lactuca sativa* Chloroplast (AP007232.1)	99%	Plastids	Timme *et al.*, 2007
			Gonystylus bancanus chloroplast from rainforst tree species (EU849490.1)			Unpublished
13	Sample	199	*Burkholderia sp.* from the weathering feldspars (EU876657.1)	95%	Beta Proteobacteria	Unpublished
14	Control filter	210	*Burkholderia sp.* from the weathering feldspars (EU876657.1)	95%	Beta Proteobacteria	Unpublished
15	Blank control	199	*Burkholderia sp.* from the weathering feldspars (EU876657.1)	95%	Beta Proteobacteria	Unpublished
16	+ve control	210	*Bacillus thuringiensis* (EF638801.1)	100%	Firmicutes	Unpublished

Table 4-6: Phylogenecity of each isolated DGGE gel bands. Actinobacteria (Band 1 and 2) and Plastids are identified from the stratospheric sample. Contamination of *Burkholderia sp.* is also found in many controls and sample filter. Proteobacteria (Band 3), Thermotogae (Band 5) and Metazoa (Band 7) are too short sequences to be fully reliable identification.

4.3.2 Phylogenetic Analysis of Bacterial community in the Stratosphere

Table 4-6 shows summarised phylogenetic data of species sequenced from the targeted DGGE bands. Band 1 and 2 from the stratospheric sample are 96% similar to the partial 16S rRNA sequences of an uncultured biphenyl-utilizing bacterium strain from a polychlorinated biphenyl contaminated pine root zone (Leigh *et al.*, 2007) and *Jiangella gansuensis* isolates from a desert soil north-west China (Song *et al.*, 2005) **(Fig. 4-6)** within the phylum Actinobacteria. Actinomycetes are Gram-positive bacteria known to survive in extreme conditions. They are further discussed later.

GGATGCCCTCCGTCGTCACCCCTTATAACGTGTTACCCGCT
TTCGGACTACGTCGTTGCGGCGCACTCCCTACTGCCGGAAG
CCCAACATTTGGAGAAAGCCGCGGCTGCTTCGGAAGCCCA
CTGACATCCGCGTCTTCTTCGTGGCCGGT

Figure 4-6: Identified partial 16S rRNA sequence of Actinomycete from DGGE band 1 (*J. gansuensis*)

Band 3 (stratospheric sample) is 100% similar to the partial 16S rRNA gene sequence of Alphaproteobacteria from a diseased region of Caribbean corals (Pantos *et al.*, 2003). They are Gram-negative bacteria and comprise many phototrophs, methylotrophs (e.g. *Methylobacterium sp.*) and nitrogen-fixing symbionts (e.g. *Rhizobium sp.*) (Kersters *et al.*, 2006). Those phototrophs include purple non-sulfur bacterium which contains bacteriochlorophylls for photosynthesis and uses organic substrates instead of CO_2 for food production (Bryant *et al.*, 2006). The amplified sequence from this band, however, was very short (72 bp) and obtained very low score from the BLASTN, which left some uncertainty to this result.

Identification of archaea *Thermococcus sp.* (Postec *et al.*, 2005) from band 5 (stratospheric sample) is also uncertain due to its very short sequence (21 bp).

Thermococcus sp. is a Gram-negative spherical thermophile, known to thrive above 80°C, and also an organothrophic anaerobe where it requires sulphur for decent growth. This is ideal characteristics for the extraterrestrial extremophile entering the Earth's atmosphere possibly thriving in the sulfide chodule of chondritic meteorites. Since we used bacterial 16S rRNA primers, finding of archaea is a bit strange and it is possible due to low score from the BLASTN. Therefore this is not conclusive.

One of the intriguing results from the DGGE excise of the stratospheric sample is our discovery of chloroplast from band 12. It is 99% similar to the chloroplast of *Lactuca sativa* (Timme *et al.*, 2007) and *Gonystylus bancanus* (Cannon *et al.*, EU849490.1) **(Fig. 4-7)**. *L. sativa* is a flowering plant in the family of Asteraceae, commonly found in many countries around the world, and *G. bancanus* is a flowering plant in the family of Thymelaeaceae, and native at Brunei, Indonesia and Malaysia. They are both seed-forming plants called spermatophyte.

Chloroplast is photosynthetic organelle found in plants, algae and protists. It is formerly free-living photosynthesizing organism (generally considered to be cyanobacteria) that has been sequestered by eukaryotic hosts with a process called endosymbiosis. The close studies of chloroplast genomes of *L. sativa* found fast-evolving DNA sequences indicating its possible contribution to the primitive endosymbiotic evolution of plastids (Timme *et al.*, 2007). They are further discussed later.

GGATGCCCTCCGTCGTCACCCCTTAAAAGGCGTTACCCGCT
TTCGGACTGCCTCGTTACGGCGCACCTCCATCTTCCGCGTG
CCCAGTACTTGAAGAAAAGGGCCTCTTCTTCGTTACTGCCA
TAGACCCCTTATTC

Figure 4-7: Identified partial 16S rRNA sequence of chloroplast (*L. sativa and G. bancanus*)

4.3.3 Contamination Aspects of PCR-DGGE Work

All the procedures throughout the whole experiments were carried under maximum sterility to avoid contamination. All the disposable plasticware and the pipettes were autoclaved and/or UV treated prior to use. Laminar air-flow cabinet was used to eliminate the contamination from the atmosphere.

The problem with working with low biomass samples as ours and those of similar environments, such as deep biosphere (Webster *et al.*, 2003, 2006), is the sensitivity of nested PCR, which can detect any small contaminants from the reagents as well. Therefore the negative and the blank controls were introduced. Table 4-6 shows 95~96% sequence similarity to the partial 16S rRNA gene of potassium-solubilising bacterium *Burkholderia sp.* from the weathering feldspars (Fei, EU876657.1) was identified in sample filter (bands 4, 11, 13), blank control (bands 9 and 15), negative control (band 10), and control filter (band 14). Contaminant of 97% sequence similarity to hexane-degrading bacteria (Lee *et al.*, AY903892.1) was identified in the control filter (band 6). Other bands with short sequences were also identified from the blank control (bands 7 and 8) giving an unreliable results.

DGGE profile **(Fig. 4-5)** shows that the contaminants from the reagents were found in many different lanes including the controls, and were different to those bacteria found in stratospheric sample filters. Therefore we are confident that our results are robust and the bacteria found have probably come from the stratosphere.

4.4 Discussion

The Earth's upper atmosphere has been extensively studied for many decades to identify any sign of extraterrestrial life coming into Earth (Bruch, 1967; Imshenetsky *et al.*, 1976). While the placement of the upper bundary of the biosphere has been argued by many scientists for a long time, it is now generally accepted that only a very few terrestrial microorganisms can cross the troposphere and unlikely to reach the upper stratosphere (Rogers *et al.*, 1936). In 2001, a balloon-borne probe carring the prototype cryogenic sampler was flown to an altitude of upto 41 km, high in the upper stratosphere, in an attempt to collect any extratterestrial life-forms that may be entering our atmosphere from space. Although a bacterium and a fungus was cultured from such sampling by Wainwright *et al.* (2003), the possibility of terrestrial organisms lofted from below cannot be excluded. More convincingly, Harris *et al.* (2002) and Wainwright *et al.* (2004) obtained evidence of VBNC microbes that could have had a cometary origin.

4.4.1 Actinobacteria

The result from the PCR-DGGE analysis of the stratospheric air sample (41 km) show the identification of actinomycete, which is 96% similar to *Jiangella gansuensis*. *J. gansuensis* was recently discovered in the desert soil of north-west China (Song *et al.*, 2005). Some species of actinomycetes are known to produce external spores, which can become airborne by mechanical disturbance of the substance they are growing on (Lloyd, 1969). The past studies have managed to isolate actinomycetes from the air sample with impactor (Nevalainen *et al.*, 1991; Dawson *et al.*, 1996). Further details of characteristics of airborne actinomycete spores are given in Reponen *et al.* (1998).

Many microorganisms are known to travel within clouds of desert dust for large distances therefore *J. gansuensis* found in the Chinese desert is probably no expection. However, the study of atmospheric movement shows the microorganisms containing Chinese desert dusts travel east and not to Hyderabad, India where the balloon was launched (Griffin, 2007). This indicates that actinomycete found in our sample is very unlikely to be those airborne terrestrial contaminants.

Although the survival of actinomycetes on the surface of toxic metals and soils are well studied (e.g. Watanabe, 2001; Ahmad *et al.*, 2005), only a little of their survival in the harsh condition of space is understood. The initial study of the same stratospheric air sample (41 km) by Wainwright *et al.* (2003) indentified firmicutes *B. simplex*. These spore-forming bacilli are known to thrive in exposure to the solar radiation if they are embedded in clay or rock materials (Horneck *et al.*, 2001). The present study shows that even non-spore-forming actinomycetes, such as *arthrobacter sp.* (same family as *Jiangella sp.*) and *Microbacterium sp.*, can survive in the same solar UV flux as at the Martian surface if they are shielded by Martian dusts (Osman *et al.*, 2008).

4.4.2 Chloroplasts

From our PCR-DGGE analysis, we identified chloroplast 99% similar to flowering plants of *Lactuca sativa* and *Gonystylus bancanus*. Chloroplast is a member of plastid genera and its evolutionary history of endosymbiosis has been widely investigated. Major controversies exist with respect to the number of primary endosymbioses leading to an individual chloroplast. Despite the diversity in ultrastructure of chloroplasts and chemical composition of chlorophyll within different species, it is now generally accepted that a single endosymbiosis event gave rise to the evolution of plastids. Those plastids surrounded by two membranes, such as green/red algae and from plants, arose by primary endosymbiosis, possibly from cyanobacteria (Whatley *et al.*, 1981; Cavalier-Smith, 1982), whereas those surrounded by three (e.g. dinoflagellate) and four membranes (e.g. cryptophyte) arose by secondary endosymbiosis, possibly from red or green algae (Gibbs, 1978, 1981).

Since chloroplasts in the flowering plants are inherited from the female ovule and not from the male pollen, only possible way of conveying them from a terrestrial origin to the stratosphere is by seeds. However, the possibility of such a large and heavy particle (smallest seed known is orchid seed with 0.2~0.6 mm) reaching to the upper stratosphere is inconceivable. The only remaining option is importation from space. Tepfer *et al.* (2006) argues that plant seeds are a possible vector of introspermia. He

demonstrated that seeds can survive in harsh environments, such as extreme cold, heat and desiccating conditions. The seed coat also can impede the penetration of UV light thus protecting multiple genomes as well as the endosymbionts, such as chloroplasts, within their tissues.

The limitation of this interpretation is that if chloroplasts exist as independent entities in space, evolutionary endosymbiosis must have had happen somewhere in an extraterrestrial setting in near-identical direction to that on Earth. It is, however, worth noting that even 1% difference of partial sequences of such a short plasmid of chloroplast may produce many different characteristics.

CHAPTER 5

Investigation of Red Rain Phenomenon

5.1 Introduction

5.1.1 General Introduction

The early reports on observations and investigation of a Red Rain type phenomenon goes as far back as early nineteenth century. Although Red Rain was occasionally observed even before that, people thought the red colour was caused by dust particles from a nearby desert, meteorite, or volcano. Intensive investigation began when Ehrenberg started to study the basics of what is now known as aerobiology in 1830's. He was very interested in the amount of organic particles and living or dead microorganisms in the atmosphere. He investigated so called 'paper meteorite' that flew from the sky near Rauden, Courland in 1687 and found blue-green algae or cyanobacteria, which are normally found in the marine microbial mats. He also found several other cyanobacteria and diatoms typical of microbial mats of the North Sea. He concluded that all of these paper-like substances were actually microbial mats that can be easily picked up by storms and transported over large distances, greater than 1000 miles, in some cases, until they fell with rainwater to the ground (Krumbein, 1995).

Around the same time, Brun from University of Geneva investigated red rain which fell in Djebel-Sekra, Morocco, and found that the red colour was caused by alga *Protoccocus fluvialis* (Fort, 1931). There were also newspaper reports of coloured rain at Kerala, India in 1896. Many phenomena concerning organic matter falling from the sky all over the world in the 1880's and 1890's are summarised in McAtee (1917).

Although it is common knowledge to us now that microorganisms do stay afloat in the troposphere, as many atmospheric scientists in twentieth century had proved, nobody actually knows the origin of most of those microorganisms in the atmosphere. In relation to Panspermia theory, McCafferty (2008) examined the historical accounts of red rain events and found 23 out of 80 references since 30 BC were possibly meteorite or comet related. It remains a possibility that some of the red-coloured microorganisms in the rainwater were originally conveyed from space within the meteorites.

5.1.2 Red Rain Phenomenon in Kerala

Early in the morning on 25th July 2001, local people at Changanacherry town in Kottayam district of Kerala, India, experienced an extraordinary red-coloured rainfall **(Fig. 5-1)**. This mysterious phenomenon continued to occur in many different parts of Kerala for next two months **(Fig. 5-2)**, in which the colour of the rain varied and in some of the cases was yellow, however in most of the cases the rain was red.

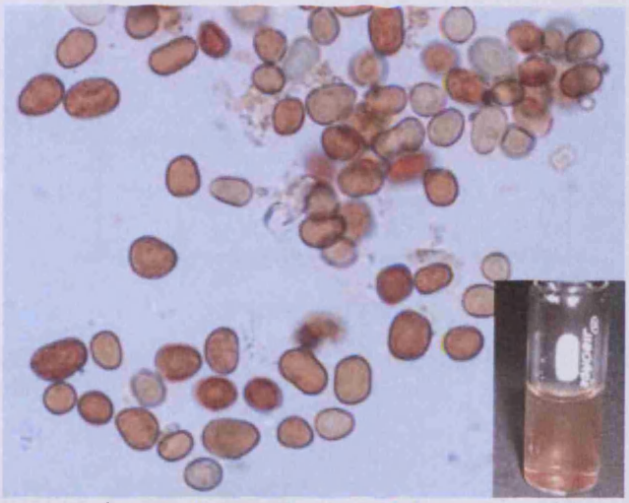

Figure 5-1: Optical microscopic image of the red rain particles under 1000x magnification. Particles have size variation from 4 to 10 μm. Inset shows red rainwater contained in a 5 ml sample bottle.

For those locals concerned about adverse health effects, the Centre for Earth Science Studies first investigated red rain samples. Sampath *et al.* (2001) and other co-workers reported that under the microscope, the red particles appeared to be spores of some microorganisms. They then managed to culture on corn meal agar growth media and identified as alga *Trentepohlia*. They concluded that lichen-forming algal spores from local sources were lifted by warm air in the morning and fell with the rainfall.

However, the story didn't end there since it didn't explain the mechanism of a huge amount of red rain cells falling over 2 months (one rainfall typically lasted less than 20 minutes). It is also puzzling that the red rain cells fell only over small areas, no more than a few square kilometres of south-west of India, and not other places where same *Trentepohlia* can be found. In fact, some people experienced the rainfall before the sunrise, therefore the lifting of local microorganisms by warm air or wind can be ruled out.

Figure 5-2: The geographical area marked by the dotted ellipse is where the red rain incidences mainly occurred in Kerala. (Louis and Kumar, 2006)

5.1.3 Further Studies of Red Rain

Louis and Kumar from Mahatma Gandhi University in Kerala have carried out further studies of the red rain cells (Louis and Kumar, 2006). They have visited most of the areas that reported the red rain events and estimated that ~50 tons of cells had fallen during this phenomenon. They have observed these cells under a scanning electron microscope (SEM) and transmission electron microscope (TEM), and found spore-forming microorganisms with very thick cell walls and possibly lacking a nucleus. They also compared the red rain cells with *Trentepohlia* but found that the red rain cells had different morphological properties.

The result from EDX analysis and CHN analyzer revealed that the red rain cells contain high abundances of carbon (49.53% wt) and oxygen (45.42% wt) with presence of some hydrogen and nitrogen. They next tested the samples using ethidium bromide fluorescent dye, which should fluoresce in the presence of DNA or RNA. They searched for fluorescence emission using a spectrofluorimeter, and the results

were negative. According to an unpublished paper Louis and Kumar (2003) have observed the growth of red rain cells at an extremely high temperature of 300°C. They concluded it is possible that these cells do not contain DNA or RNA but carry an alternative genetic material which allows them to survive at high temperatures. However, this has remained a speculative argument since it is very hard to prove.

Interviews with local people carried out by both Sampath and Louis recorded hearing an extremely loud thunder and seeing a lightning a few hours before the red rain. It is very unlikely to get thunderstorms during the south-west monsoon (July) in India, and one also expects to see multiple lightening if there is a thunderstorm. These testimonies can be explained if the cometary boride impacted the atmosphere at a high speed causing a flash of light and thunderous sound. The red rain phenomenon can be related to this event but again it is hard to prove with absolute conviction since no chondritic material was detected from the rain water.

It is of scientific interest to probe further the red rain cells and discover their origin from a biological standpoint. In this chapter I report further properties of the red rain cells obtained by using SEM, TEM, other types of fluorescent dye, and DNA isolation work. I also report SEM and fluorescent dye examination of the red rain cells heated at 300°C by Louis, which were sent to Centre for Astrobiology, Cardiff University for investigation.

5.2 Materials & Methods

In this section, the procedures used for morphological analysis, fluorescence dye analysis and DNA isolation on the red rain cells are explained. In morphological analysis, the techniques used are scanning electron microscopy (SEM), which can produce high-resolution images of a cell surface, and the microtome, which cuts a cell in a thin layer to observe the cell interior under the transmission electron microscopy (TEM). For the fluorescence dye analysis, Live/Dead stains and DAPI stains are used, and the DNA isolation was carried out by the same technique used as in chapter 4.

All the procedures were aseptically done by using the fully sterilised tools and avoided contamination. The red rain cells were washed to remove any microscopic debris in the solution before every experiment. The red rain solution was transferred to a 1 ml sterile tube. The tube was centrifuged at 2,000 rpm for 5 minutes. The supernatant liquid was removed and the resulting pellet was resuspended in DNase/RNase free water (Bioline) to wash and centrifuged again for 5 minutes. After three washes, the pellet was suspended in 1 ml DNase/RNase free water and taken to further experiments.

5.2.1 Preparation for Scanning Electron Microscopy (SEM)

The washed 1 ml red rain sample was filtered through 0.22 μm pore-sized Nuclepore Track-Etch Membrane. The filter was then dehydrated sequentially with 30%, 55%, 70%, 95% and 100% ethanol for 10 minutes each time. The alcohol was then drained out by using the critical point dryer for overnight. Approximately 25 mm^2 of the filter was cut with sterile scissors and attached to an aluminium stub 12 mm in diameter, which was then stabilised by gold sputter-coating at 40mA. The images of the red rain cells were taken by SEM with 20 keV of the electron beam under 7 x 10^{-9} bar vacuum (Philips XL20 SEM FEI). More detailed SEM techniques are explained in chapter 3.

5.2.2 Preparation for Transmission Electron Microscopy (TEM)

The washed 1ml red rain sample was centrifuged at 2,000 rpm for 5 minutes. The resulting pellet was embedded in 6% agar and fixed in 2.5% glutaraldehyde in 0.1 M phosphate buffer (pH 7.4) for 1 hour at room temperature. The fixed pellet was then rinsed in the same buffer for 30 minutes (3 x 10 minutes) and post-fixed for 1 hour in 1% osmium tetroxide. Following the post-fixation, the sample was dehydrated in a graded series of ethanol concentrations (50, 70, 80, 90 and 100%) each for 10 minutes. After another three changes of pure ethanol each for 10 minutes, the pellet was transferred into propylene oxide for 20 minutes (2 x 10 minutes), infiltrated overnight on a rotary mixer in a 1:1 (v/v) mixture of propylene oxide and araldite CY212 **(Table 5-1)** and finally embedded in pure araldite at 60°C for 2 days.

Reagents	Amounts
Aradite CY212	5.0g
DDSA	5.0g
BDMA	0.15g

Table 5-1: Recipe for Aradite embedding resin.

The polymerised resin block containing the sample was cut into 60-90 nm thick sections using a glass knife on a Reichert ultracut E microtome (Reichert-Jung, Leica, UK). The thin sections were collected on a pioloform coated copper grid and counterstained in 2% uranyl acetate for 10 minutes and Reynolds lead citrate for 5 minutes prior to examination. Ultrastructural observations were carried out using a transmission electron microscope (Philips TEM 208) operated at 80 kV accelerating voltage with magnifications ranging from 3,000x to 5,000x. The images were recorded on 4489 kodak film plates and developed according to a standard photographic method using D19 developer.

5.2.3 Fluorescence Dye Analysis

The red rain sample was treated with a fluorescence reagent called Live/Dead stains. It is used for observing the viability and the gram sign in living bacteria. All the reagents for Live/Dead stains were included in the LIVE *Bac*Light™ Bacterial Gram Stain Kit (Molecular Probers). It includes green fluorescent 3.34 mM SYTO 9 and red fluorescent 4.67 mM hexidium iodide nucleic acid stains. The SYTO 9 stain labels gram +ve and –ve bacteria, whereas hexidium iodide effectively displaces the SYTO 9 of only gram +ve bacteria. Therefore under the UV light, excitation/emission maxima for the gram +ve bacteria are about 480 nm/500 nm and gram –ve are about 480 nm/625 nm. Any dead bacteria will not fluoresce in these wavelength regions. The detailed properties of the kit can be found in the manufacturer's instructions.

To stain the cells, 1.5 μl of each reagent was first mixed together thoroughly, and then added into the washed 1 ml red rain sample. After mixing the sample with the stains thoroughly and incubating at room temperature in the dark for 15 minutes, 5 μl stained sample was trapped between a sterile glass slide and 18 mm square coverslip. It was observed under the UV fluorescence microscope (incident wavelength of 360 ~ 390 nm). The sample without the fluorescence reagents was also observed at the same wavelength for a negative control.

The red rain sample was also treated with DAPI stains (Sigma). DAPI (4', 6-diamidino-2-phenylindole) is a fluorescence reagent that binds strongly to DNA, and under the UV light, its excitation/emission maxima are about 358 nm/461 nm. 1 μl DAPI stain was mixed with the washed 1 ml red rain sample thoroughly and incubated at room temperature in the dark for 15 minutes. 5 μl of stained sample was transferred to a sterile glass slide and trapped with 18 mm square coverslip. It was observed under the UV fluorescence microscope (incident wavelength of 340 ~ 380 nm).

5.2.4 Isolation of DNA from the Red Rain Cells

In this experiment, the same FastDNA® SPIN Kit for Soil (Bio101® Systems) as in chapter 4 was used. The tools such as tips and pipettes were autoclaved in the CL-1000 Ultraviolet crosslinker for 5 minutes. The experiment was carried out in a sterile laminar flow chamber and maintained the aseptic conditions at all the time.

The washed 5 ml red rain sample was centrifuged at 2,000 rpm for 5 minutes and resuspended in 100 µl DNase/RNase free water (Bioline). It was then transferred into Lysing Matrix E Tube with 900 µl Sodium Phosphate buffer and 120 µl MT buffer. The tube was secured in FastPrep® Instrument and processed for 30 seconds at speed 5.5. The rest of the procedure was carried out as same as in chapter 4.2.1. The same procedure was carried out without the red rain sample for the negative control and with known bacteria (*Bacillus thuringiensis*) for the positive control. To quantify DNA yield, the DNA extracts were examined by agarose (1.2% w/v) gel electrophoresis, which was stained with 0.5 µg/ml ethidium bromide and compared with HyperLadder I DNA quantification marker (Bioline).

5.3 Results

5.3.1 Observation of Scanning Electron Microscope (SEM) Images

To obtain the detailed morphologies of the red rain cells, we first looked at them under SEM. The cells had an average size of 4~6 μm, and had in general oval shapes **(Fig. 5-3)**. These properties are in general agreement with the observation of Louis and Kumar's (2006). However, most of red rain cells we observed were squashed in such a way that they looked like the red blood cells **(Fig. 5-4)**. This was probably due to the dehydration procedures that we used, which caused tension over the cell-surfaces and squashing of the cells. This is supported by the observation under the optical microscope where the long exposures to the light's heat dehydrated the cells and the core has started to get squashed **(Fig. 5-5)**.

The red rain cells, which were heated at 300°C by Louis, were also observed. It can be separated into two types, one with smooth surface and another with wrinkled surface. The size varied from 10 μm to 1 μm **(Fig. 5-6)**. We observed 3~4 μm smooth and wrinkled particles and budding smaller smooth particles **(Fig. 5-7)**. We also observed a 10 μm near-complete spherical particle producing a small wrinkled surface with a hole which looks like the location of a small particle that was made before **(Fig. 5-8)**. Although we have observed many aspects of particle budding in the heated sample, it is hard to tell whether they are the red rain cells or not because morphologically they are very different from the original red rain cells.

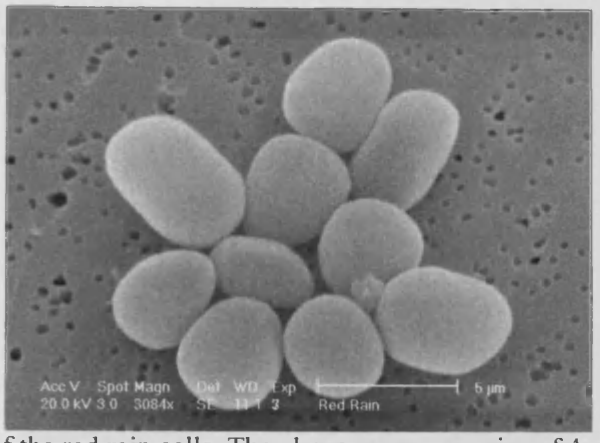

Figure 5-3: SEM image of the red rain cells. They have an average size of 4~6 µm and have square-oval shapes.

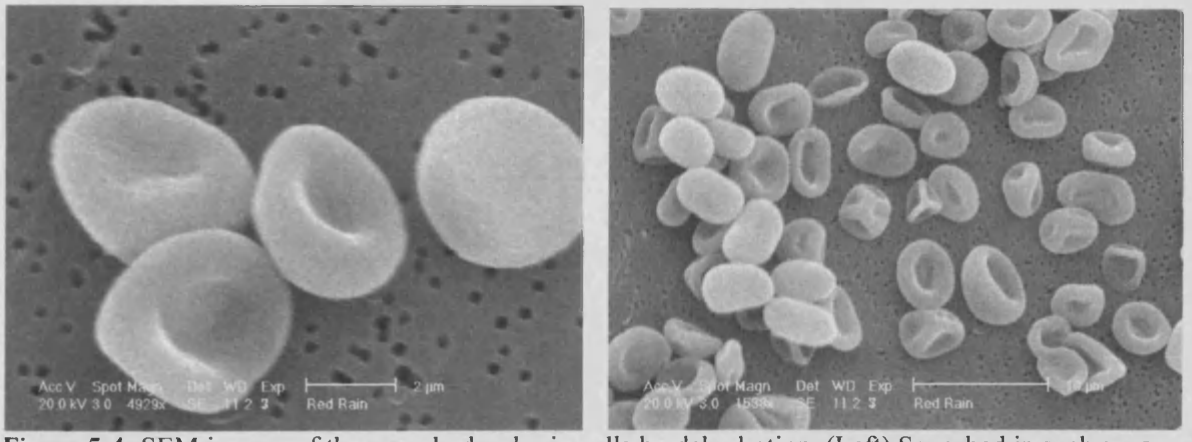

Figure 5-4: SEM images of the squashed red rain cells by dehydration. (Left) Squashed in such a way that looks like red blood cells. (Right) Many other squashed morphology of the red rain cells.

Figure 5-5: Optical microscopic images of the squashed red rain cells, which were dehydrated by the long exposure to the microscope's heat.

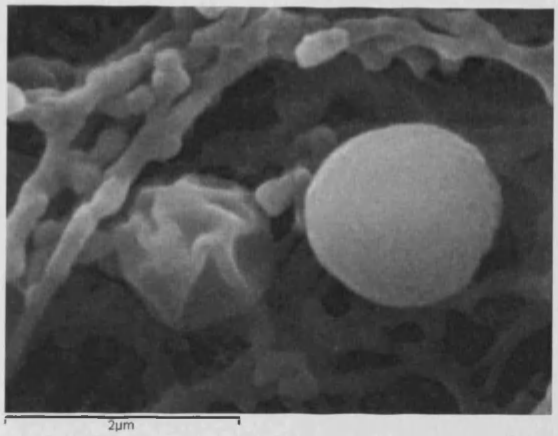

Figure 5-6: SEM image of 1~2 μm smooth and wrinkled particles from the 300°C heated red rain sample on cellulose nitrate filter.

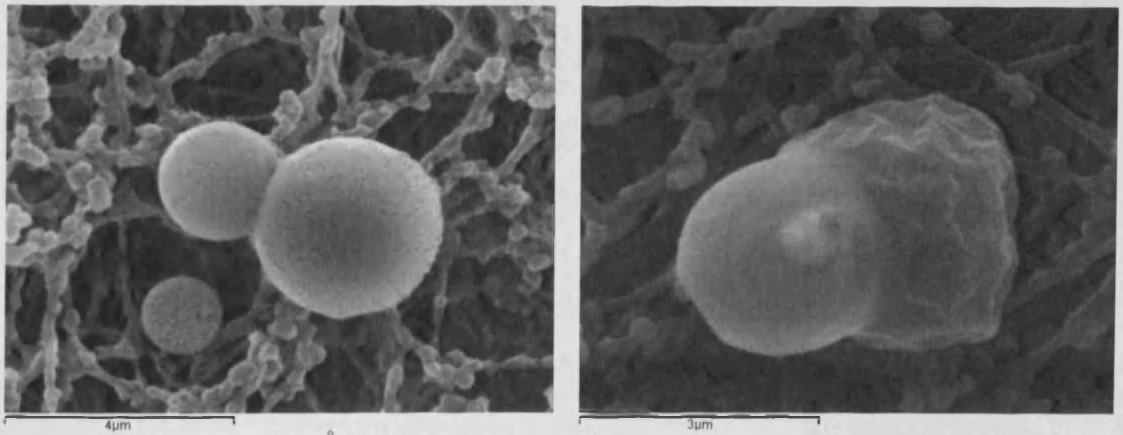

Figure 5-7: SEM image of 300°C heated red rain sample on cellulose nitrate filter. (Left) 4 μm smooth particle producing a smaller one. (Right) 3 μm wrinkled particle producing a smaller one.

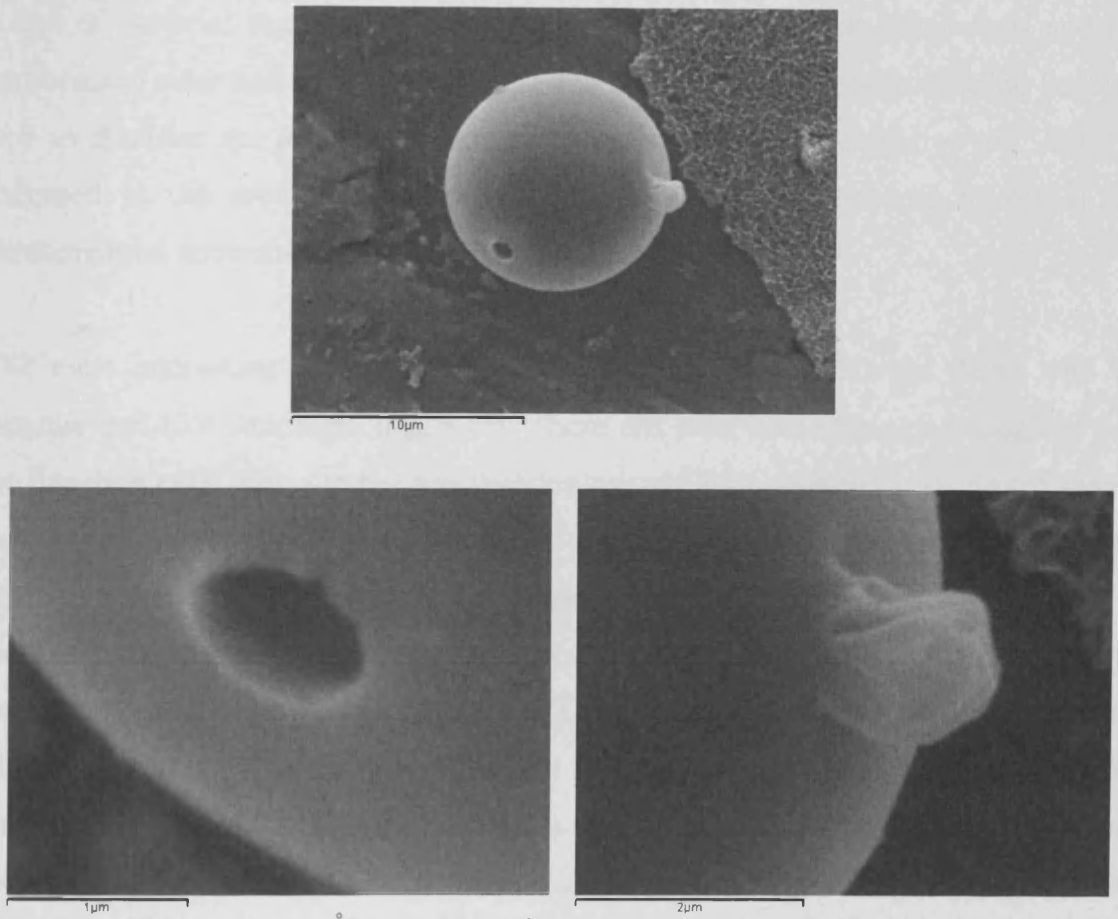

Figure 5-8: SEM image of 300°C heated red rain sample on Anodisc 47. (Top) 10 µm near-complete spherical smooth particle. (Bottom Left) A hole where it looks like a small particle budded out. (Bottom Right) A small wrinkled particle budding out.

5.3.2 Observation of Transmission Electron Microscope (TEM) Images

To obtain the interior properties of the red rain cells, they were cut in cross sections and observed under TEM. Figure 5-9 shows cells with very thick coating, and under the coats double envelopes containing a variety of structures, mainly comprised of strand or cytoskeleton-like materials. They also luck the nucleus as Louis and Kumar observed before. The ultrastructure characteristics of the red rain cells are very similar to that of bacterial endospores **(Fig. 5-10)**. They also have thick spore coats and two membranes (outer and inner) enveloping the core cells. Endospore-forming bacteria, such as *Bacillus sp.* found in the upper stratosphere (Wainwright *et al.*, 2003) as discussed in the previous chapter, can survive in many extreme terrestrial and extraterrestrial environments (Nicholson *et al.*, 2000).

The most interesting ultrastructures that we have observed were those with the daughter cell-like structures **(Fig. 5-10)**. There are cells containing one daughter cell, two daughter cells with another one developing, and four daughter cells. In the case of the cell with four daughters, we identified another one in the different TEM sample, which has the same orientation with one pointed daughter cell. Sporulations of bacteria generally undergo binary fission and only a few unusual species produce daughter cells within the parent cell, for example *Epulopiscium sp.* and *Metabacterium sp.* (Angert *et al.*, 1996, 2004; Robinow *et al.*, 1998). They are symbionts which sporulate one to twelve daughter cells inside and those daughter spores are active unlike other dormant endospores. Figure 5-11 (A), however, shows that sporulation of those bacteria are morphologically different from that of the red rain cells. In fact, the sporulation of Ascus **(Fig. 5-11 (B))** is far more similar. It is the sexual spore-bearing cell produced in ascomycete fungi. Ascospores like those daughter cells were made by meiosis within ascus and burst out when the time comes (Honnegger, 1985). Unfortunately they are eukaryotes, therefore contains nucleus which the red rain cells do not have.

We have also observed many other unusual ultrastructures, such as those with the squashed inner envelopes and core **(Fig. 5-12)**. It looks like a squashed cell caused by dehydration as observed under the optical microscope. We also identified the empty exosporium, perhaps with the daughter cells already ejected **(Fig. 5-13)**. There was also a cell with two other envelopes, one within another, inside the double envelopes **(Fig. 5-14)**.

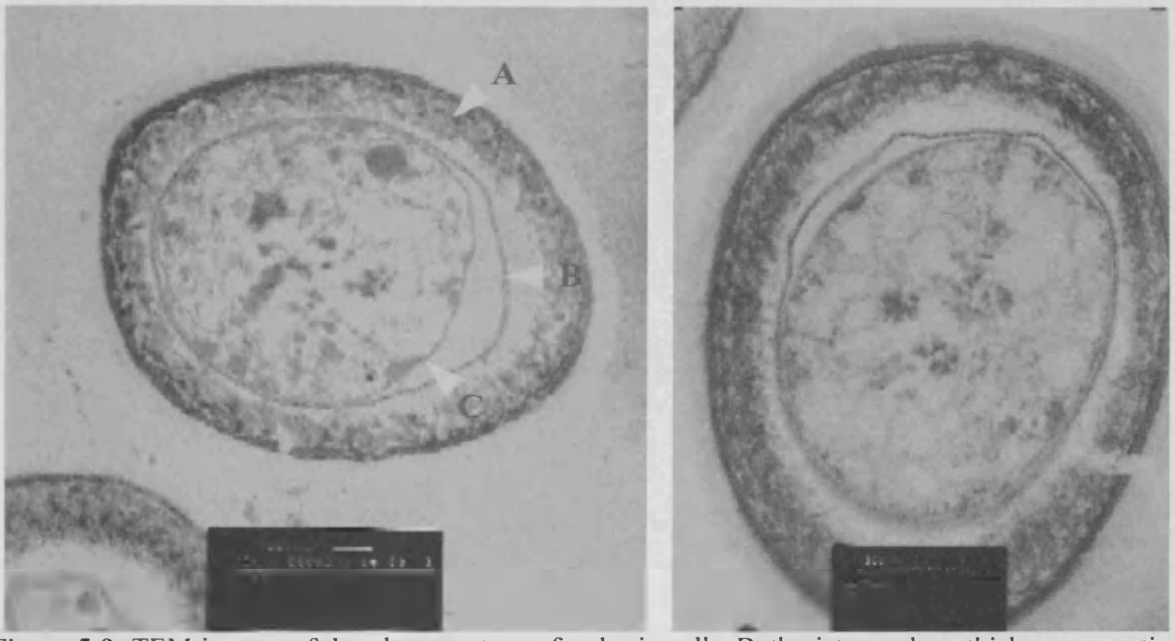

Figure 5-9: TEM images of the ultrastructure of red rain cells. Both pictures show thick spore coating (A) with double envelopes underneath (outer (B) and inner (C)). They seem to contain many materials inside the core but no nuclei are present.

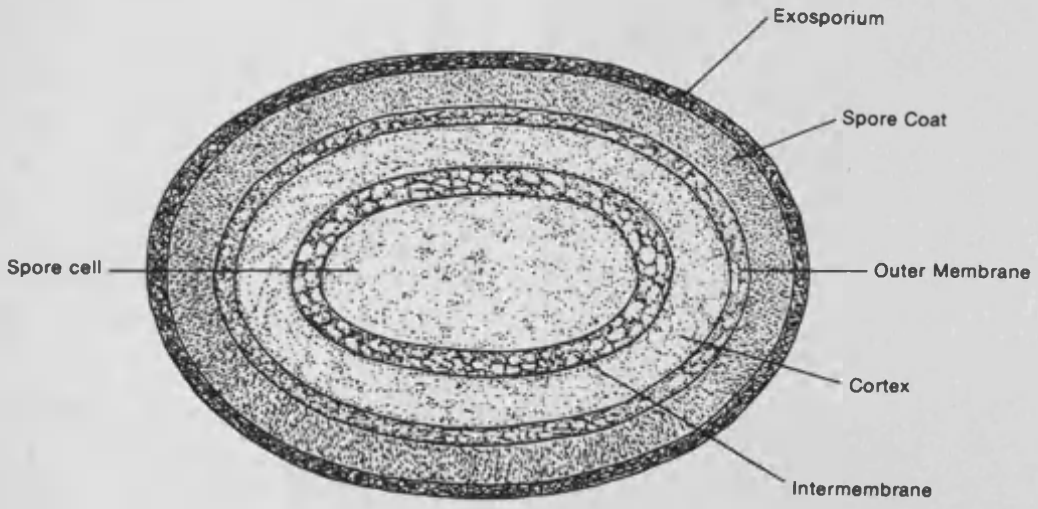

Figure 5-10: Illustration of typical endospore ultrastructure. ©Howie, University of Georgia

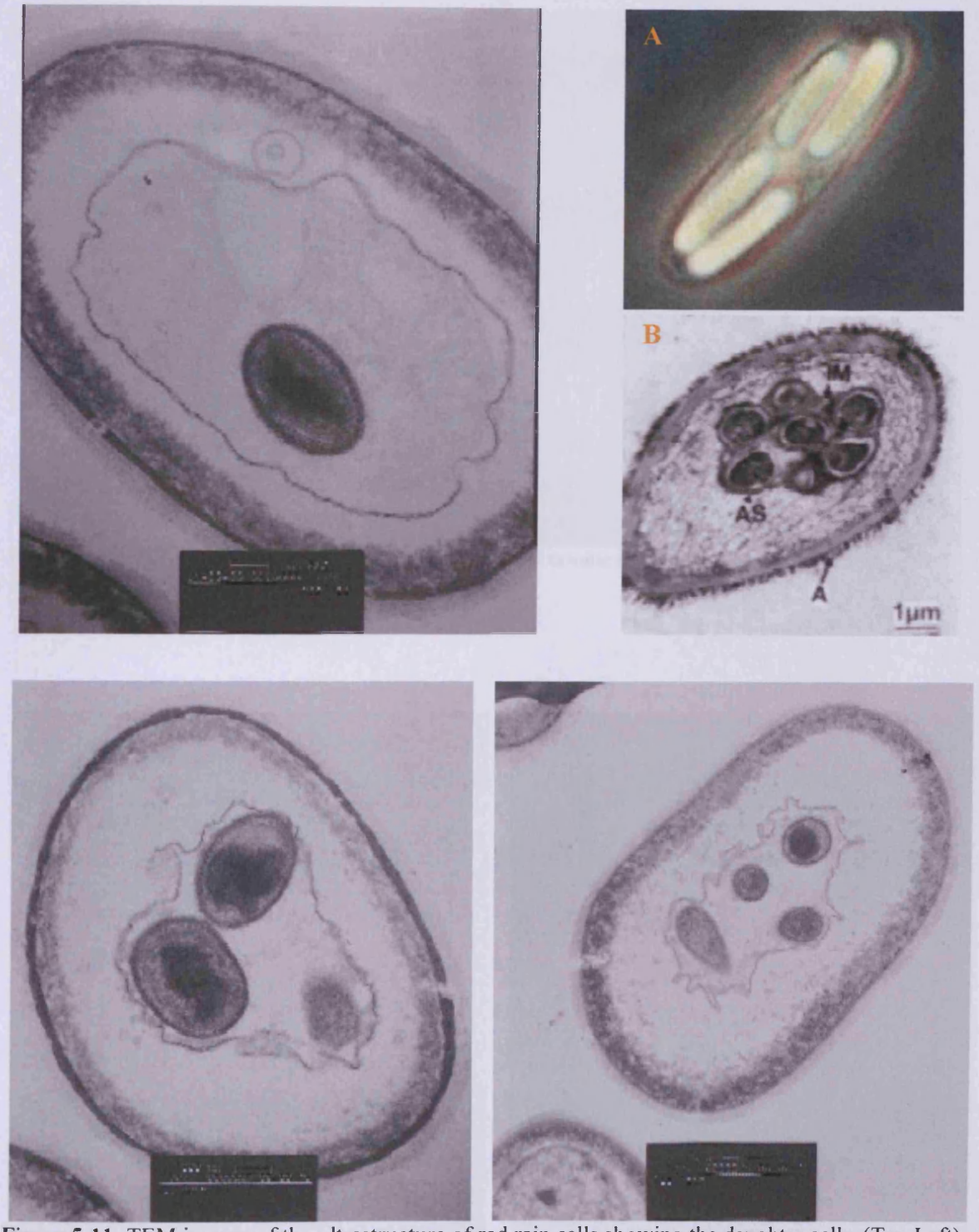

Figure 5-11: TEM images of the ultrastructure of red rain cells showing the daughter cells. (Top Left) A single daughter. (Bottom Left) Two daughter cells with another one developing. (Bottom Right) Four daughter cells. (Top Right) A – Endospores of *Metabacterium polyspora* (©Department of Microbiology, Cornell University). B – Ascospores of yeast *D. tothii* (Smith *et al.*, 2000).

Figure 5-12: TEM image showing the squashed internal double envelopes and the core cell.

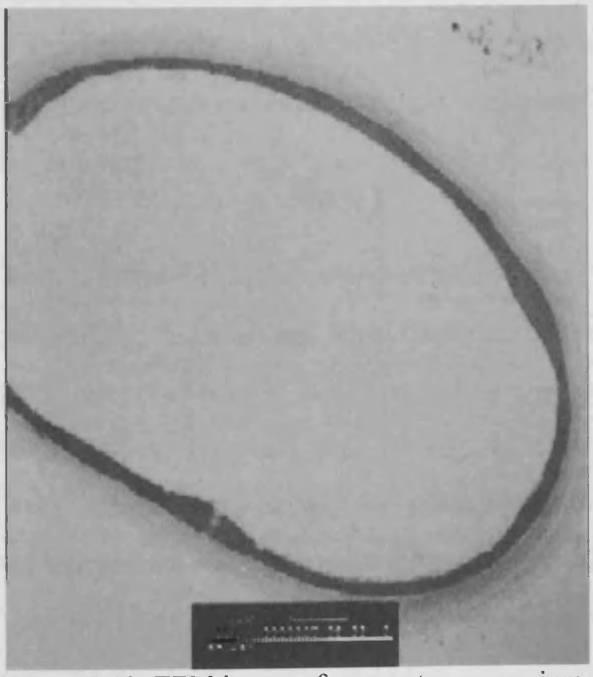

Figure 5-13: TEM image of an empty exosporium.

Figure 5-14: TEM image showing many extra envelopes inside.

5.3.3 Results from the Fluorescence Dye Analysis

Florescence properties of the cells can give a firm evidence for the presence of biological materials. First the viability of the red rain cells were analysed by using Live/Dead stains. After the cells were stained, they were observed under UV light and any cells that are living expected to fluoresce either in green colour (gram +ve bacteria) or red colour (gram –ve bacteria). The result showed a confirmation of red fluorescence emission by some of the cells **(Fig. 5-15)**. However, when the negative control of the cells without the stains were observed under UV light, red fluorescence emission were still observed from many cells **(Fig. 5-16)**. This shows that the red rain cells can actually autofluoresce in red under the UV light. Therefore we conclude that the results from the Live/Dead stains were not reliable.

Next the red rain cells were treated with DAPI stains. DAPI combines with DNA and fluoresce in blue colour under UV light. Since we discovered that the red rain cells autofluoresce in red colour, the emission by DAPI stains with the presence of DNA can be easily distinguished. The results show multiple number of the red rain cells fluoresced in blue, which confirmed the presence of DNA **(Fig. 5-17)**. We also found one of the cells containing four fluorescing daughter cells **(Fig. 5-18)**. This confirms that they are indeed the daughter cells and DNA must have separated into those cells by meiosis.

The red rain cells that were heated at 300°C by Louis had also been treated by DAPI stains. Fig. 5-19 shows blue fluorescence emission by one of the cells confirming the presence of DNA. It is difficult to believe that the DNA had survived heating to this temperature. The cell wall in Fig. 5-19 seem to be bumpy, this is may be due to the wrinkled cell surface that we observed under SEM. However, it has lost the red colour which was the best characteristic of the red rain cells and now it is hard to tell whether they are identifiable as descendants of red rain cells.

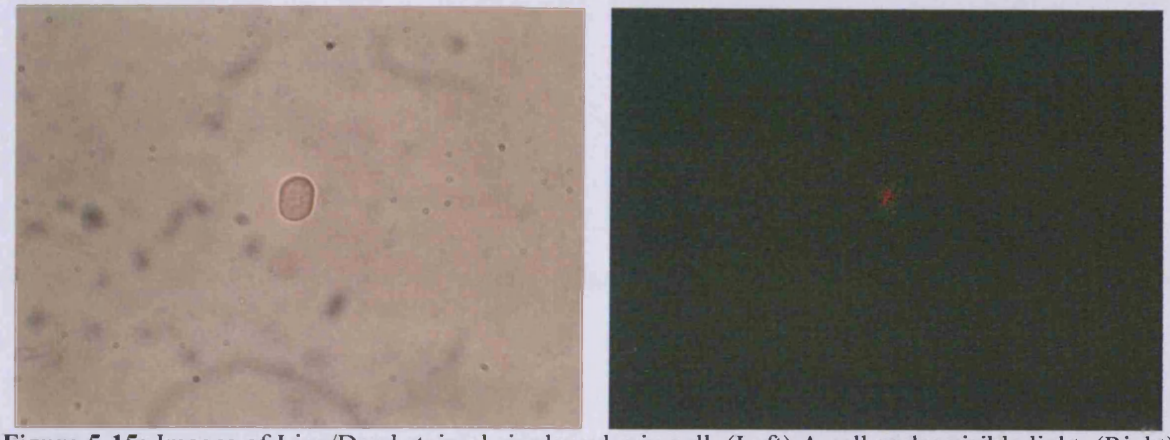

Figure 5-15: Images of Live/Dead stained single red rain cell. (Left) A cell under visible light. (Right) A cell fluorescing in red under UV light.

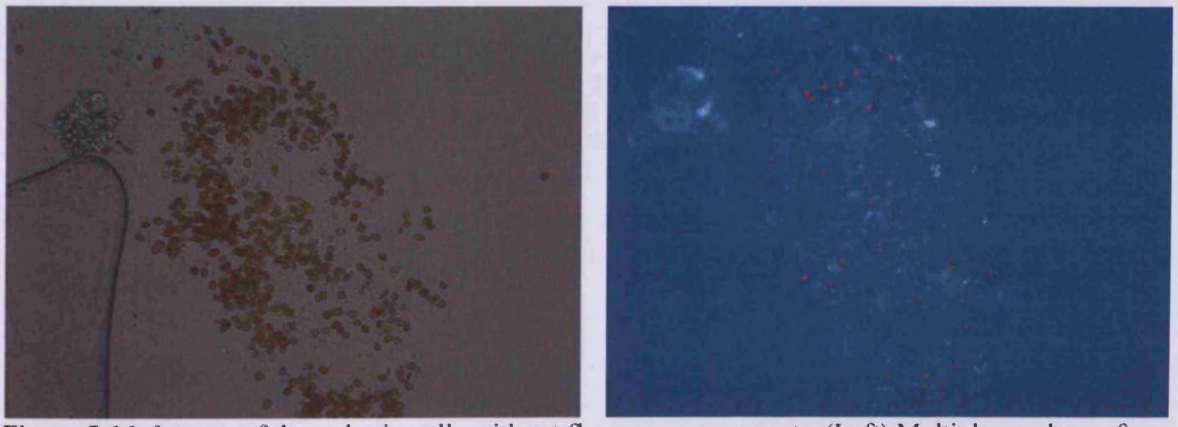

Figure 5-16: Images of the red rain cells without fluorescence reagents. (Left) Multiple numbers of cells under visible light. (Right) A number of cells autofluorescing in red under UV light.

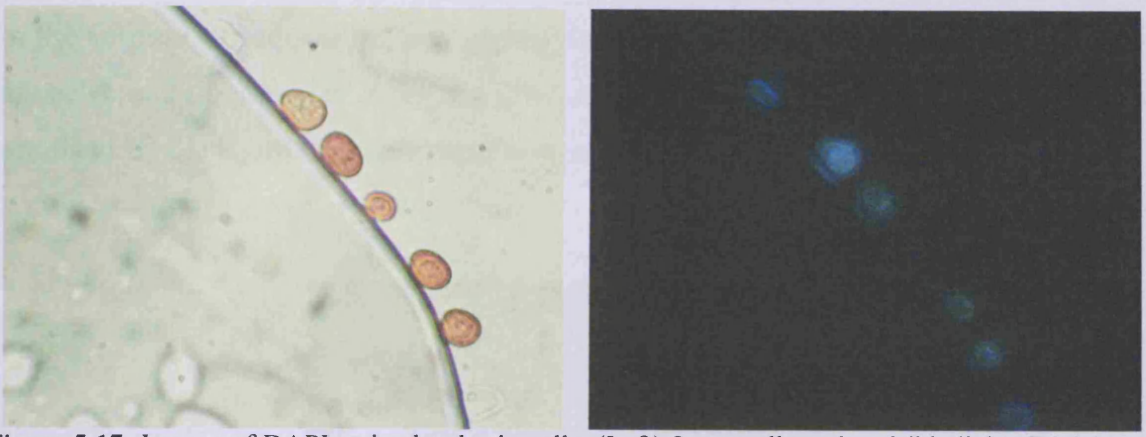

Figure 5-17: Images of DAPI stained red rain cells. (Left) Some cells under visible light. (Right) One of the cells fluorescing in blue under UV light.

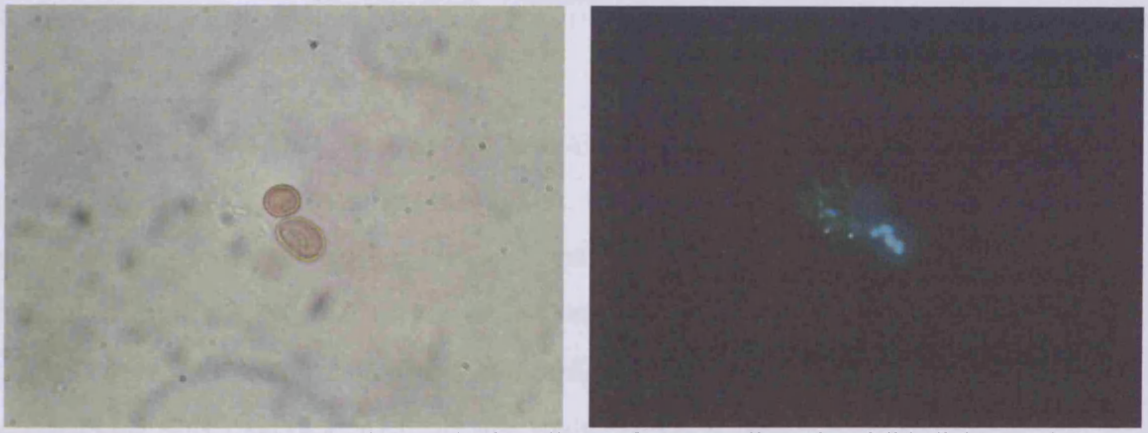

Figure 5-18: Images of DAPI stained red rain cells. (Left) Two cells under visible light. (Right) one of the cell contains four daughter cells, which are fluorescing in blue under UV light.

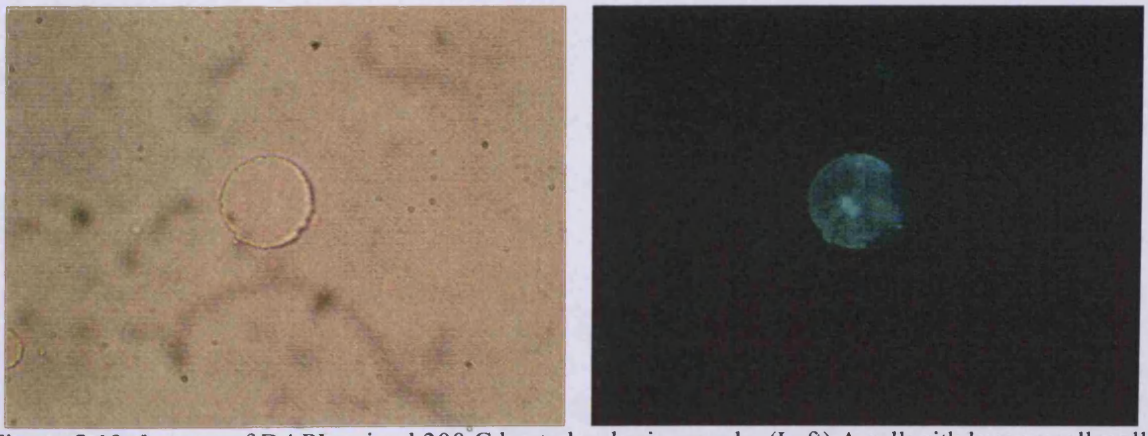

Figure 5-19: Images of DAPI stained 300 C heated red rain sample. (Left) A cell with bumpy cell wall under visible light. (Two small fluoresced areas within the cell under UV light.

5.3.4 Results from the DNA Isolation

Having observed the presence of DNA by DAPI stains, we next tried to isolate DNA for the purpose of sequencing and identifying which species of microorganism the red rain cells really belong to. After the DNA extract was obtained by lysis, its yield was examined by the agarose gel electrophoresis under the UV light **(Fig. 5-20)**.

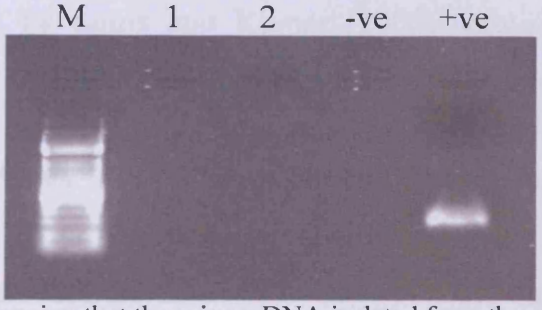

Figure 5-20: Agarose gel showing that there is no DNA isolated from the red rain sample. M – Marker. 1 and 2 – Red rain sample. –ve – Blank Work. +ve – known Bacteria (*B. thuringiensis*).

As Fig. 5-20 shows that we had not managed to isolate any DNA from the red rain cells. To identify any reason for this result, I extracted the solution after the lysis work and observed under the optical microscope **(Fig. 5-21)**. We observed only a couple of cells were crushed and rest of the cells were still intact. Since the technique we used can lyse most of the spores and the bacteria, it shows that the red rain cells have much tougher cell wall structure than any known microorganisms.

Figure 5-21: Optical microscopic images of the red rain cells treated with lysis work. Only a couple of cells were crushed and the rest of the cells were still intact.

5.4 Discussion

The mysterious red rain phenomenon were observed in many different parts of Kerala, India, in 2001. The studies of similar phenomena in the past have pointed to a connection with terrestrial microorganisms to the cause red colour (Fort *et al.*, 1931; McAtee, 1917). Early investigations of the red rain samples from India suggested that the lichen of *Trentepohlia sp.* was the cause of the red colour (Sampath *et al.*, 2001). However, closer study by Louis and Kumar (2006) showed that they are spore-forming microorganisms significantly different from *Trentepohlia sp.*.

Our TEM analysis shows that ultrastructures of red rain cells have similar characteristics of those of prokaryotic endospores and eukaryotic ascospores. They have a thick spore coat with no nucleus in the core, pointing to their prokaryotic nature. They, however, show sporulation of up to four daughter cells within a parent cell, similar to the meiotic reproductive cycles of ascospores by ascomycota (Honnegger, 1985). An unpublished paper of Louis *et al.* (2003) argued that the red rain cells can also reproduce at high temperatures of up to 300°C, by both binary fission and sporulation, within the parent cells. Our own SEM analysis of Louis's reproduced cells at high temperature, however, show loss of the original cell's characteristics. Therefore it is difficult to draw definite conclusions regarding their nature. These problems can be resolved if we are able to carry out the genomic analysis on the red rain cells.

After our confirmation of DNA within the cells by DAPI staining, we carried out their DNA isolation by the same lysis work used in the study of low biomass extremophiles found in deep biosphere (Webster *et al.*, 2003). The results, however, showed the only a few cells were lysed and not enough DNA yield was obtained. This is another characteristic indication of an unusually tough spore coat around the cells.

For the future work, I suggest that techniques, such as a French press (Milner *et al.*, 1950) or a Fuse press (Hughes *et al.*, 1971), can be trialled for breaking these tough cell walls. Cellular metabolic analysis, such as ATP synthesis, can also be studied. At

present, the phylogenicity of the red rain cells remains to be determined, as indeed the origin of those cells.

CHAPTER 6

Conclusion and Prospects

According to the theory of cometary panspermia the process of abiogenesis, normally thought to have occurred on Earth, took place as a rare event on a cosmic scale. Once microorganisms were originated, possibly in comets as proposed by Napier *et al.* (2007), its subsequent spread occurs through the agency of comets. Comets pick up a viable component of microbes (spores) present in interstellar dust clouds, amplify this in the warm interior of radioactively melted comets, and distributes this to other star and planet forming systems.

On this basis, life on Earth was introduced by comets nearly 4 Gyr ago, but the process did not stop there. Comets are still bringing debris to the Earth at the rate of ~100 tonnes per day. Some fraction of this debris must contain viable as well as 'fossilised' microorganisms.

The work described in this thesis set out to find evidence of bacterial material – viable as well as fossilised – amongst cometary debris and IDP's collected by the cryosampler collection technique in 2001. Samples from this collection were made available to me and I conducted SEM/EDX studies on over 30 IDP's cataloguing the types/compositions/mineralogies that I discovered. I found a class of carbonaceous IDP's with a probable biological provenance – fossilised and viable cells including nanobacterial shapes/compositions.

Since morphology and composition alone could prove deceptive, I next proceeded to carry out PCR investigation of a part of the collected filter material. Significantly I found evidences of 16S rRNA corresponding to an actinomycete (96% homology to *J. gansuensis*) and a chloroplast (99% homology to *L. sativa* and *G. bancanus*), both of which are most unlikely to be the contaminants, and can therefore be inferred as being indigenous to the cometary sample. The presence of chloroplasts as an independent symbiont in the cometary environment provides strong support for cometary panspermia and its contribution to the evolution of terrestrial life. Clearly, the work

has to be reconfirmed by future studies, possibly including isotope analysis using nanoSIMS techniques.

In the final chapter, my preliminary analyses of the Kerala Red Rain sample leads to an inconclusive result as to its origin. Consistency with an extraterrestrial origin is established on the grounds of unusual morphologies exhibited in my SEM/TEM work but is not proved.

More stratospheric samples, obtained relatively inexpensively using the cryosampler collection technique could have an important pay-off in confirming the work of this thesis and firmly establishing the concreteness of the theory of cometary panspermia.

Appendix A

Isosilicates:

Olivine group

Forsterite	– Mg_2SiO_4
fayalite	– Fe_2SiO_4

Garnet group

Almandine	– $Fe_3Al_2(SiO_4)_3$
Pyrope	– $Mg_3Al_2(SiO_4)_3$

Inosilicates:

Pyroxene group

Enstatite	– $MgSiO_3$
Ferrosite	– $FeSiO_3$

Sodium pyroxene group

Jadeite	– $NaAlSi_2O_6$
Aegirine	– $NaFe^{3+}Si_2O_6$

Phyllosilicate:

Clay mineral group

Pyrophyllite	– $Al_2Si_4O_{10}(OH)_2$
Talc	– $Mg_3Si_4O_{10}(OH)_2$

Spinel:

Spinel	– $MgAl_2O_4$
Hercynite	– $FeAl_2O_4$
Magnetite	– Fe_3O_4
Chromite	– $(Fe, Mg)Cr_2O_4$

Haematite: – Fe_2O_3

Wüstite: – FeO

Pyrrhotite: – FeS (weekly magnetic)

Pyrite: – FeS_2

Taenite: – FeNi

Bibliography

A'HEARN, M. F. *et al.* (2005) Deep Impact: excavating comet Tempel 1. *Science,* 310, 258-64.

AHMAD, I., HAYAT, S., AHMAD, A. & INAM, A. (2005) Effect of heavy metal on survival of certain groups of indigenous soil microbial population. *J Appl Sci Envion Manag*, 9, 115-21.

ALLEN, C. C. *et al.* (1997) Nanobacteria in Carbonates. *28th LPSC*, 29.

ALLEN, D. A. & WICKRAMASINGHE, D. T. (1981) Diffuse interstellar absorption bands between 2.9 and 4.0 μm. *Nature*, 294, 239-40.

ALLEN, M., DELITSKY, M., HUNTRESS, W., YUNG, Y., IP, W. H., SCHWENN, R., ROSENBAUER, H., SHELLEY, E., BALSIGER, H. & GEISS, J. (1987) Evidence for methane and ammonia in the coma of comet P/Halley. *Astron Astrophys,* 187, 502-12.

ANGERT, E. R., BROOKS, A. E. & PACE, N. R. (1996) Phylogenetic analysis of Metabacterium polyspora: Clues to the evolutionary origin of *Epulopiscium* spp., the largest bacteria. *J Bacteriol,* 178, 1451-6.

ANGERT, E. R. & CLEMENTS, K. D. (2004) Initiation of intracellular offspring in Epulopiscium. *Mol Microbiol,* 51, 827-35.

ARRHENIUS, S. (1903) Die Verbreitung des Lebens im Weltenraum. *Die Umschau,* 7, 481-5.

BECQUEREL, P. (1924) La Vie Terrestre provient-elle d'un Autre Monde? *Bull Soc Astron*, 38, 393-417.

BERZELIUS, J. J. (1834) Uber Meteorstein, 4. Meteorstein von Alais. *Ann Phys Chem*, 33, 113-23.

BHANDARI, N., ARNOLD, J. R. & PARKIN, E. (1968) Cosmic dust in the stratosphere. *J Geophys Res*, 73, 1837-45.

BRADLEY, J. P. & BROWNLEE, D. E. (1983) Pyroxene whiskers and platelets in interplanetary dust: evidence of vapour phase growth. *Nature*, 301, 473-7.

BRADLEY, J. P., BROWNLEE, D. E. & FRAUNDORF, P. (1984) Discovery of nuclear tracks in interplanetary dust. *Science*, 226, 1432-4.

BRADLEY, J. P., HARVEY, R. P. & MCSWEEN, H. Y., JR. (1996) Magnetite whiskers and platelets in the ALH84001 Martian meteorite: evidence of vapor phase growth. *Geochim Cosmochim Acta,* 60, 5149-55.

BRIDGES, J. C. *et al.* (2008) Iron Oxide Grains in Stardust Track 121 Grains as Evidence of Comet Wild 2 Hydrothermal Alteration. *39th LPSC,* 2193.

BROWNLEE D. E. & HODGE, P. W. (1973) The physical nature of interplanetary dust as inferred by particles collected at 35 km. *NASA SP-319*, 291-5.

BROWNLEE, D. E. *et al.* (1974) Elemental abundances in interplanetary dust. *Nature*, 252, 667-9.

BROWNLEE, D. E. (1976a). An atlas of extraterrestrial particles collected with NASA U-2 aircraft 1974-1976. *NASA TMX*, 73, 152-68.

BROWNLEE, D. E., FERRY, G.V. & TOMANDL, D.A. (1976b) Stratospheric aluminium oxide. *Science*, 191, 1270-1.

BROWNLEE, D. E., (1978) Microparticle Studies by Sampling Techniques. COSMIC DUST, *Wiley Interscience Publications*, 295-336.

BROWNLEE, D. E., OLSZEWSKI, E. & WHEELOCK, M. (1982) A working taxonomy for micrometeorites. *Lunar Planet Sci*, 12, 71-2.

BROWNLEE, D. E. (1985) Cosmic Dust: Collection and Research. *Annu Rev Earth Planet Sci*, 13, 147-73.

BRYANT, D. A. & FRIGAARD, N. U. (2006) Prokaryotic photosynthesis and phototrophy illuminated. *Trends Microbiol,* 14, 488-96.

BRUCH, C. W. (1967) Airborne Microbes Symposium of the Society for Microbiology, *Cambridge University press,* 17, 345-73.

CAVALIER-SMITH, T. (1982) The origins of plastids. *Biol J Linn Soc*, 17, 289-306.

CISAR, J. O., XU, D. Q., THOMPSON, J., SWAIM, W., HU, L. & KOPECKO, D. J. (2000) An alternative interpretation of nanobacteria-induced biomineralization *Proc Natl Acad Sci U S A,* 97, 11511-5.

COOPER, G., KIMMICH, N., BELISLE, W., SARINANA, J., BRABHAM, K. & GARREL, L. (2001) Carbonaceous meteorites as a source of sugar-related organic compounds for the early Earth. *Nature,* 414, 879-83.

COULSON, S. G. & WICKRAMASINGHE, N. C. (2003) Frictional and radiation heating of micron-sized meteoroids in the Earth's upper atmosphere. *Mon Notic Roy Astron Soc*, 343, 1123-30.

DAWSON, M. W., SCOTT, J. G. & COX, L. M. (1996) The medical and epidemiological effects on workers of the levels of airborne *Thermoactinomyces spp.* Spores present in Australian raw sugar mills. *Am Ind Hyg Assoc J,* 57, 1002-12.

DELONG, E. F. (1992) Archaea in coastal marine environments. *Proc Natl Acad Sci U S A,* 89, 5685-9.

DIETZEL, H., NEUKUM, G. & RAUSER, P. (1972) Micrometeoroid simulation studies on metal targets. *J Geophys Res*, 77, 1375-95.

DUBOS, R. (1950) Louis Pasteur: Free Lance of Science. *Da Capo Press, Inc.*, 187.

DU NOÜY, L. (1947) Human Destiny. *New York: Longmans, Green & Co.,* 289.

EHRENFREUND, P., GLAVIN, D. P., BOTTA, O., COOPER, G. & BADA, J. L. (2001) Extraterrestrial amino acids in Orgueil and Ivuna: Tracing the parent body of CI type carbonaceous chondrites. *Proc Natl Acad Sci U S A,* 98, 2138-41.

FLYNN, G. J. (2008) Physical, Chemical, and Mineralogical Properties of Comet 81P/Wild 2 Particles Collected by Stardust. *Earth, Moon and Planets*, 102, 447-59.

FORT, C. (1931) Lo!. *Ace Books*, 583.

FRAUNDORF, P. (1980) The distribution of temperature maxima for micrometeorites decelerated in the Earth's atmosphere without melting. *Geophys Res Let*, 7, 765-8.

FRAUNDORF, P., BROWNLEE, D. E. AND WALKER, R. M. (1982) Laboratory studies of interplanetary dust. COMETS, *Tucson,* 384-409.

GELINAS, L. J. *et al.* (1998) First observation of meteoritic charged dust in the tropical mesosphere. *Geophys Res Let*, 25(21), 4047-50.

GIBBS, S. P. (1978) The chloroplasts of Euglena may have evolved from symbiotic green algae. *Can J Bot*, 56, 2883-9.

GIBBS, S. P. (1981) The chloroplasts of some algal groups may have evolved from endosymbiotic eukaryotic algae. *Ann N Y Acad Sci,* 361, 193-208.

GILBER, W. (1986) The RNA World. *Nature*, 319, 618.

GRADY, M. & WRIGHT, I. (1990) A Cosmic Cake Mix: Can primitive meteorites tell us what happened before the Solar System was formed? *New Scientist*, 127, 46-7, 50-2.

GRAPS, A. L. *et al.* (2006) Geo Debris and Interplanetary Dust: Fluxes and Changing Behavior. *Astrophys.*, http://arxiv.org/abs/astro-ph/0609341

GRIFFIN, D. W. (2007) Atmospheric Movement of Microorganisms in Clouds of Desert Dust and Implications for Human Health. *Clin Microbiol Rev,* 20, 459-77.

HALDANE, J. B. S. (1929) The Origin of Life. *London: Chatto and Windys.*

HALLGREN, D. S. & HEMENWAY, C. L. (1976a) Analysis of impact craters from the S-149 skylab experiment. *Proc IAU Coll 31, Lecture Notes in Physics*, 48, 270-4.

HALLGREN, D. S., HEMENWAY, C. L. & WLOCHOWICZ, R. (1976b) Magellan collections of large cosmic dust particles. *Proc IAU Coll 31, Lecture Notes in Physics*, 48, 284-8.

HANIC, F. *et al.* (2000) Thermochemical aspects of the conversion of the gaseous system CO_2-N_2-H_2O into a solid mixture of amino acids. *J Therm Anal Cal*, 60, 1111-21.

HARNISCH, J. *et al.* (2000) Natural fluorinated organics in fluorite and rocks. *Geophys Res Let*, 27, 1883-6.

HARRIS, M. J. *et al.* (2002) The detection of living cells in stratospheric samples. *SPIE*, 4495, 192-8.

HEMENWAY, C. L. & SOBERMAN, R. K. (1962) Studies of micrometeorites obtained from a recoverable sounding rocket. *Astro J*, 67, 256-66.

HEMENWAY, C. L., HALLGREN, D. S. & COON, R. E. (1967) High altitude balloon-top collection of cosmic dust. *Space Res*, 7, 1423-31.

HEMENWAY, C. L. (1976) Submicron particles from the Sun. *Proc IAU Coll 31, Lecture Notes in Physics*, 48, 251-69.

HONEGGER, R. (1985) The hyphomycetous anamorph of Coniocybe furfuracea. *Lichenol*, 17, 273-9.

HOOVER, R. B. *et al.* (1998) Further Evidence of Microfossils in Carbonaceous Chondrites. *SPIE*, 3441, 203-16.

HOOVER, R. B. *et al.* (2004) Indigenous microfossils in carbonaceous meteorites. *SPIE*, 5555, 1-17.

HOOVER, R. B. (2006) Microfossils of Cyanobacteria in Carbonaceous Meteorites. *NTRS*, http://ntrs.nasa.gov/archive/nasa/casi.ntrs.nasa.gov/20070038326_2007036997.pdf

HOPPE, H. *et al.* (2004) Nanoscale Morphology of Conjugated Polymer/Fullerene-Based Bulk - Heterojunction Solar Cells. *Adv Func Mat*, 14(10), 1005-11.

HORNECK, G. (1993) Responses of *Bacillus subtilis* spores to space environment: Results from experiments in space. *Orig Life Evol Biosph,* 23, 37-52.

HORNECK, G., ESCHWEILER, U., REITZ, G., WEHNER, J., WILLIMEK, R. & STRAUCH, K. (1995) Biological responses to space: results of the experiment "Exobiological Unit" of ERA on EURECA I. *Adv Space Res,* 16(8), 105-18.

HORNECK, G., RETTBERG, P., REITZ, G., WEHNER, J., ESCHWEILER, U., STRAUCH, K., PANITZ, C., STARKE, V. & BAUMSTARK-KHAN, C. (2001) Protection of bacterial spores in space. A contribution to the discussion on Panspermia. *Orig Life Evol Biosph,* 31, 527-47.

HOYLE, F. & WICKRAMASINGHE, N. C. (1977) Identification of the λ2200A interstellar absorption feature. *Nature*, 270, 323-4.

HOYLE, F. & WICKRAMASINGHE, N. C. (1978) Lifecloud: the origin of life in the galaxy. *London: J.M. Dent.*

HOYLE, F. & WICKRAMASINGHE, N. C. (1981) *In:* C. Ponnamperuma, ed. Comets and the Origin of Life. *Dordrecht: D. Reidel*, 227.

HOYLE, F. & WICKRAMASINGHE, N. C. (1982) Proofs that Life is Cosmic. *Colombo: Govt. Press, Sri Lanka.*

HOYLE, F. & WICKRAMASINGHE, N. C. (1985) Living Comets. *Cardiff Univ College, Cardiff Press.*

HUEBNER, W. F. *et al.* (1987) Polyoxymethylene in comet Halley. *Astrophys J*, 320, 149-52.

HUGHES, D. E., WIMPENNY, J. W. T. & LLOYD, D. (1971) The disintegration of Microorganism. *Meth Microbiol*, 5B, 1-54.

IMSHENETSKY, A. A., LYSENKO, S. V. & KAZAKOV, G. A. (1978) Upper Boundary of the Biosphere. *Appl Environ Microbiol*, 35, 1-5.

JEFFS, W. (2006) NASA's Stardust findings may alter view of comet formation. *NASA News*, 06-091.

JESSBERGER, E. K. (1999) Rocky Cometary Particulates: Their Elemental, Isotopic and Mineralogical Ingredients. *Space Sci Rev*, 90, 91-7.

JUNGE, K., EICKEN, H. & DEMING, J.W. (2004) Bacterial Activity at -2 to -20°C in Arctic Wintertime Sea Ice. *Appl Environ Microbiol*, 70, 550-7.

JUNGE, K., EICKEN, H., SWANSON, B. D. & DEMING J. W. (2006) Bacterial incorporation of leucine into protein down to −20 °C with evidence for potential activity in sub-eutectic saline ice formations. *Cryobiol*, 52, 417-29.

KASHEFI, K. & LOVLEY, D. R. (2003) Extending the Upper Temperature Limit for Life. *Science,* 301, 934.

KASTEN, F. (1968) Falling Speed of Aerosol Particles. *J Appl Meteol*, 7, 944-7.

KAZMIERCZAK, J. & KEMPE, S. (2003) Modern terrestrial analogues for the carbonate globules in Martian meteorite ALH84001. *Naturwissenschaften,* 90, 167-72.

KERSTERS, K., LISDIYANTI, P., KOMAGATA, K. & SWINGS, J. (2006) The Family Acetobacteraceae: The Genera *Acetobacter*, *Acidomonas*, *Asaia*, *Gluconacetobacter*, *Gluconobacter*, and *Kozakia. Prokaryotes,* part 1, 163-200.

KHULLAR, M., SHARMA, S. K., SINGH, S. K., BAJWA, P., SHEIKH, F. A., RELAN, V. & SHARMA, M. (2004) Morphological and immunological characteristics of nanobacteria from human renal stones of a north Indian population. *Urol Res,* 32, 190-5.

KROT, A. N. *et al.* (2005) Evolution of oxygen isotopic composition in the inner solar nebula. *Astrophys J*, 622, 1333-42.

KRUMBEIN, W. E. (1995) Gone with the wind – a second blow against spontaneous generation: In memoriam, Ehrenberg, C.G.. *Aerobiologia*, 11, 205-11.

LACY, J. H. *et al.* (1991) Discovery of interstellar methane - Observations of gaseous and solid CH_4 absorption toward young stars in molecular clouds. *Astrophys J*, 376, 556-60.

LANE, M. D. & CHRISTENSEN, P. R. (1998) Thermal Infrared Emission Spectroscopy of Salt Minerals Predicted for Mars. *Icarus*, 135, 528-36.

LEIGH, M. B., PELLIZARI, V. H., UHLIK, O., SUTKA, R., RODRIGUES, J., OSTROM, N. E., ZHOU, J. & TIEDJE, J. M. (2007) Biphenyl-utilizing bacteria and their functional genes in a pine root zone contaminated with polychlorinated biphyenyls (PCBs). *ISME J,* 1, 134-48.

LISSE, C. M. *et al.* (2006) Spitzer Spectral Observations of the Deep Impact Ejecta. *Science,* 313, 635-40.

LLOYD, A. B. (1969) Dispersal of Streptomyces in air. *J Gen Microbiol,* 57, 35-40.

LLOYD, D. & HAYES, A. J. (1995) Vigour, vitality and viability of microorganisms. *FEMS Microbiol Let,* 133, 1.

LOPEZ-AMOROS, R., MASON, D. J. & LLOYD, D. (1995) Use of two oxonols and a fluorescent tetrazolium dye to monitor starvation of *E. coli* in sea water by flow symmetry. *J Microbiol Meth,* 22, 165.

LOVE, S. G. & BROWNLEE, D. E. (1993) A Direct Measurement of the Terrestrial Mass Accretion Rate of Cosmic Dust. *Science,* 262, 550-3.

LOUIS, G. & KUMAR, A. S. (2003) New biology of red rain extremophiles prove cometary panspermia. *Astrophys,* http://arxiv.org/abs/astro-ph/0312639

LOUIS, G. & KUMAR, A. S. (2006) The Red Rain Phenomenon of Kerala and its Possible Extraterrestrial Origin. *Astrophys Space Sci,* 302, 175-87.

MANDEVILLE, J. C. (1991) Study of cosmic dust particles on board LDEF: The FRECOPA experiments AO138-1 and AO138-2. *LDEF First Post-Retrieval Symp, NASA CP,* 3134, 419-34.

MCATEE, W. L. (1917) Showers of Organic Mater. *Mon Weather Rev,* 17, 217-24.

MCCAFFERTY, P. (2008) Bloody rain again! Red rain and meteors in history and myth. *Int L Astrobiol,* 7, 9-15.

MCKAY, D. S. *et al.* (1996) Search for past life on Mars: Possible relic biogenic activity in Martian meteorite ALH84001. *Science,* 273, 924-30.

MILEIKOWSKY, C. *et al.* (2000) Natural Transfer of Viable Mcrobes in Space: 1. From Mars to Earth and Earth to Mars. *Icarus,* 145, 391-427.

MILLER, S. L. & UREY, H. C. (1959) Organic Compound Synthesis on the Primitive Earth. *Science,* 130, 245-51.

MILNER, H. W., LAWRENCE, N. S. & FRENCH, C. S. (1950) Colloidal Dispersion of Chloroplast Material. *Science,* 111, 633-34.

MILOSHEVICH, L. M. & HEYMSFIELD, A. J. (1997) Al Balloon-borne Continuous Cloud Particle Replicator for Measuring Vertical Profiles of Cloud Microphysical Properties: Instrument Design, Performance, and Collection Efficiency Analysis. *J Atm Ocean Tech*, 14, 753-68.

MURPHY, C. D., SCHAFFRATH, C. & O'HAGAN, D. (2003) Fluorinated natural products: the biosynthesis of fluoroacetate and 4-fluorothreonine in *Streoptomyces cattleya. Chemosphere,* 52, 455-61.

MUYZER, G., DE WAAL, E. C. & UITTERLINDEN, A. G. (1993) Profiling of complex microbial populations by denaturing gradient gel electrophoresis analysis of polymerase chain reaction-amplified genes coding for 16S rRNA. *Appl Environ Microbiol,* 59, 695-700.

NAGASHIMA, K., KROT, A. N. & YURIMOTO, H. (2004) Stardust silicates from primitive meteorites. *Nature,* 428, 921-4.

NAPIER, W. M., WICKRAMASINGHE, J. T. & WICKRAMASINGHE, N. C., 2007. The origin of life in comets. *Int J Astrobiol*, 6(4), 321-3.

NEVALAINEN, A. *et al.* (1991) The indoor air quality in Finnish homes with mold problems. *Environ Int*, 17, 299-1302.

NICASTRO, A. J., VREELAND, R. H. & ROSENZWEIG, W. D. (2002) Limits imposed by ionizing radiation on the long-term survival of trapped bacterial spores: beta radiation. *Int J Radiat Biol,* 78, 891-901.

NICHOLSON, W. L., MUNAKATA, N., HORNECK, G., MELOSH, H. J. & SETLOW, P. (2000) Resistance of Bacillus Endospores to Extreme Terrestrial and Extraterrestrial Environments. *Microbiol Mol Biol Rev,* 64, 548-72.

O'HAGAN, D. AND HARPER, D.B. (1999) Fluorine-containing natural products. *J Fluorine Chem*, 100, 127-33.

OPARIN, A. I. (1924) The Origin of Life, *Moscow Worker Publisher.*

OSMAN, S., PEETERS, Z., LA DUC, M. T., MANCINELLI, R., EHRENFREUND, P. & VENKATESWARAN, K. (2008) Effect of Shadowing on Survival of Bacteria under Conditions Simulating the Martian Atmosphere and UV Radiation. *Appl Environ Microbiol,* 74, 959-70.

PANTOS, O., COONEY, R. P., LE TISSIER, M. D., BARER, M. R., O'DONNELL, A. G. & BYTHELL, J. C. (2003) The bacterial ecology of a plague-like disease affecting the Caribbean coral *Montastrea annularis. Environ Microbiol,* 5, 370-82.

PAUL, S., BAG, S. K., DAS, S., HARVILL, E. T. & DUTTA, C. (2008) Molecular signature of hypersaline adaptation: insights from genome and proteome composition of halophilic prokaryotes. *Genome Biol,* 9(4), R70.

POSTEC, A., URIOS, L., LESONGEUR, F., OLLIVIER, B., QUERELLOU, J. & GODFROY, A. (2007) Continuous Enrichment Culture and Molecular Monitoring to Investigate the Microbial Diversity of Thermophiles Inhabiting Deep-Sea Hydrothermal Ecosystems. *Cur Microbiol.* 50, 138-44.

RAPP, M. *et al.* (2005) Observations of positively charged nanoparticles in the night time polar mesosphere. *Geophys Res Let*, 32, L23821.

REPONEN, T. A., GAZENKO, S. V., GRINSHPUN, S. A., WILLEKE, K. & COLE, E. C. (1998) Characteristics of Airborne Actinomycete Spores. *Appl Environ Microbiol,* 64, 3807-12.

ROBINOW, C. & ANGERT, E. R. (1998) Nucleoids and coated vesicles of "Epulopiscium" spp.. *Arch Microbiol,* 170, 227-35.

RODE, B. M. (1999) Peptides and the origin of life. *Peptides,* 20, 773-86.

ROGERS, L. A. & MEIER, F. C. (1936) The collection of microorganisms above 36,000 feet. *Nat Geograph Soc Strato Series,* 2, 146–51

SAMPATH, S, ABRAHAM, T.K., SASI KUMAR, V. & MOHANAN, C.N. (2001) Coloured Rain: A Report on the Phenomenon. *Cen Earth Sci Stud Trop Bot Garden Res. Ins.*, CESS-PR-114-2001. [Abstract]

SANDFORD, S. A. (1983) Spectral matching of astronomical data from Comet Kohoutek with infrared data on collected interplanetary dust. *Meteoritic*, 18, 391.

SECKER, J., WESSON, P. S. & LEPOCK, J. R. (1994) Damaging due to ultraviolet and ionizing radiation during the ejection of shielded micro-organisms from the vicinity of $1M_{\Theta}$ main sequence and red giant stars. *Astrophys Space Sci*, 219, 1-28.

SEE, T. H. *et al.* (1991) Meteoroid and Debris Special Investigation Group preliminary results: size-frequency distribution and spatial density of large impact features on LDEF. *LDEF First Post-Retrieval Symp, NASA CP,* 3134, 477-86

SHARMA, A., SCOTT, J. H., CODY, G. D., FOGEL, M. L., HAZEN, R. M., HEMLEY, R. J. & HUNTRESS, W. T. (2002) Microbial Activity at Gigapascal Pressures. *Science,* 295, 1514-6.

SHYAMLAL, A. *et al.* (1996) Balloon-borne cryogenic air sampler experiment for the study of atmospheric trace gases. *Ind L Radio Space Phys*, 25, 1-7.

SMITH, D. P., KOCK, J. L., MOTAUNG, M. I., VAN WYK, P. W., VENTER, P., COETZEE, D. J. & NIGAM, S. (2000) Ascospore aggregation and oxylipin distribution in the yeast *Dipodascopsis tothii*. *Antonie Van Leeuwenhoek,* 77, 389-92.

SOMMER, A. P., MCKAY, D. S., CIFTCIOGLU, N., ORON, U., MESTER, A. R. & KAJANDER, E. O. (2003) Living Nanovesicles-Chemical and Physical Survival Strategies of Primordial Biosystems. *J Proteome Res,* 2, 441-3.

SOMMER, A. P., MIYAKE, N., WICKRAMASINGHE, N. C., NARLIKAR, J. V. & AL-MUFTI, S. (2004) Functions and Possible Provenance of Primordial Proteins. *J Proteome Res,* 3, 1296-9.

SONG, L., LI, W. J., WANG, Q. L., CHEN, G. Z., ZHANG, Y. S. & XU, L. H. (2005) *Jiangella gansuensis* gen. nov., sp. nov., a novel actinomycete from a desert soil in north-west China. *Int J Syst Evol Microbiol,* 55, 881-4.

SUNSHINE, J. M., CONNOLLY, H. C., JR., MCCOY, T. J., BUS, S. J. & LA CROIX, L. M. (2008) Ancient Asteroids enriched in Refractory Inclusions. *Science*, 320, 514-7.

TAN, W. C. & VANLANDINGHAM, S. L. (1967) Electron Microscopy of biological-like structures in the Orgueil carbonaceous meteorite. *Geophys J Royal Astr Soc*, 12, 237.

TIMME, R. E., KUEHL, J. V., BOORE, J. L. & JANSEN R. K. (2007) A comparative analysis of the *Lactuca* and *Helianthus* (Asteraceae) plastid genomes: identification of divergent regions and categorization of shared repeats. *American J Bot*, 94, 302-12.

TEPFER, D. & LEACH, S. (2006) Plant seeds as model vectors for the transfer of life through space. *Astrophys Space Sci*, 306, 69-75.

VREELAND, R. H., ROSENZWEIG, W. D. & POWERS, D. W. (2000) Isolation of a 250 million-years-old halotolerant bacterium from a primary salt crystal. *Nature*, 407, 897-900.

WÄCHTERSHÄUSER, G. (1988) An all-purine precursor of nucleic acids. *Proc Natl Acad Sci U S A,* 85, 1134-5.

WAINWRIGHT, M., WICKRAMASINGHE, N. C., NARLIKAR, J. V. & RAJARATNAM, P. (2003) Microorganisms cultured from stratospheric air samples obtained at 41 km. *FEMS Microbiol Lett,* 218, 161-5.

WAINWRIGHT, M. *et al.* (2004) Confirmation of the presence of viable but non-cultureable bacteria in the stratosphere. *Int J Astrobiol*, 3, 13-5.

WALLIS, M. K. (1980) Radiogenic melting of primordial comet interiors. *Nature*, 284, 431-3.

WALLIS, M. K., AL-MUFTI, S., WICKRAMASINGHE, N. C., RAJARATNAM, P. & NARLIKAR, J. V. (2002) SEM Imaging of Stratospheric Particles of Non-terrestrial Origin. *Presentation at University of the West of England, Bristol.*

WATANABE, K. (2001) Microorganisms relevant to bioremediation. *Curr Opin Biotechnol,* 12, 237-41.

WEBSTER, G., EMBLEY, T. M. & PROSSER, J. I. (2002) Grassland Management Regimens Reduce Small-Scale Heterogeneity and Species Diversity of β-Proteobacterial Ammonia Oxidizer Populations. *Appl Environ Microbiol,* 68, 20-30.

WEBSTER, G., NEWBERRY, C. J., FRY, J. C. & WEIGHTMAN, A. J. (2003) Assessment of bacterial community structure in the deep sub-floor biosphere by 16S rDNA-based techniques: a cautionary tale. *J Microbiol Methods,* 55, 155-64.

WEBSTER, G., PARKES, R. J., CRAGG, B. A., NEWBERRY, C. J., WEIGHTMAN, A. J. & FRY, J. C. (2006) Prokaryotic community composition and biogeochemical processes in deep subseafloor sediments from the Peru Margin. *FEMS Microbiol Ecol,* 58, 65-85.

WEBSTER, G., YARRAM, L., FREESE, E., KOSTER, J., SASS, H., PARKES, R. J. & WEIGHTMAN, A. J. (2007) Distribution of candidate division JS1 and other Bacteria in tidal sediments of the German Wadden Sea using targeted 16S rRNA gene PCR-DGGE. *FEMS Microbiol Ecol,* 62, 78-89.

WHATLEY, J. M. & WHATLEY, F. R. (1981) Chloroplast Evolution. *New Phytol*, 87, 233-47.

WICKRAMASINGHE, N. C. (1974) Formaldehyde polymers in interstellar space. *Nature*, 252, 462-3.

WICKRAMASINGHE, D. T. & ALLEN, D. A. (1986a) Discovery of organic grains in comet Halley. *Nature*, 323, 44-6.

WICKRAMASINGHE, D. T., HOYLE, F., WICKRAMASINGHE, N. C. & AL-MUFTI, S. (1986b) A model of the 2-4 micron spectrum of comet Halley. *Earth, Moon and Planets*, 36, 295-9.

WICKRAMASINGHE, N. C., HOYLE, F. & MAJEED, Q. (1989) Mineral and organic particles in astronomy. *Astrophys Space Sci*, 158(2), 335-46.

WICKRAMASINGHE, N. C., WAINWRIGHT, M., NARLIKAR, J. V., RAJARATNAM, M. J., HARRIS, M. J. & LLOYD, D. (2003) Progress towards the vindication of panspermia. *Astrophys Space Sci*, 283, 403-13.

WICKRAMASINGHE, J. T. (2007) *PhD thesis. Cardiff University.*

WICKRAMASINGHE, J. T., WICKRAMASINGHE, N. C. & WALLIS, M. (2008) Liquid water and organics in comets: implications for exobiology. *Int J Astrobiol*, in press.

WILDE, S. A., VALLEY, J. W., PECK, W. H. & GRAHAM, C. M. (2001) Evidence from detrital zircons for the existence of continental crust and oceans on the Earth 4.4 Gyr ago. *Nature*, 409(6817), 175–8.

WLOCHWICZ, R., HEMENWAY, C. L., HALLGREN, D. S. & TACKETT, C. D. (1976) Magellan: balloon-borne collection technique for large cosmic dust particles. *Canadian J Phys*, 54, 317-21.

WOESE, C. (1968) The Genetic Code. *Harper and Row.*

WRIGHT, I.P. *et al.* (1995) EURECA Multi-Layer Insulation Impact Morphology and Residue Analysis. *EURECA MLI Final Report, MADWEB Arch*, http://space-env.esa.int/madweb/eureca/mli/reports/oumli/oumlirp.php

ZINNER, E., PAILER, N. & KUCZERA, H. (1983) Laboratory measurements of D/H ratios in interplanetary dust. *Nature*, 305, 119-21.

ZWART, G & BOK, J. (2004) Protocol DGGE. *Netherlands Inst Ecol*, http://www.nioo.knaw.nl/CL/MWE/protocol_DGGE.pdf